Advances and Applications of Capillary Electrophoresis-Mass Spectrometry

By

Ryan Tyler Johnson

B.S, Drake University

Des Moines, IA

Submitted to the graduate degree program in Chemistry and the Graduate Faculty of the University of Kansas in partial fulfillment of the requirements for the degree of Doctor of Philosophy.

_____

Dr. John Stobaugh (Chairperson)

_____

Dr. Susan Lunte

_____

Dr. Heather Desaire

_____

Dr. Bob Dunn

_____

Dr. Teruna Siahaan

Date Submitted: 12/08/16

The dissertation committee for Ryan Tyler Johnson

certifies that this is the approved version of the following dissertation:

Advances and Applications of Capillary Electrophoresis-Mass Spectrometry

_____

Chairperson: John F Stobaugh

Date approved: 12/13/16

Abstract

Ryan Tyler Johnson Ph.D
Ralph N. Adams Institute for Bioanalytical Chemistry
University of Kansas, 2016

Capillary electrophoresis-mass spectrometry (CE-MS) is a useful analytical technique capable of high efficiency separations from complex and low volume samples. However, the interface between CE and MS is not nearly as robust as that for LC-MS. Herein, we describe applications of CE-MS that demonstrate the technique's utility and effectiveness. Additionally, advancements to the CE-MS interface design are presented.

Firstly, we developed a CE-UV and CE-ESI-MS method that utilizes a borate background electrolyte for the investigation of 14 natural flavonoid glycones and aglycones. Borate complexes with catechol containing flavonoids were detected in MS spectra. These complexes can aid in unknown flavonoid identification as well as mass isomer differentiation of flavonoids with varying hydroxylation patterns. Secondly, we fabricated a novel sheathless CE-ESI-MS interface with better mechanical stability than other similar interfaces. The interface was capable of nM LODs and robust electrophoresis and electrospray. Lastly, the novel interface was used to develop a CE-MS method for several biomarkers of lipid peroxidation from low volume microdialysis samples. The method utilizes charge reversal derivatization to achieve superior detection limits compared to native lipid biomarkers. Post-derivatization and sample clean up, approximately 25 nM LODs were achievable.

Acknowledgements

I would like to first thank my parents, Toby and Julie, who have supported me in every way imaginable over the past 27 years. They have been the sounding board for nearly every decision I have made, including the decision pursue a Ph.D. To my dad, thank you for always being available when I needed anything. I'll always remember when you said "anything that is mine, is yours" as I smuggled toilet paper on one my trips back home. To my mom, thank you for always being in my corner (even when I'm probably wrong) and putting up with me never calling or coming home enough. I would also like to thank my brother, Derrick, who is a computer and internet wizard willing to help me solve an odd-problem at the drop of a hat. I sincerely cannot be more indebted to you guys and love you with all of my being.

I would like to thank my late research advisor, Dr. Craig Lunte, for providing me the opportunity to do research in his lab. His "hands-off" style allowed me to flourish as a scientist. He taught me that life should be serious as much as it should be joyous. He also taught me that people actually eat at Arby's. Craig was there to provide patience, guidance, and to talk me off the ledge when times were tough. I will continue to miss his mentorship and his big jovial personality.

I would like to thank Dr. John Stobaugh for going out on a limb to accept an orphan student who was too stubborn to change research projects. John dedicated a lot of his time toward helping me get through the final 1.5 years of my graduate work, which included editing two manuscripts and this entire

dissertation, constant visits to MRB, and providing guidance on various half-finished projects. In the same vein, I would like to thank Dr. Susan Lunte and Dr. Heather Desaire for reading manuscripts and providing guidance in hard times. They have been incredibly supportive over the years and I am grateful.

I would also like to thank Dr. Mark Vitha, my undergraduate advisor and analytical professor, for providing me with the tools to think, write, edit, and present effectively. I'd also like to thank Dr. Todd Williams and Bob Drake, who helped me fix multiple old mass spectrometers and pumps.

During the past five years, I developed a great and lifelong friendship with Nhan To. I feel we have exchanged our best traits to become better overall chemists. We have shared many awesome memories throughout graduate school, including hitting Mass street when KU made the final four and travelling to Columbia, South America for a CE conference. I also want to acknowledge Daniel Kim, who, while he was part of the Dunn lab, was an honorary member of our lab. I enjoyed our white-board sessions, coffee sessions, and random conversations about whatever was on our minds on a given day.

Lastly, I would like to thank past members of the C. Lunte group (Carl, Sara, Alex, Michael, Yunan, Hasitha, Kavisha, Rob, Nurullah, Senem, and many more) for all of their support.

Table of Contents

Chapter 1: Introduction

1.1 Introduction…….....1

1.2 Fundamentals of Capillary Electrophoresis……...1

1.2.1 Advantages and Disadvantages……2

1.2.2 Detection Platforms……..4

1.3 Coupling CE to MS Detection……..6

1.3.1 Electrospray Ionization……6

1.3.2 MS Detectors for CE-MS……8

1.3.3 CE-MS Interface Considerations……9

1.3.4 Interface Types……..……14

1.3.4.1 Sheath Flow Interface……....14

1.3.4.2 Liquid Junction Interface……16

1.3.4.3 Sheathless Interface……..18

1.4 Dissertation Synopsis……19

1.5 References……..……21

Chapter 2: A Capillary Electrophoresis Electrospray Ionization-Mass Spectrometry Method using a Borate Background Electrolyte for Fingerprinting Analysis of Flavonoids in Ginkgo Biloba Herbal Supplements

2.1 Introduction……..……24

2.2 Experimental…….…...26

2.2.1 Reagents……..26

2.2.2 Instrumentation……..……26

2.2.3 Capillary Preparation and Infusion Experiments……...28

2.2.4 Preparation of *Ginkgo biloba* Herbal Supplement……28

2.3 Results and Discussion……..29

2.3.1 Optimization of Capillary Electrophoresis Conditions……...29

2.3.2 Flavonoid Characterization by CE-MS/MS……33

2.3.3 Flavonoid Fingerprint Analysis of *Ginkgo biloba* Ethanolic Extracts……..…39

2.4 Conclusions……..……41

2.5 References……..…..42

Chapter 3: The Development of a Sheathless Interface for Capillary Electrophoresis Ionization Mass Spectrometry using a Cellulose Acetate Cast Capillary

3.1 Introduction……...46

3.2 Tip Shaping……..….46

3.3 Sheathless CE-ESI-MS……..48

3.3.1 Two-piece Interfaces……..48

3.3.2 One-piece Interfaces……..49

3.4 Experimental……...……52

3.4.1 Reagents……..52

3.4.2 Instrumentation and Apparatus……...…52

3.4.2.1 CE-UV……..…52

3.4.2.2 CE-ESI-MS Interface Fabrication…….....53

3.5 Results and Discussion……..54

3.5.1 Interface Design……...…54

3.5.2 Interface Fabrication……..55

3.5.3 Perspectives and Operational Aspects……..……57

3.5.4 Comparison of CE-ESI-MS Interface to Commercial CE-UV System……59

3.5.5 Post-Junction pH Modification……..…….60

3.6 Conclusions……..63

3.7 References……..……64

Chapter 4: CE-ESI-MS Method Development for Lipid Peroxidation Biomarkers of Oxidative Stress

4.1 Introduction……...…67

4.1.1 Oxidative Stress……..67

4.1.2 Lipid Peroxidation……...68

4.1.3 Biomarkers of Enzymatic Lipid Peroxidation……..69

4.2 Microdialysis Sampling……..…….73

4.3 Experimental……...….75

4.3.1 Reagents……..75

4.3.2 Instrumentation……..……75

4.3.3 Sample Preparation……76

4.3.4 Microdialysis……77

4.4 Method Development……..78

4.4.1 CE-UV and CE-MS of Native Eicosanoids……...…….…….78

4.4.1.1 CE-UV Studies……78

4.4.1.2 CE-MS Studies……83

4.4.2 CE-MS of Derivatized Eicosanoid Standards……85

4.4.3 Application of CE-ESI-MS Method for Eicosanoids in Microdialysis Samples….97

4.5 Conclusions……..……..……99

4.6 References……..……99

Chapter 5: Conclusions and Future Directions

5.1 Introduction……..103

5.2 Future Directions……...…105

5.3 References…….……107

Chapter 1

Introduction

1.1 Introduction

Online coupling of gas chromatography (GC), liquid chromatography (LC), and capillary electrophoresis (CE) to mass spectrometry (MS) is analytically advantageous because it provides a second dimension of separative analysis with molecular weight and structural information. GC-MS and LC-MS are routinely used in industrial, academic, and governmental laboratories. However, CE-MS has not been as widely applied despite its many advantages and applications. Coupling the high resolution capabilities of CE with analytical strength of MS creates a powerful tool for the analysis of complex mixtures of ionic species.

1.2 Fundamentals of Capillary Electrophoresis

Capillary electrophoresis (CE) is an analytical technique that separates ions in a fused silica capillary based on their electrophoretic mobility within an electric field (Figure 1.1A). Electrophoretic mobility ($\boldsymbol{\mu_{ep}}$) is defined as

$$\boldsymbol{\mu_{ep}} = \frac{\boldsymbol{q}}{\boldsymbol{6\pi\eta r}}$$

where $\boldsymbol{q}$ is ion charge, $\boldsymbol{r}$ is hydrated radius, and $\boldsymbol{\eta}$ is the viscosity of the separation medium (background electrolyte (BGE)). The electrophoretic velocity of the ion ($\boldsymbol{v}$) is directly proportional to the electric field ($\boldsymbol{E}$) as governed by the following equation

$$\boldsymbol{v} = \boldsymbol{\mu_{ep}E} = \frac{\boldsymbol{\mu_{ep}V}}{\boldsymbol{L}}$$

where $\boldsymbol{V}$ is the potential applied across the capillary and $\boldsymbol{L}$ is the length of the

capillary[1].

Electroosmotic flow (EOF) occurs when a potential is applied to the BGE-filled capillary. BGE cations electrostatically interact with the anionic silanol walls of the capillary, resulting in formation of an electrical double layer (Figure 1.1B). Solvated cations from the diffuse layer migrate toward the cathode. The result is a uniform plug-shaped bulk flow that is usually faster than an analyte's electrophoretic velocity[2]. Thusly, the EOF is capable of carrying anions, cations, and neutral molecules to the cathode for detection. The mobility of the EOF is governed by the following equation

$$\mu_{EOF} = \frac{\in}{4\pi\eta} E\zeta$$

where $\in$ is the dielectric constant of the BGE and ζ is the zeta potential at the wall[3]. EOF strength is an important parameter to optimize during method development. For compounds with drastically different electrophoretic mobilities, for example, a fast EOF is desirable to minimize analysis time. In contrast, compounds with similar mobilities require slower EOF to resolve. The common ways to modify the EOF velocity are through buffer identity, ionic strength, pH, and electric field strength.

1.2.1 Advantages and Disadvantages

CE has several advantages and applications. Due to the low overall volume of the CE capillary, it is particularly useful when precious sample is limited (<100 nL). An example application where this is useful is *in vivo* microdialysis sampling[4-6]. When microdialysis samples are analyzed by a separation system, the temporal resolution is determined by the sample volume

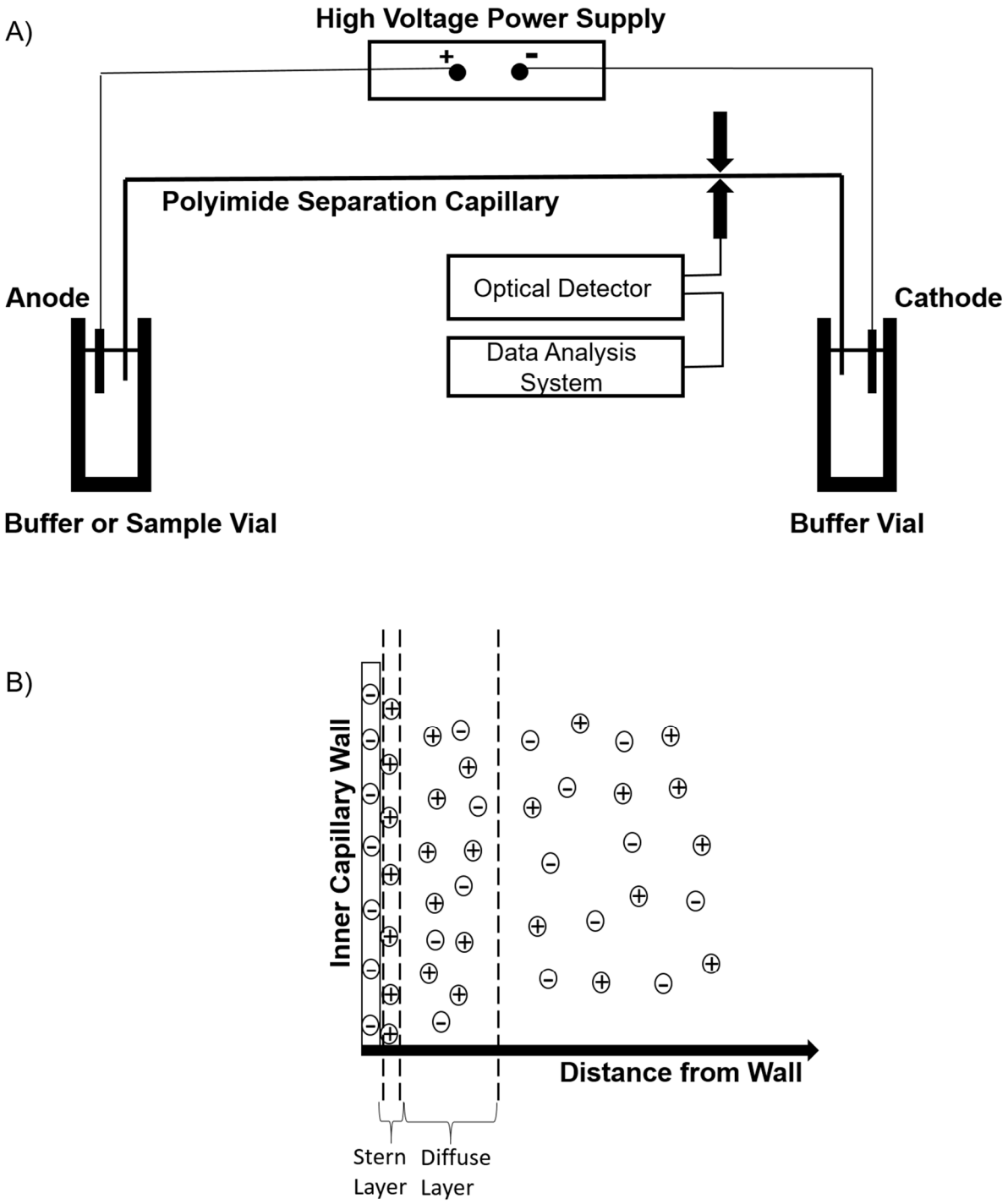

Figure 1.1: A) schematic of a typical normal mode CE system, B) electrical double layer formation at the wall of a CE capillary

requirements and detection limits of the instrument[7]. The low injection volumes of CE permit sub-second temporal resolution and reproducibility studies from a single microdialysis sample. Another advantage of CE is that it is capable of separating cations, anions, and neutrals in a single analytical run, which is particularly useful in fields like metabolomics[8,9] and proteomics[10,11]. Lastly, the mechanism of separation for CE is orthogonal to liquid chromatography (LC), as it separates molecules based on charge and hydrated size rather than hydrophobicity. CE is capable of higher peak efficiencies than LC and is more proficient at separating polar charged compounds.

CE does possess disadvantages compared to other separation techniques. CE is not widely applied in industrial labs due to migration time irreproducibility caused by run-to-run fluctuations in EOF. Between runs, thorough hydroxide and BGE rinses can minimize these fluctuations[12]. Another drawback of CE is that it is not well-equipped to separate neutral, enantiomeric, or hydrophobic compounds without the aid of cyclodextrins[13], micelles[14], or organic solvent additives in the BGE. In these cases, it is likely easier to use an alternative separation platform if the application is not sample limited.

1.2.2 Detection Platforms

In a typical CE experiment, both ends of the capillary are submerged in BGE along with the anodic (inlet) and cathodic (outlet) electrodes. The EOF carries analytes to the cathodic end of the capillary, where detection occurs. Analytes can be detected in-capillary or off-capillary depending on the method of detection.

UV/Vis is the most commonly employed detection platform for CE. It is inexpensive, capable of detecting a wide range of analytes, and easy to implement. However, the path-length in CE-UV/Vis is defined by the narrow inner diameter (I.D.) of the capillary, which is usually 25-100 μm. Because absorbance is proportional to path length, the technique is limited to the analyses of concentrated samples or to compounds that possess high molar absorptivity.

CE coupled to fluorescence detection is capable of sub-nM limits of detection (LOD) for fluorescent analytes when a laser excitation source is used. An obvious disadvantage of this system is that the analyte must be natively fluorescent or reacted with a fluorophore for detection to occur. Additionally, the laser's wavelength must be close to the fluorophore's wavelength of maximum absorption (λ_{max}) to achieve the lowest possible LODs. This requirement is cumbersome if a variety of lasers or derivatization agents are not readily available.

CE-electrochemical (EC) systems are inexpensive and detection can be conducted in-capillary and off-capillary. CE-EC usually refers to amperometric detection, in which current is measured from the oxidation or reduction of an electroactive species by an applied potential. The advantages of CE-amperometric detection are its high selectivity and sensitivity. The disadvantages are that the analyte must be electroactive, the fabrication of the working electrode can be difficult, and the difficulty in decoupling the CE current from the working electrode.

CE-MS systems, typically interfaced through electrospray ionization

sources, provide a breadth of information about complex and small volume samples. However, advances in CE-ESI-MS technology have been slower than LC-ESI-MS in terms of robustness and automation. This is because there are several technical details that require careful optimization to make the interface routine and transferrable to all electrospray sources. Recent CE-ESI-MS research focuses on making the fabrication and use of the interface easier so that routine analyses are possible.

1.3 Coupling CE to MS Detection

CE can be coupled to MS by atmospheric pressure chemical ionization (APCI)[15,16], fast atom bombardment (FAB)[17], or electrospray ionization (ESI). ESI is the most common ionization technique for CE. It is a soft ionization technique, which means a low occurrence of source fragmentation and relatively clean spectra. Additionally, ESI is relatively easy to implement at the CE outlet compared to APCI and FAB. In CE, the analytes are pre-ionized in the separation buffer, making it so that the only job of ESI is to volatilize the CE effluent.

1.3.1 Electrospray Ionization

ESI was first described by Yamashita and Fenn in 1984[18] and has since become the most popular ionization method for MS. In ESI, solution flows through a conductive needle with a positive or negative voltage applied across it for cation or anion ion analysis, respectively. A positively charged ESI needle adds protons to the solution passing through it, while a negatively charged needle causes the solution to be devoid of protons.

The mechanism of ionization for ESI takes place in several steps, so only positive ionization is considered in this section. The first step in ESI is the formation of charged droplets. When the electric field is applied, it penetrates the electrolytic solution at the spray tip causing charge polarization at the meniscus of the liquid. Cations migrate toward the surface of the meniscus and anions migrate away. The balance between the repulsive forces from the ion polarization and the surface tension of the liquid results in the formation of a "Taylor cone." In the presence of an electric field, a fine jet emerges from the Taylor cone whose surface is made up of an excess of cations. Positively charged droplets from the jet form when the repulsion of the surface cations overcomes the surface tension of solution[19].

The second step in the ESI mechanism is the shrinkage and Columbic explosion of the droplets. As in the Taylor cone, cations in the newly formed droplets migrate toward the surface. As the droplet migrates toward the MS counter electrode, the solvent begins to evaporate. This evaporation is often aided by the addition of drying gas and heat. The droplet decreases in size causing the repulsion between surface cations to grow. When the Coulombic repulsive forces overcome the surface tension of the droplet [20], it becomes unstable and fissions into progeny droplets. This point is known as the Rayleigh stability limit and is defined as

$$\boldsymbol{q = 8\pi(\varepsilon_o \gamma R^3)^{1/2}}$$

where q is charge of the droplet, ε_o is the vacuum permittivity, γ is the surface tension of the liquid, and R is the radius of the droplet[19].

The final step in the ESI mechanism is the formation of a gas phase ion from the charged droplets. There is contention as to exactly how gas phase ions are formed, but two models are presented[21]. In the 'charge residue' model, the concluding droplet contains only one ion. The ion is released when the solvent evaporates. In the 'ion evaporation' model, the droplet continues to evaporate until the field strength at the surface is large enough to cause ion expulsion. Currently, these models are only described by computer simulations and little experimental evidence has been produced that confirms either model.

1.3.2 MS Detectors for CE-MS

CE has been coupled to magnetic sector[22], quadrupole[23], fourier transform ion cyclotron resonance[24], time-of-flight (TOF)[25], and ion trap[26] mass spectrometers. The most important parameter to consider when coupling a mass spectrometer to CE is the mass analyzer's scan rate. Ideally, the time required to scan a particular mass range is fast relative to the width of the analytical peak. In CE, the peaks tend to be quite narrow (< 10 s), so slow scanning instruments like magnetic sector mass spectrometers are not suitable for many applications. Quadrupole instruments are the most prevalent MS detector and are therefore often employed for CE-MS. Quadrupole and ion-trap instruments have less qualitative ability due to their relatively low mass accuracy and narrow mass range characteristics. TOF detectors are the most suitable for online CE coupling[25] due to ~1 millisecond scan speeds and the ability to detect almost unlimited mass range.

1.3.3 CE-MS Interface Considerations

The first combination of CE and MS by ESI was introduced by Olivares and coworkers in 1987[27]. In their design, the capillary outlet was covered in a metal sheath to replace the terminal electrode used in traditional CE systems. However, the publications that followed highlighted flaws in the design, such as the requirement of high EOF to achieve robust electrospray or the need to use a limited selection of volatile BGEs[28]. The addition of a high flow rate sheath solution at the CE outlet minimized these drawbacks at the cost of sensitivity. Early commercial CE-MS platforms utilized sheath flow designs in favor of robustness over sensitivity, but were only used if the application's limiting factor was not concentration. More recently, "sheathless" interfaces, which are simply improvements upon Olivares's original model, have been created and are capable of sub-nanomolar detection limits. These designs still suffer from a lack of robustness and difficult fabrication, but commercial sources are now manufacturing them.

Capillary electrophoresis has become a popular alternative to liquid chromatography in the proteomic and metabolomic fields. Thusly, the importance of being able to reliably interface CE with MS is growing. Unfortunately, there are several complications associated with this coupling. One complication is that the EOF rate in a CE capillary is nL/min, while commercial sources operate at μL/min. This aspect limits the feasibility of simply threading the CE capillary into a standard ESI manifold. Modified commercial nanospray manifolds have been used for online CE-ESI-MS[29]. Nanospray

sources possess small diameter spray needles and on-axis positioning relative to the MS orifice ideal for low flow ESI. Additionally, the outer diameter (O.D.) of the CE outlet must be reduced to accommodate the low flow rate of the CE effluent. This can be done by using lower O.D. capillaries compared to traditional 360 μm O.D. capillaries or by tip sharpening. When small tip O.D.s in combination with low flow rates are used, smaller droplets are ejected from the Taylor cone. Smaller droplets require less solvent evaporation and are therefore more efficiently transferred to the mass spectrometer. Additionally, nanoflow systems have higher tolerance for salt content than traditional sources[30]. If the tip O.D. is not decreased, high ESI voltages (>5 kV) that are not conducive for robust ESI are required for spray formation and sensitivity is diminished.

The most important design consideration for CE-ESI-MS interfaces is the electrical connections. The CE circuit (anode to cathode) must be maintained simultaneous to the ESI circuit (ESI needle to MS orifice)[31]. To achieve this, the terminal electrode at or near the CE outlet must serve a dual purpose: complete the CE circuit while providing the voltage necessary for electrospray. Several methods to introduce a 'shared' CE/ESI electrode to the effluent have been created and will be discussed in later sections.

The arrangement of the voltage supplies is critical to achieve successful CE-ESI-MS and depends on the type of ESI source and mass spectrometer being used. The least complicated arrangement is one where the ion source of the mass spectrometer is the high voltage end of the electrospray circuit[32]. In this scenario, the CE circuit operates normally with the inlet at high voltage and

the outlet at ground. More commonly, however, the ESI needle is the high voltage end of the ESI circuit. In this scenario, the CE inlet and the CE outlet/ESI needle are at high voltage, while the mass spectrometer is at ground. Only a small percentage of the current from the CE circuit is necessary for spray formation, so the excess current is left to sink into the ESI voltage supply (Figure 1.2A). This destabilizes the voltage output and in turn the electrospray. Voltage dividers are often implemented to protect the voltage source by increasing the resistance of the circuit. A schematic of a CE-ESI-MS system with a voltage divider is shown in Figure 1.2B. This forces the electrospray voltage source to supply current instead of sinking it[33].

The polarity of the inlet and outlet power supplies is an important factor for CE-ESI-MS analysis. The polarity of the CE inlet power supply dictates the direction of the EOF and is typically between 10 kV and 30 kV in magnitude. The polarity of the CE outlet supply dictates whether cations or anions are being sent to the MS and is typically between 1 kV and 5 kV in magnitude. For 'normal mode' CE analysis, where the EOF flows toward the cathodic end of the capillary, the inlet power supply must be operated in positive mode. If the inlet power supply is operated in negative mode, the EOF will go the wrong direction due to the large magnitude of the negative voltage. For 'reverse polarity mode' CE, where EOF is toward the anodic end of the capillary due to cationic wall coating, the inlet supply must be operated in negative mode. Figure 1.3 depicts these relationships.

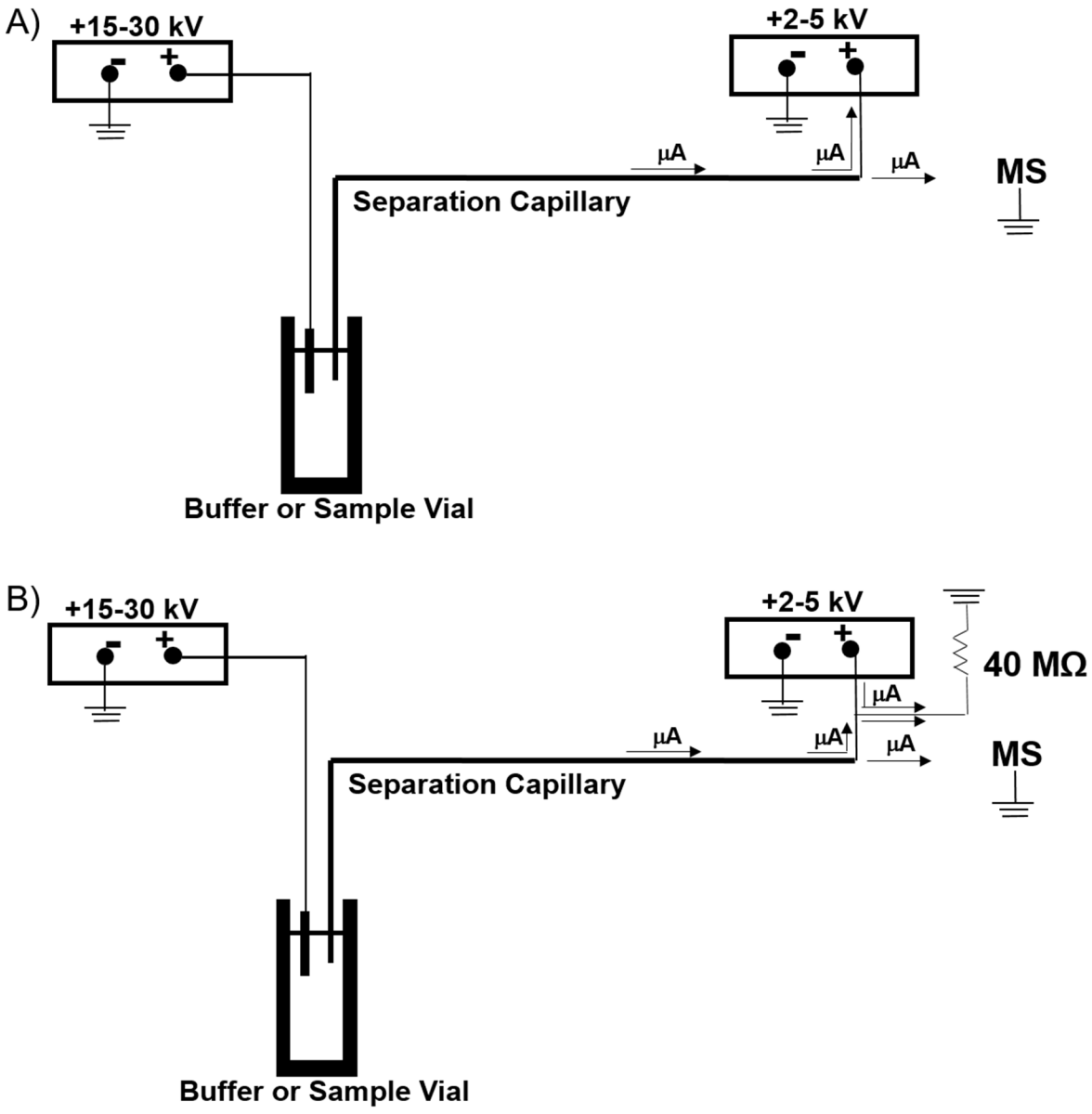

Figure 1.2: A) CE-ESI-MS system without a voltage divider. Current (μA) flows into terminal voltage supply. B) CE-ESI-MS system with a voltage divider. Terminal voltage supply forced to deliver current instead of sinking it.

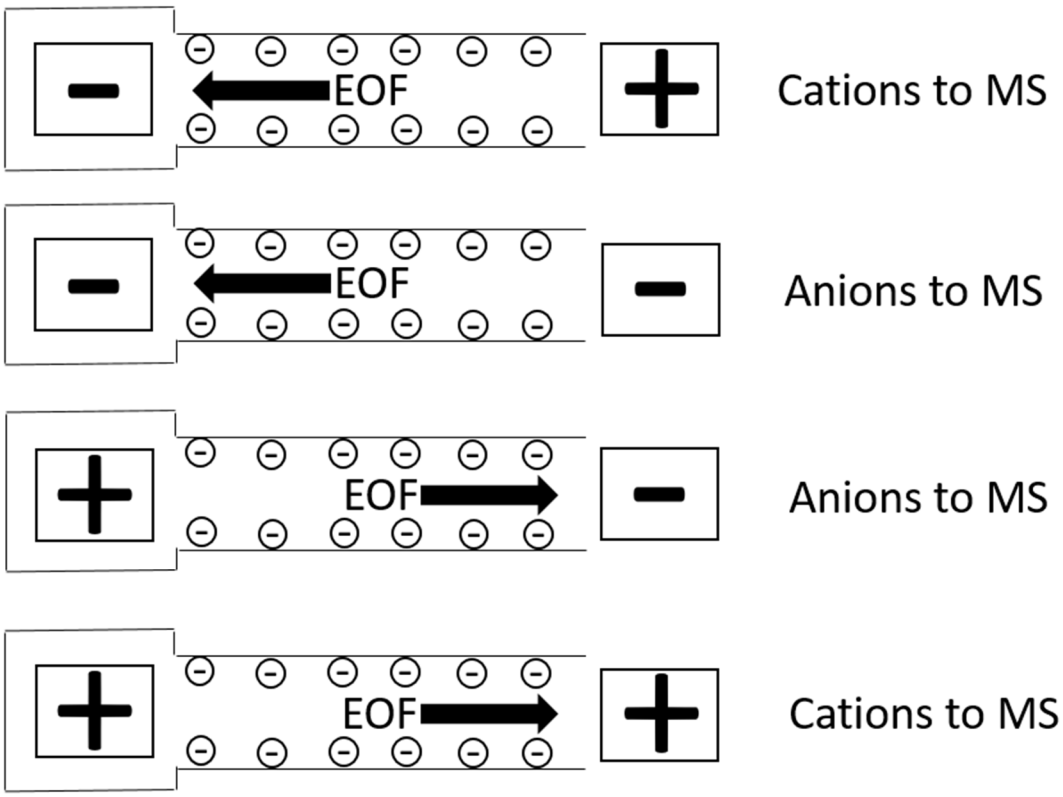

Figure 1.3: EOF direction when different inlet and outlet voltages are applied. When the EOF is toward the inlet, positive wall coating or applied pressure is required to detect ions.

Another consideration when conducting CE-ESI-MS is the BGE conditions. The BGE must be volatile for ESI to occur directly from the capillary outlet. Ammonium acetate and ammonium formate are the most frequently used BGEs for CE-MS. Common BGE additives like borate, cyclodextrin, and surfactant molecules are used in low concentrations to minimize arcing and chemical buildup of non-volatiles on the MS orifice. High BGE concentrations also hinder electrospray performance. Lastly, the pH of the BGE directly effects spray stability. Higher pH BGEs provide faster EOFs and stable spray. This is especially true for the analysis of anionic compounds in normal mode CE. Reports for anion analysis describe a 'conductivity gap' when the EOF reaches the spray tip[34], resulting in a current drop that can be overcame at pH >8.

1.3.4 Interface Types

1.3.4.1 Sheath Flow Interface

The first CE-ESI-MS interface introduced by Olivares et al. was a sheathless interface that suffered from several practical issues[27]. The sheath flow interface was quickly innovated to overcome these issues[35].

In the sheath flow interface design, the CE capillary is inserted within a hollow metal ESI needle. The capillary outlet is usually flush or slightly protruding from the ESI needle. A sheath solution is introduced through a T-junction, then enters the ESI needle and mixes with the CE effluent. An electrospray voltage is applied to either the T-junction or the ESI needle. A schematic of a sheath flow interface is shown in Figure 1.4A. The sheath solution contains a low concentration of electrolyte to complete the CE circuit.

An ideal sheath solution is miscible with the CE BGE and increases the volatility of the spray. The sheath solution may contain chemical modifiers that improve ionization, such as ammonium acetate, ammonium formate, or ammonia. The flow rate of the sheath solution directly impacts the sensitivity of the detection. An ideal sheath flow rate is low enough to limit dilution of the CE effluent while still providing stable spray. Common sheath flow rates are in the μL/min range delivered by syringe perfusion, but recent advancements in sheath flow interface technology have reduced operational flow rates to nL/min. This is done by electrokinetically driving the sheath solution to the ESI tip and by decreasing the diameter of the CE capillary to 10 μm and the ESI needle to 2-40 μm. At these flow rates, low nM detection limits were achievable for a standard peptide[36].

Sheath flow interfaces are generally more rugged and easy to construct relative to other interface types. First, the capillary tip does not need to be tapered because the sheath flow compensates for the low flow from the CE. This simplifies fabrication and decreases the likelihood of clogging. Second, difficult structural modifications to the body of the capillary are not necessary to introduce the terminal voltage. Third, some sheathless designs suffer from short lifetimes (1-2 days) due to an easily oxidized thin metal coating layer at the outlet. Conversely, the CE capillary used in sheath liquid designs demonstrates long lifetimes. Fourth, the sheath flow allows more freedom in terms of CE BGE and additives that are beneficial to the separation but not as compatible with MS detection. Lastly, the sheath solution can be used to modify the CE effluent to achieve better ionization than spraying directly from the CE BGE. This would be

ideal if, for example, an analyte could only be separated by CE as an anion but provided better detection as a cation. Organic acids are an example of an analyte that would require this treatment.

There are drawbacks to sheath flow CE-ESI-MS interfaces, such as the inherent dilution of the sample by the sheath solution. As researchers try to achieve lower LODs, the use of sheathless designs is becoming more desirable. Typical LODs for sheath flow systems are mid-high nM while those of sheathless designs are sub-low nM. The sheath flow can also cause irreproducibility in migration times. It has been reported that hydroxide ions produced at the ESI tip due to electrochemical processes can migrate into the CE outlet[37]. The result is a conductivity barrier at the CE outlet that will cause run-to-run deviation in migration times. Additionally, the hydroxide ions can alter the EOF velocity at the outlet, leading to more irreproducibility.

1.3.4.2 Liquid Junction Interface

The liquid junction interface was developed by Lee et al. in 1989[38]. In this interface, the CE capillary and ESI emitter are situated 25-50 μm apart within a sheath solution reservoir where the terminal voltage is applied. A schematic of this interface is shown in Figure 1.4B. The positive aspects of this interface are the lower dilution factor compared to sheath flow interfaces and longer lifetimes relative to sheathless interfaces of the time. The sheath solution can also be used to improve the MS compatibility of the CE effluent. However, the liquid junction interface is the least utilized design due to the dead volumes and peak broadening caused by the gap between the capillary and emitter.

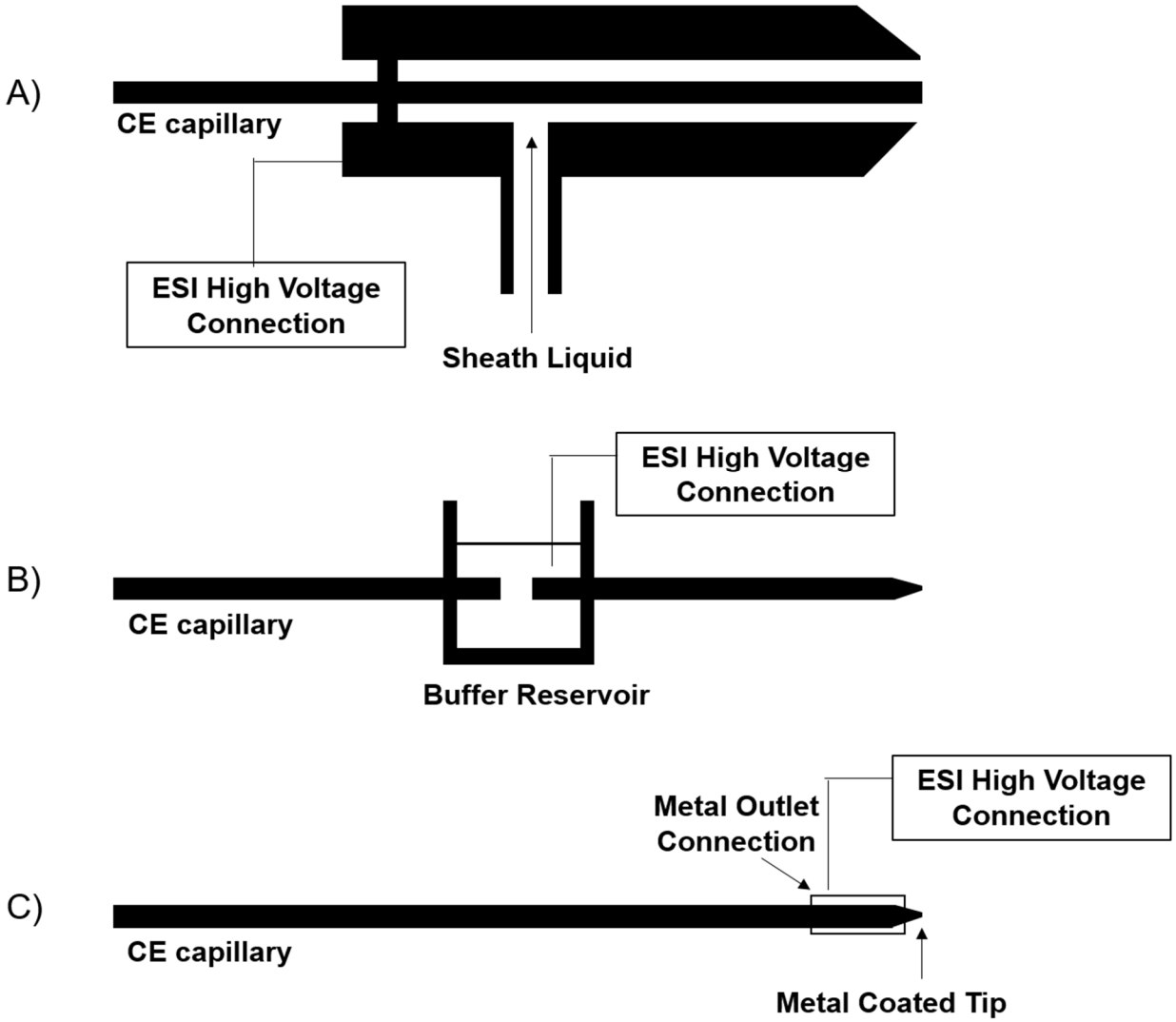

Figure 1.4: A) Sheath Flow Interface, B) Liquid-Junction Interface, C) Metalized CE Tip Sheathless Interface

Additionally, the alignment of the capillary and emitter can be tedious and difficult to reproduce. Self-aligning liquid junctions have been created to overcome this problem[39]. More recently, a pressurized liquid junction interface was developed to help minimize band-broadening and improve ESI stability[40].

1.3.4.3 Sheathless Interface

To achieve lower detection limits than interfaces that utilize a sheath solution, substantial research has been dedicated to improving upon the original sheathless design (Figure 1.4C). In that design, which suffered from short capillary lifetimes and unstable spray, the capillary was coated in either copper, silver, or gold[27]. The tip was encased and in contact with a metalized tube where the ESI voltage was applied. The metal coating on the capillary was subject to oxidation and was often stripped within a few days. The next sheathless design utilized the insertion of an electrode into the capillary outlet for the application of an ESI voltage. This design improved the lifetime of the interface but perturbed the EOF and destabilized the electrospray[41].

Eventually, it became standard in sheathless interfaces to decrease the capillary outlet tip diameter to achieve robust ESI from the EOF alone. Common methods used to fabricate tapered emitters are heat-assisted tip-pulling, etching with HF acid, or mechanical sharpening. Further modification at or near the capillary outlet has been used for the application of terminal voltage. For example, insertion of an electrode into a drilled hole in the capillary wall has been used for ESI voltage application. Similarly, a small crack made in the capillary wall and submerged in BGE containing the terminal electrode has been

developed for CE-ESI [42]. Detailed aspects of tip and capillary modifications for CE-ESI-MS will be discussed in Chapter 3. In general, many of the sheathless designs require complicated and often irreproducible fabrication procedures. Further, the resultant capillary is typically quite fragile and incapable of robust EOF and ESI. However, the improved sensitivity of sheathless relative to sheath flow interfaces has driven researchers to develop interfaces that can minimize these drawbacks. This push has led to the first commercialization of a sheathless interface by Ab SCIEX.

1.4 Dissertation Synopsis

The goal of this dissertation is to demonstrate the utility of CE-ESI-MS for bioanalytical challenges while also taking steps toward advancing interface use and technology. In Chapter 2, a simple sheath flow CE-ESI-MS interface developed in our laboratory will be described. The interface utilizes narrow O.D. CE capillary to permit low sheath flow rates for efficient ESI. The interface will be used to investigate prominent natural flavonoids found in herbal supplements. Unlike other CE-ESI-MS methods for flavonoids, our method utilizes a borate BGE, greatly increasing the selectivity of the separation compared to ammonium acetate and formate BGEs. CE-ESI-MS method development and optimization will be discussed in terms of separation parameters, sheath flow composition, and various technical parameters of the interface. Finally, the method will be demonstrated using *Ginkgo biloba* as a flavonoid test mixture.

In Chapter 3, a novel sheathless interface for CE-ESI-MS will be presented. The interface is an elaboration of a design developed by Damon

Osbourn in our laboratory for on-column CE-EC detection. The design combines the benefits of sheathless CE-ESI-MS, such as good sensitivity and low LODs, with the solution modification capabilities of sheath liquid interfaces. To validate the design, a comparison of the separation of four peptide standards will be made between a commercial CE-UV system and the novel interface. The migration time reproducibilities and LODs using the interface will also be presented. Lastly, we demonstrate pH modification of the CE BGE post-separation at the interface's outlet reservoir to improve sensitivity for the peptide Val-Tyr-Val.

In Chapter 4, we apply the novel interface presented in Chapter 3 to develop a method for eicosanoids found in microdialysis samples. Eicosanoids are important biomarkers for determining the extent of lipid peroxidation that has occurred during an oxidative stress event. Monitoring these biomarkers can also be useful when determining the efficacy of drugs that aim to increase or decrease lipid peroxidation. However, there are many difficulties associated with the analysis of eicosanoids from microdialysis samples such as the low volume-high salt content nature of the sample, the separation of like-structured analytes, and the low ionization efficiency of eicosanoids. The strategies implemented to overcome these analytical challenges will be described in detail.

Chapter 5 will present conclusions and future directions of the research shown in this dissertation. The overall utility of CE-ESI-MS to the scientific community will be discussed. A short review of recent innovations to CE-ESI-MS will be presented with particular attention paid to microchip platforms.

1.5 References

[1] Jorgenson, J. W.; Lukacs, K. D. *Anal. Chem.*, **1981,** *53* (8), 1298-1302.

[2] Harris, D. C. Quantitative Chemical Analysis. 5th ed.; W.H. Freeman: New York, 1999.

[3] Ewing, A. G.; Wallingford, R. A.; Olefirowicz, T. M. *Anal. Chem.*, **1989**, *61* (4), 292-303.

[4] Huynh, B. H.; Fogarty, B. A.; Martin, R. S.; Lunte, S. M. *Anal. Chem.*, **2004**, *76* (21), 6440-6447.

[5] Bowser, M. T.; Kennedy, R. T. *Electrophoresis*, **2001**, *22* (17), 3668-3676.

[6] Hogan, B. L.; Lunte, S. M.; Stobaugh, J. F.; Lunte, C. E. *Anal. Chem.*, **1994**, 66 (5), 596-602.

[7] Hogerton, A. L.; Bowser, M. T. *Anal. Chem.*, **2013**, *85* (19), 9070-9077.

[8] Soga, T.; Ohashi, Y.; Ueno, Y.; Naraoka, H.; Tomita, M.; Nishioka, T. *J. Proteome Res.*, **2003**, *2* (5), 488-494.

[9] Barbas, C.; Vellejo, M.; Garcia, A.; Barlow, D.; Hanna-Brown, M. *J. Pharma. Biomed. Anal.*, **2008**, *47* (2), 388-398.

[10] Schiffer, E.; Mischak, H.; Novak, J. *Proteomics*, **2006**, *6* (20), 5615-5627.

[11] Fonslow, B. R.; Yates III, J. R. *J. Sep. Sci.*, **2009**, *32* (8), 1175-1188.

[12] Schaeper, J. P.; Sepaniak, M. J. *Electrophoresis*, **2000**, *21* (7), 1421-1429.

[13] Fanali, S. *J. Chroma. A.*, **2000**, *875* (1), 89-122.

[14] Kaul, S.; Faiman, M. D.; Lunte, C. E. *Anal. Methods*, **2011**, *3*, 1514-1520.

[15] Takada, Y.; Sakairi, M.; Koizumi, H. *Anal. Chem.*, **1995**, *67* (8), 1474-1476.

[16] Takada, Y.; Otsuka, K.; Terabe, S. *J. Pharma. Biomed.*, **2003**, *30* (6), 1889-1895.

[17] Moseley, M. A.; Deterding, L. J.; Tomer, K. B. *J. Chroma. A.*, **1990**, *516* (1), 167-173.

[18] Yamashita, M.; Fenn, J. B. *J. Phys. Chem.*, **1984**, *88* (20), 4451-4459.

[19] Kebarie, P. *J. Mass Spectrom.*, **2000**, *35* (7), 804-817.

[20] Fenn, J. B.; Mann, M.; Meng, C. K.; Wong, S. F.; Whitehouse, C. M. *Science*, **1989**, *246*, 64-71.

[21] Kebarle, P.; Peschke, M. *Anal. Chim. Acta*, **2000**, *406*, 11-35.

[22] Perkins, J. R., Tomer, K. B., *Anal Chem.*, **1994**, *66* (18), 2835-2840.

[23] Loo, J. A.; Udseth, H. R.; Smith, R. D. *Anal. Biochem.*, **1989**, *179* (2), 404-412.

[24] Hofstadler, S. A.; Wahl, J. H.; Bakhtiar, R.; Anderson, G. A.; Bruce, J. E.; Smith, R. D. *J Amer. Soc. Mass Spectrom.*, **1994**, *5* (10), 894-899.

[25] Banks Jr., J. F.; Dresch, T. *Anal. Chem.*, **1996**, *68* (9), 1480-1485.

[26] Henion, J. D.; Mordehal, A. V.; Cal, J. *Anal Chem.*, **1994**, *66* (13), 2103-2109.

[27] Olivares, J. A.; Nguyen, N. T.; Yonker, C. R; Smith, R. D. *Anal. Chem.*, **1987**, *59* (8), 1230-1232.

[28] Smith, R. D.; Olivares, J. A.; Nguyen, N. T.; Udseth, H. R. *Anal. Chem.,* **1988**, *60* (5), 436-441.

[29] Krisko, R. M.; Schieferecke, M. A.; Williams, T. D.; Lunte, C. E. *Electrophoresis*, **2003**, *24* (14), 2340-2347.

[30] Juraschek, R.; Dulcks, T.; Karas, M. *J. Amer. Soc. Mass. Spectrom.*, **1999**, *10* (4), 300-308.

[31] Kelly, J. F.; Ramaley, L.; Thibault, P. *Anal. Chem.,* **1997**, *69* (1), 51-60.

[32] Ingendoh, A.; Kiehne, A.; Greiner, M. *Chromatographia*, **1999**, *49* (1), 87-92.

[33] Cole, R. B. *Electrospray and MALDI Mass Spectrometry: Fundamentals, Instrumentation, Practicalities and Biological Applications*, 2nd Ed., Wiley, 2010.

[34] Soga, T.; Ueno, Y.; Naraoka, H.; Matsuda, K.; Tomita, M.; Nishioka, T. Anal. Chem., 2002, 74 (24), 6224-6229.

[35] Smith, R. D.; Barinaga, C. J.; Udseth, H. R. *Anal. Chem.* **1988**, *60* (18), 1948-1952.

[36] Sun, L.; Zhu, G.; Zhang, Z.; Mou, S.; Dovichi, N. *J. Proteome Res.*, **2015**, *14*, 2312-2321.

[37] Foret, F.; Thompson, T. J.; Voures, P.; Karger, B. L. *Anal. Chem.*, **1994**, *66* (24), 4450-4458.

[38] Lee, E. D.; Muck, W.; Henion, J. D.; Covey, T. R. *Biol. Mass Spectrom.*, **1989**, *18* (9), 844-850.

[39] Wachs, T.; Sheppard, R. L.; Henion, J. *J. Chroma. B. Biomed. Sci. App.*, **1996**, 685 (2), 335-342.

[40] Kusy, P.; Kleparnik, K.; Aturki, Z.; Fanali, S.; Foret, F. *Electrophoresis*, **2007**, *28* (12), 1964-1969.

[41] Fang, L.; Zhang, R.; Williams, E. R.; Zare, R. N.; *Anal. Chem.*, **1994**, *66* (21), 3696-3701.

[42] Moini, M. *Anal. Chem.* **2001**, *73* (14), 4241-4246.

Chapter 2

A Capillary Electrophoresis Electrospray Ionization-Mass Spectrometry Method using a Borate Background Electrolyte for Fingerprinting Analysis of Flavonoids in Ginkgo Biloba Herbal Supplements

2.1 Introduction

Flavonoids are a class of polyphenolic compounds found in all plants, providing pigmentation and protecting the plants against pathogens and ultraviolet radiation. They are the most consumed polyphenolic compound in the human diet and are attributed with several therapeutic effects, including increased resistance to oxidants[1,2] and decreased occurrence of inflammation[3], cardiovascular disease[4], hypertension and cancer[5,6]. Studies have shown that flavones and flavonols contain the highest antioxidant capacity[5] and that their glycosidic forms retain some antioxidant activity[7,8].

Plant extracts have been used as medicinal treatments in most cultures for thousands of years. The popular *Ginkgo biloba* flavonoid extract EGb761, for example, has been reported to improve cognitive function by increasing dopamine levels in the brain, thereby improving memory[9]. In a population study, Gingko biloba flavonoid supplements were found to decrease the rate of cognitive decline in non-demented patients over 65 years of age when compared to patients not taking the supplement[10]. Additionally, these flavonoid supplements have also been shown to act as an agonist to 5-HT_{1A}, resulting in relief to stress and depression[11].

To identify potentially bioactive flavonoids from plant material, HPLC and GC are traditionally employed[12-15]. Capillary electrophoresis (CE) has potential advantages for flavonoid analysis, including faster analysis times, less consumption of precious sample, and high separation efficiencies for charged compounds. Conventional CE and micellar electrokinetic chromatography (MEKC)[16] have been coupled to UV detection[17-19], electrochemical[20-22], and MS detection[18, 23, 24] for the analysis of flavonoids. Of these detection systems, MS is capable of providing an additional dimension of separation based on mass, as well as pertinent structural information garnered from fragmentation studies. However, as noted by Rijke et al., little work has been conducted using CE-MS for flavonoid analysis[25]. This is because flavonoid separations by CE typically require selective background electrolyte components, such as borate, that can complex phenolic compounds, and micelles, that can act as a pseudo-stationary phase for flavonoids. These components are not volatile and are therefore rarely employed in CE-ESI-MS applications in favor of acetate and formate containing electrolytes[18, 24]. However, at low concentrations, additives can be used without significant spray degradation or instrument contamination due to the low mass loads of the electrophoresis capillary[26-28].

Herein, we describe qualitative CE-ESI-MS method in negative ion mode for the detection of 14 common flavonoids utilizing an ammonium borate buffer as the BGE. The method is capable of separating and detecting five flavonoid glycones and nine aglycones in 13 minutes with separation efficiencies of up to 75,000 theoretical plates. Additionally, the catechol containing flavonoids were

detected as borate adducts in the MS^1 scans, adding an extra dimension of structural diagnostic information. Fragmentation data on these adducts is presented. Finally, the method was applied to the analysis of flavonoids in *Ginkgo biloba* herbal supplements.

2.2 Experimental

2.2.1 Reagents

Apigenin, chrysin, eriodoctyl, galangin, kaempferol, luteolin, naringenin, naringin, pinocembrin, quercetin, quercitrin, rutin, and ammonium biborate were purchased from Sigma (St. Louis, MO, USA). Apiin and apigetrin were purchased from Carl Roth (Karlsruhe, Germany). No further purification of the standards was conducted. Methanol, ethanol, isopropyl alcohol, acetic acid and ammonium hydroxide were purchased from Fisher Scientific (Pittsburg, PA, USA). Ultrapure water was obtained from a Milli-Q water purification system (Millipore, Bedford, MA, USA).

Stock solutions of the flavonoids were prepared by dissolving 1 mg of standard in 1 mL of methanol for aglycones and 70:30 methanol:water for glycones. The solutions were stored in the dark at 4°C. Prior to dilution, the stock solutions were sonicated for 5 min to ensure flavonoid dissolution. The buffer pH was investigated in the range 8.7-10.0 and was adjusted using 0.1 M ammonium hydroxide. The BGE was degassed and replaced daily to avoid current drops due to bubbles in the CE capillary.

2.2.2 Instrumentation

The separation of 14 flavonoid standards was optimized using a P/ACE MDQ Capillary Electrophoresis System equipped with a diode array detector (Beckman Coulter, Palo Alto, CA, USA). A 65 cm x 50 □m i.d. x 360 □m o.d. capillary (Polymicro Technologies, Tucson, AZ, USA) was used with a 55 cm effective length for all CE-UV studies.

A sheath liquid CE-MS interface was fabricated on a Micromass Quattro Ultima triple quadrupole instrument (Waters, Millford, MA, USA) using a modified nanospray flange. The interface was constructed using a model MT1CS6 Valco mixing tee (VICI, Houston, TX, USA). The electrospray needle was made by cutting 30 gauge metal tubing (Component Supply Co., Fort Meade, FL, USA) into a 2 cm segment and sharpening the tip using a metal file in order to allow the use of lower electrospray voltages. The ESI needle was then secured into the front of the mixing tee using a 0.3 mm I.D Valco one piece fused silica adapter. Sheath liquid was supplied to the mixing tee via an infusion pump at 3 μL/min. The laboratory-built CE system was connected to the interface by threading a 65 cm length x 40 μm i.d. (105 μm o.d.) fused silica capillary through the back of the mixing tee using PEEK tubing and subsequently into the electrospray needle. The CE capillary was flush with the electrospray tip during analysis. Two separate Spellman power supplies provided separation and electrospray voltages. The CE power supply was operated in positive mode while the electrospray power supply was operated in negative mode. The mass spectrometer was operated at a cone voltage of -35 V and a cone temperature of

100 °C with 40 psi nitrogen bath gas flooding into the fish bowl flange. No drying gas was used.

2.2.3 Capillary Preparation and Infusion Experiments

CE capillaries were sequentially rinsed with methanol, 0.1 M HCl, nanopure water, 0.1 M ammonium hydroxide, and BGE at 10 psi for 10 min. The capillary was also rinsed at 10 psi for 5 min with 0.1 M ammonium hydroxide and for 10 min with BGE between injections. Samples were injected onto the capillary hydrodynamically using 10 psi for 2 sec, which corresponds to 13.3 nL or 1.63% of the total capillary volume. Prior to daily CE-MS analysis, the sheath liquid line was rinsed with two tubing volumes of methanol and 80:20 IPA:water sheath liquid. The electrospray tip was rinsed with 50:50 water:methanol between runs to prevent the accumulation of salts. Infusion experiments to determine flavonoid fragment ions were conducted using 10 μm standards in BGE and infusing through the CE capillary using electroosmotic flow. The CID energy was increased in 5 eV steps until significant fragmentation of the parent was observed, which typically occurred at ~20 eV.

2.2.4 Preparation of *Gingko biloba* Herbal Supplement

Herbal supplements of 120 mg *Ginkgo biloba* were purchased at a local market. The plant material from the supplement was removed from a capsule and dissolved in 70:30 ethanol:water. The solution was sonicated for 1 hour and subsequently centrifuged (1000 g) for 5 minutes. The supernatant was extracted and diluted 100-fold with BGE. The resultant solution was filtered through a 0.25

μm membrane filter twice and immediately injected into the CE system to minimize oxidation of the flavonoids.

2.3 Results and Discussion

2.3.1 Optimization of Capillary Electrophoresis Conditions

The base structures of flavones, flavonols, and flavonones are shown in Figure 2.1A, and the substitution patterns on the 14 flavonoids analyzed in this study are listed in Table 2.1. For simplicity, a Beckman CE-UV system equipped with an autosampler was used for the optimization of CE separation conditions. A borate based buffer was chosen for the separation because of its ability to form complexes with polyphenolic compounds and increase their effective negative charge and size[29, 30]. Migration in CE is based on the overall charge and hydrated radius of a molecule. Similar molecules possessing different borate complex formation constants can be resolved. However, borate buffer is normally considered incompatible with MS due to its low volatility. In our experiments, significant salt accumulation was not observed and the MS orifice was cleaned regularly to prevent buildup. Ammonium ion was chosen as the BGE cation due to its high volatility.

The optimized separation of the 14 flavonoids is shown in Figure 2.1B. Biborate concentrations above 50 mM caused arcing between the ESI tip and the MS inlet, so only concentrations below this value were investigated. The effect of pH on the separation was investigated in the range of 8.7-10, where the flavonoids carry at least one negative charge. Additionally, the effect of methanol on the separation was investigated due to its ability to potentially increase

Table 2.1. Representative flavonoids and the respective fragments used in this study. Bolded flavonoids contain catechol group.

Compound Name	Monitored Mass	R1	R2	R3	R4	R5	Major Fragments
		Flavones					
1) Chrysin	253	OH	OH	H	H	-	209 (100), 181 (13)
2) Apigenin	269	OH	OH	H	OH	-	225 (100), 201 (25)
3) **Luteolin**	285	OH	OH	**OH**	**OH**	**-**	241 (100)
4) Apigetrin	431	Glu	OH	H	OH	-	269 (100) 311 (20)
5) Apiin	563	Glu-Apio	OH	H	OH	-	269 (100), 431(25)
		Flavonones					
6) Pinocembrin	255	OH	OH	H	H	-	213 (100), 211 (45)
7) Naringenin	271	OH	OH	H	OH	-	151 (100), 177 (23)
8) **Eriodictyol**	313	OH	OH	**OH**	**OH**	**-**	269 (100), 151 (10)
9) Naringin	580	Glu-Rha	OH	H	OH	-	271 (100), 459 (30)
		Flavonols					
10) Galangin	269	OH	OH	OH	H	OH	197 (100), 241 (98)
11) Kaempferol	285	OH	OH	OH	H	OH	257 (100), 213 (65)
12) **Quercetin**	345	OH	OH	OH	**OH**	**OH**	327 (100) 301 (35)
13) **Quercitrin**	491	OH	OH	OH	**OH**	Rha	473(100)
14) **Rutin**	609	OH	OH	**OH**	**OH**	Glu-Rha	301 (100), 591(20)

A)

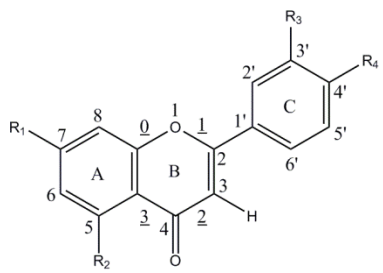

Flavone

1) Chrysin - R_1= OH, R_2= OH, R_3= H, R_4 = H
2) Apigenin - R_1= OH, R_2= OH, R_3= H, R_4 = OH
3) Luteolin - R_1= OH, R_2= OH, R_3= OH, R_4 = OH
4) Apigetrin - R_1= Glu, R_2= OH, R_3= H, R_4 = OH
5) Apiin - R_1= Glu-Apio, R_2= OH, R_3= H, R_4 = OH

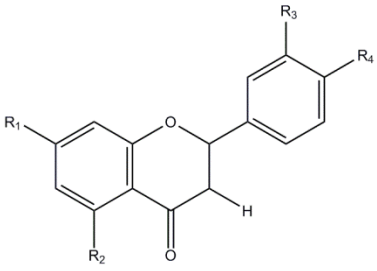

Flavonone

6) Pinocembrin - R_1= OH, R_2= OH, R_3= H, R_4 = H
7) Naringenin - R_1= OH, R_2= OH, R_3= H, R_4 = OH
8) Eriodictyol - R_1= OH, R_2= OH, R_3= OH, R_4 = OH
9) Naringin - R_1= Glu-Rha, R_2= OH, R_3= H, R_4 = OH

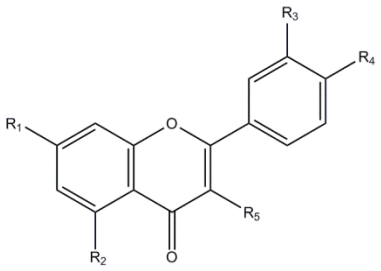

Flavonol

10) Galangin - R_1= OH, R_2= OH, R_3= H, R_4 = H R_5= OH
11) Kaempferol - R_1= OH, R_2= OH, R_3= H, R_4 = OH R_5= OH
12) Quercetin - R_1= OH, R_2= OH, R_3= OH, R_4 = OH R_5= OH
13) Quercitrin - R_1= OH, R_2= OH, R_3= OH, R_4 = OH R_5= Rha
14) Rutin - R_1= OH, R_2= OH, R_3= OH, R_4 = OH R_5= Glu-Rha

B)

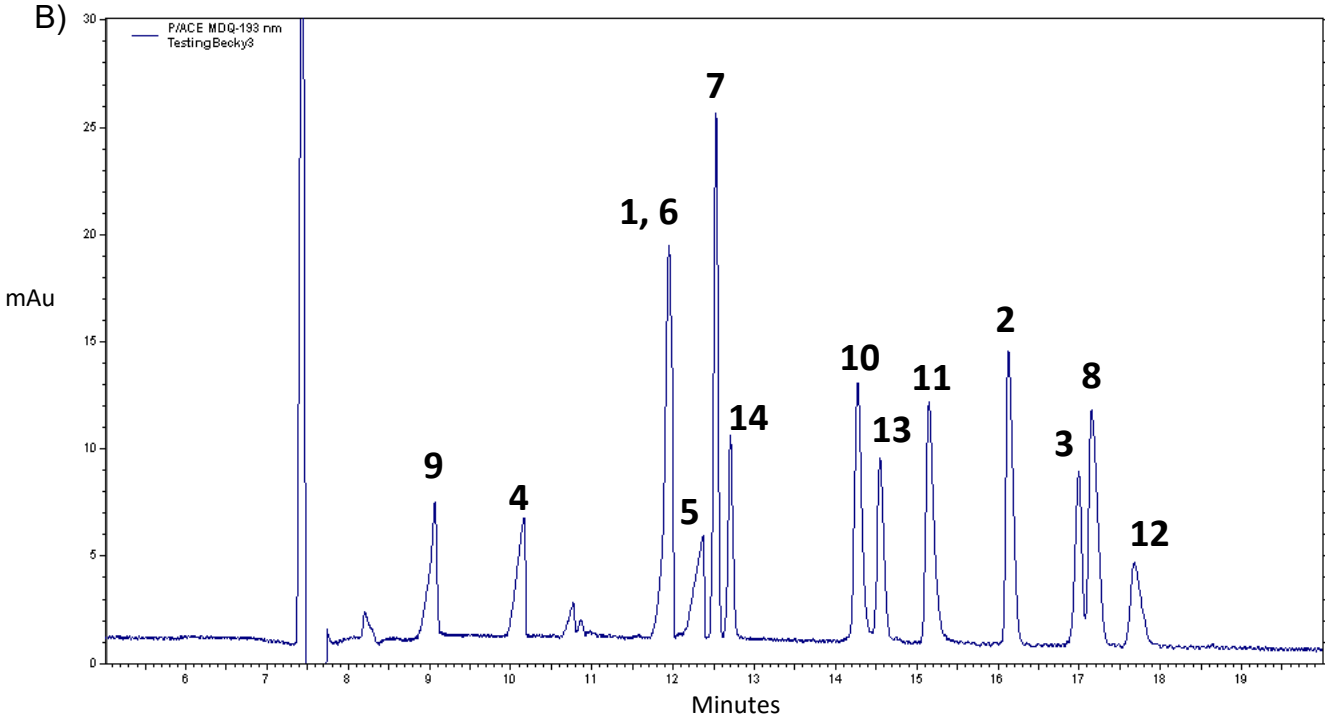

Figure 1: A) Basic structure of the flavonoids analyzed in this study. Underlined numbers represent common bond cleavages upon CID fragmentation, B) CE-UV separation of 14 flavonoid standards. Conditions: separation voltage: 25 kV, 65 cm x 50 μm i.d. x 360 μm o.d. capillary, 65 cm effective length, 25 mM ammonium biborate in 10% methanol, pH = 9.3. 100 μM standards dissolved in BGE.

separation efficiency and ESI spray volatility. Baseline resolution of the compounds was achieved in 18 min using a BGE chemistry of 25 mM ammonium biborate at pH = 9.3 with 10% methanol and a separation voltage of 25 kV. At pH values greater than 9.3, comigration of catechol containing flavonoids was observed, while methanol concentrations greater than 10% resulted in long analysis times (>20 min). Coelution of pinocembrin and chrysin, which differ by two mass units, was observed; however, if these two flavonoids are present in a single sample, they can be identified separately by mass spectrometric detection.

The migration order of flavonoids under the optimal separations conditions can be used to identify the presence of specific structural features of unknown flavonoids. A primary factor that affected the migration properties of the flavonoids was their flavonoid subclass. For example, non-catechol flavonones were detected between 9-12.5 min, while flavonols were detected after 12.5 min. Another factor that determined the migration properties of the flavonoids was the extent of B-ring hydroxylation. A higher number of B-ring hydroxyl groups increased the migration time of the flavonoids. This effect is particularly true of quercetin, eriodictyol, and luteolin, all of which contain catechol functionalities. Catechols are known to form strong complexes with borate, resulting in an increased negative charge and longer migration times in normal mode CZE. This trend was observed for flavonoid glycones as well; however, because the flavonoid glycosides are much larger in size and lower in negative charge, they migrate more quickly toward the detector than even aglycones which contain one B-ring hydroxyl group.

Borate complexation extended the migration times of catechol containing glycosylated flavonoids as well, as can be observed by the flavonoids rutin and quercitrin. Additionally, because rutin and quercitrin are 3-O-glycosides, the 7-position hydroxyl group is deprotonated at pH = 9.3, increasing their negative electrophoretic mobility relative to 7-O-glycosides. The 7-O-glycosides apigetrin and naringen are less negatively charged, resulting in fast migration times within 3 min of the neutral marker. Apiin, a 7-O-diglycoside would be expected to migrate more quickly toward the detector than apigetrin due to its size. However, it is detected 2 min after apigetrin, suggesting borate complexation could be occurring at its additional sugar substituent.

2.3.2 Flavonoid Characterization by CE-MS/MS

Sheath liquid composition was optimized by analyzing the signal stability of background ions present in the sheath solution. Without the assistance of drying gas, organic content of greater than 70% is required for spray formation at -3 kV spray voltage. Methanol based sheath liquids typically produced erratic signal fluctuations in negative mode electrospray. A fairly stable signal was observed by using 80:20 isopropyl alcohol (IPA):water. The utility of IPA sheath liquids has been reported [31, 32], but methanol is still frequently used in CE-MS [33, 34]. The organic additive triethylamine was used to increase the signal of the 7-O-glycosides naringin, apigetrin, and apiin compared to ammonium acetate and acetic acid additives. These flavonoids have a higher pKa_1, and require higher pH sheath liquids than that of the BGE to achieve a more negative charge. Sheath liquid flow rates from 1-10 μL/min were investigated, and 3 μL/min was

chosen because it provided the best signal stability without significantly diluting the analyte. Using these sheath liquid conditions in tandem with the aforementioned optimized CE conditions, nine aglycones and five glycones were separated and detected in 13 min by CE-MS (Figure 2.2). The average number of theoretical plates for the flavonoid separation was 30,000, with as high as 75,000 theoretical plates for the flavonoid naringenin. As reported by Wang et. al., these CE peak efficiencies for flavonoids are significantly higher than those obtained using reverse phase LC[35].

Negative ionization mode was chosen for this study because the flavonoids were present as negative ions in the BGE. The retro-Diels Alder product ion of the A-ring at m/z 151 was observed during MS analysis of most of the flavonoid aglycones, and represents the 1,3 cleavage of the C-ring (Figure 2.1A). The B-ring retro-Diels Alder fragment, which provides diagnostic information regarding B-ring hydroxylation and C-ring saturation, was not detected in these studies. Reports show that B-ring fragments can be detected in positive ion mode[36,37]. However, because the flavonoids were separated as anions by CE, sensitive detection of them in positive ion mode was not successful. The difference between the parent ion mass and the $[1,3\ A]^-$ ion mass can be used to infer the number of hydroxyl groups on the undetected fragment of the flavonoid; however, the location of the hydroxyl groups on the B- or C-ring cannot be determined. Losses of CO and CO_2 were also common for the aglycones. Other ions characteristic of individual aglycones are in agreement with LC-MS/MS

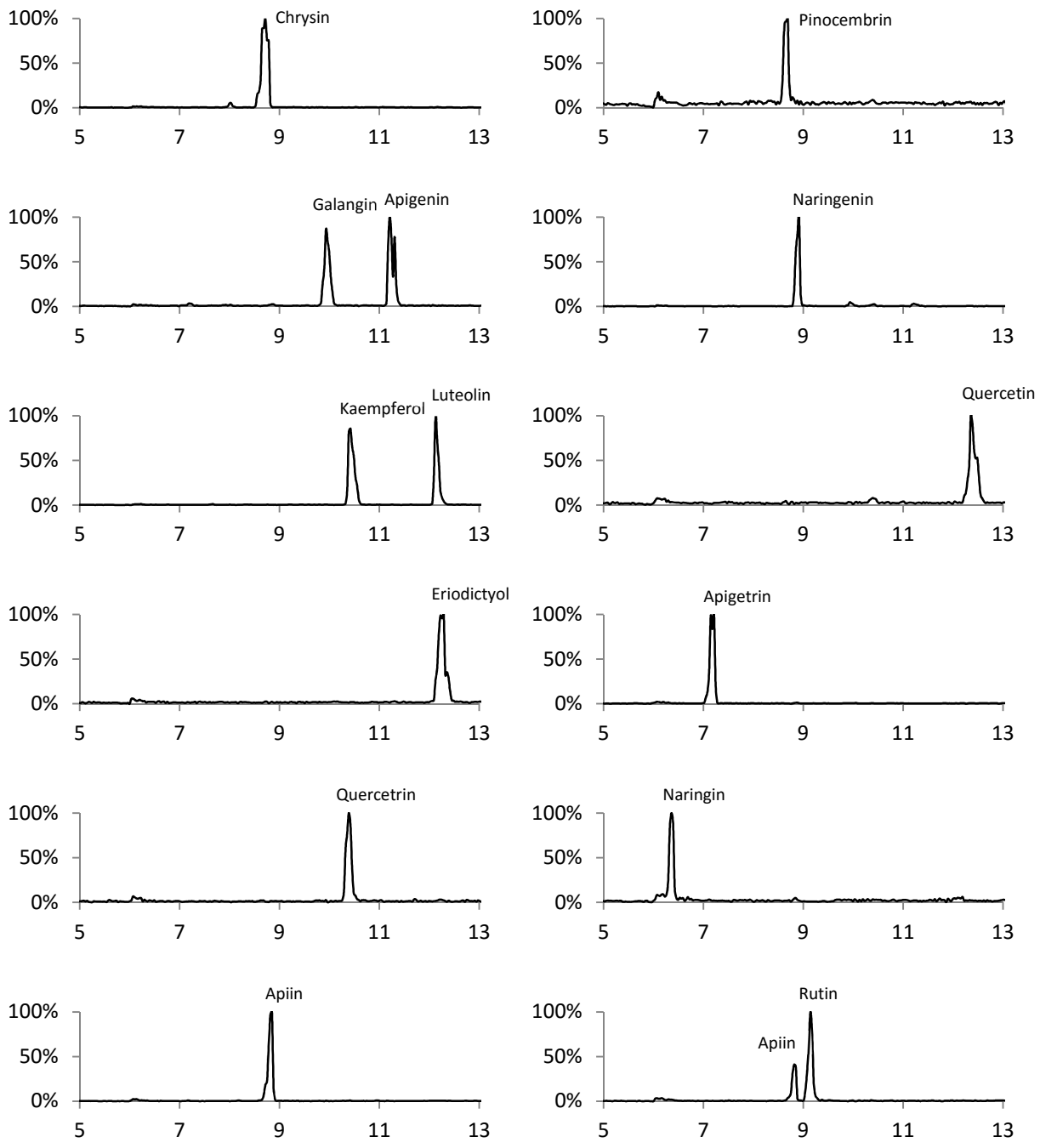

Figure 2.2: CE-MS separation of 14 flavonoid standards. Conditions: separation voltage: 25 kV, 65 cm x 40 μm i.d. x 105 μm o.d. capillary, 25 mM ammonium biborate in 10% methanol, pH = 9.3. Electrospray voltages = -3 kV. 25 μM standards dissolved in BGE.

reports and possible mechanisms for these losses have been proposed elsewhere [36-39].

The fragmentation of catechol containing flavonoid aglycones is shown in Table 2.2. Borate adduct formation corresponding to $[M + B(OH)_3 - 2H_2O - H]^-$, $[M + B(OH)_3 - H_2O - H]^-$, $[M + B(OH)_3 + CH_3OH - 2H_2O - H]^-$, and $[M + B(OH)_3 + 2CH_3OH – 3H_2O –H]^-$ were detected for all catechol containing flavonoids. For eriodictyol, $[M + B(OH)_3 - 2H_2O - H]$ was its base peak at *m/z* 313 (Figure 2.3A). For quercetin and luteolin, the adducts were fairly evenly distributed in terms of abundance. Fragmentation of the borate adducts often resulted in detection of the free aglycone ion, except for the eriodictyol borate adduct, which underwent fragmentation similar to free aglycones. In MS^1 scans, the borate adducts generate an increasing *m/z* pattern (M+26, 44, 58, and 72) that can be used to identify the presence of a catechol group on the aglycone or a *cis*-diol group on a sugar substituent. These diagnostic ions are particularly useful for flavonoids, where several isomers exist, and fragmentation pathways are fairly similar.

The fragmentation of the flavonoid glycones and their most abundant borate adducts is shown in Table 2.3. Quercitrin and rutin were detected as $[M-H]^-$ as well as borate adducts (Figure 2.3B). Additionally, apiin was detected at $[M+26-H]^-$, supporting borate complexation which would cause longer migration time relative to other non-catechol containing flavonoid glycosides. Interestingly, the base peak for rutin was $[M+8-H]^-$, with the borate adduct $[M+26-H]^-$ being the second most abundant ion in its spectrum. The former of the two adducts was not expected, but it contained a similar isotopic distribution as the other borate

Table 2.2. Fragmentation of catechol containing flavonoid aglycones. *[M+$B(OH)_3$-$2H_2O$-H]-, **[M+$B(OH)_3$-H_2O-H]-, ***[M+$B(OH)_3$+CH_3OH-$2H_2O$-H]-

	3	3**	3***	8*	12	12**
[M-H]-	285	329	344	313	301	345
[M-H_2O-H]-	-	311	-	-	-	327
[M-CO-H]-	-	-	-	-	273	-
[M-CH_3OH-H]-	-	-	312	-	-	-
[M-CO_2-H]-	241	-	-	269	-	-
[Aglycone-H]-	-	285	285	-	-	301
[M-$C_2H_4O_2$-H]-	-	-	-	253	-	285
[M-CO_2-CO-H]-	-	-	-	-	229	-
[M-B-ring-H]-	-	-	-	-	191	-
[1,2 A]-	-	-	-	-	179	-
[1,3 A]-	151	-	-	151	151	-

Table 2.3. Fragmentation of flavonoid glycosides and their borate adducts

	4	5	5*	9	13	13**
[M-H]-	431	563	589	579	447	491
[M-H_2O-H]-	-	-	571	-	-	473
[M-borate adduct-H]-	-	-	-	-	-	447
[M-apioside-H]-	-	431	-	-	-	-
[M-rhamnoside-H]-	-	-	-	-	-	327
[1,3 A]-	311	-	-	459	-	-
[Aglycone-H]-	269	269	269	271	301	301

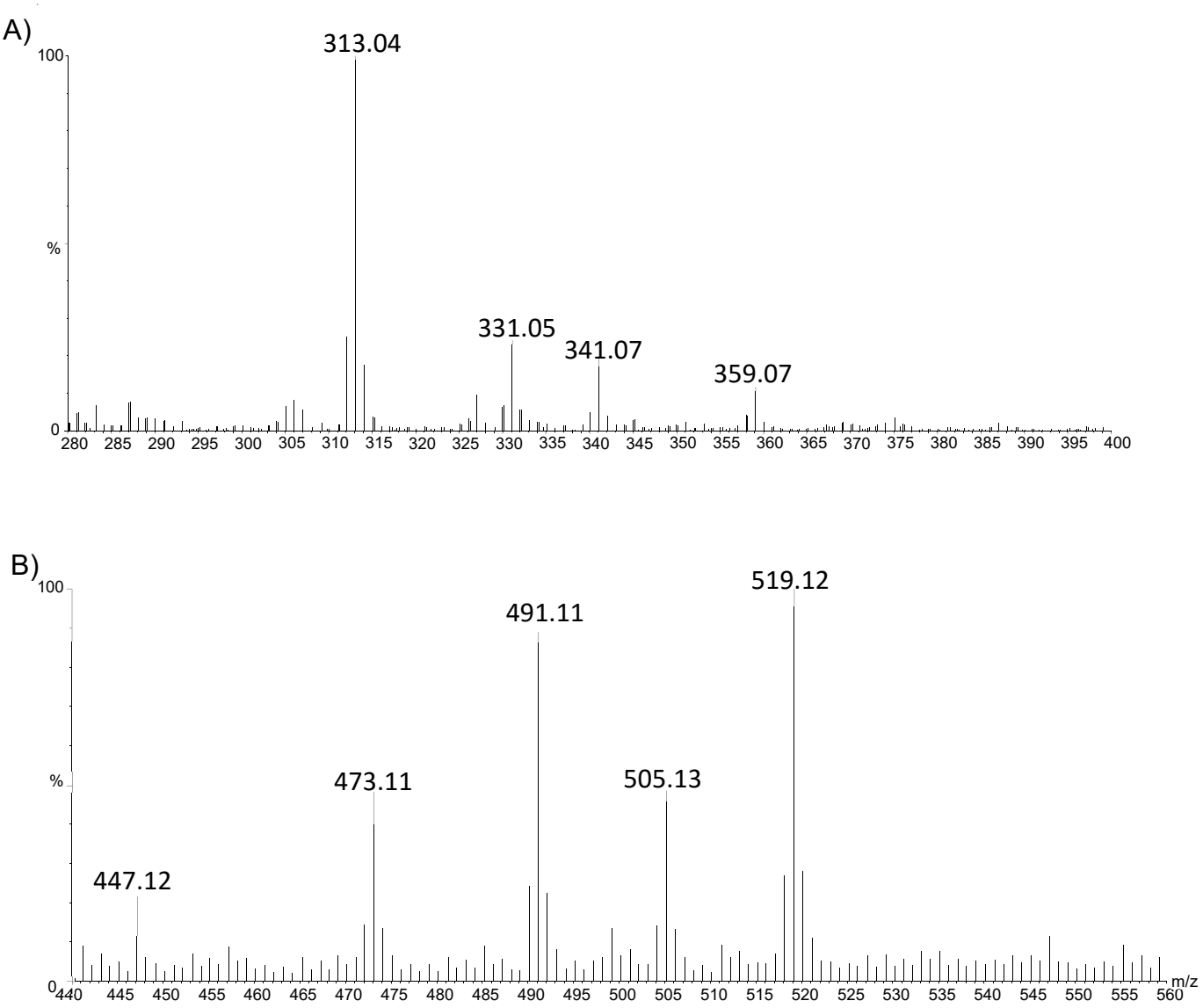

Figure 2.3: The formation of borate adducts for A) eriodictyol and B) quercitrin

adducts. Fragmentation of this adduct yielded the quercetin aglycone ion at *m/z* 301, which is expected from the quercetin derived glycoside. Upon CID fragmentation, the aglycone fragment was the base peak for all of the glycosides. For apigetrin and naringin, the $[1,3\ A]^-$ fragment ion, with the sugar groups intact, was detected at approximately 20% abundance, that has been reported previously for flavonoid glycones[40]; however, in the case of naringin, this ion could also correspond to fragmentation along the glycoside directly connected to the aglycone[38]. The neutral loss of *m/z* 132 from apiin corresponds to the loss of its pentose substituent. Single sugar group neutral losses are possible for polyglycosides; however, the corresponding product ions were not observed for the diglycosides rutin or naringin.

2.3.3 Flavonoid Fingerprint Analysis of *Ginkgo biloba* Ethanolic Extracts

Ginkgo biloba flavonoids were extracted from herbal supplements by sonication in a 70:30 ethanol:water solution in order to extract both glycones and aglycones from the plant material. Hydrolysis of the plant material was not conducted because this results in the cleavage of O-glycosidic bonds, limiting the method to only the detection of aglycones[41]. The results for the CE-MS analysis of *Ginkgo biloba* flavonoids are shown in Figure 2.4. Based on CE-MS results, the most prominent flavonoids present in Gingko biloba are kaempferol and quercetin. Peak destacking of kaempferol and quercetin occurred in the 4-fold BGE diluted ethanolic extract of the *Ginkgo biloba* supplement, so a 100-fold dilution was conducted to minimize this effect. Apigenin, rutin, and apigetrin were also detected in the supplement, which is in agreement with other reports

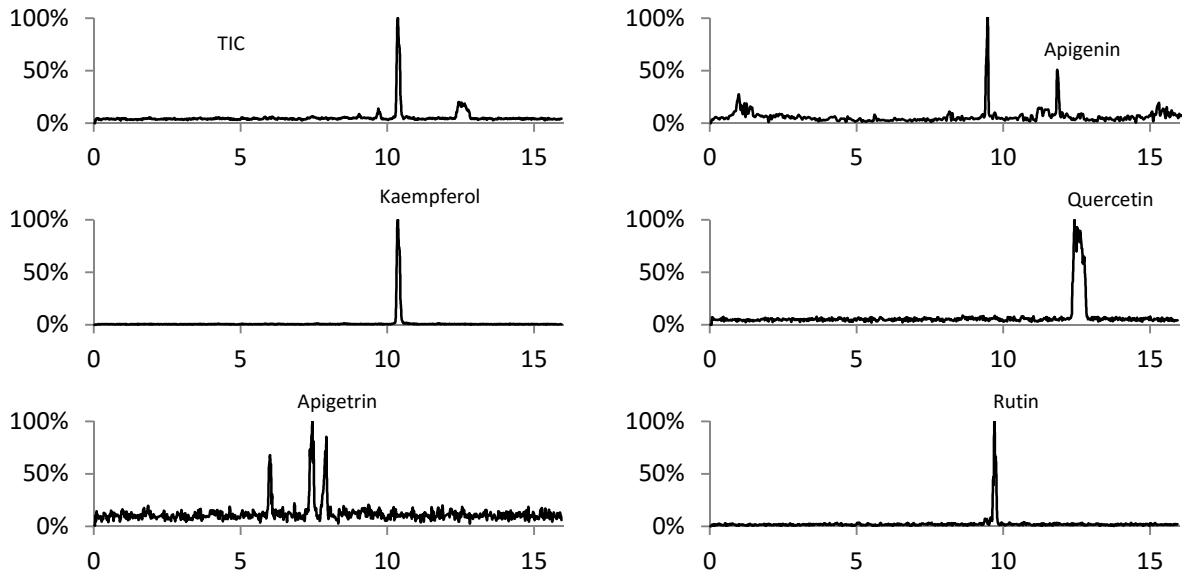

Figure 2.4: CE-MS of 100-fold dilution of the Ginkgo biloba supplement ethanol extract. *Apigenin (2) was not detected in the 100-fold dilution, but was detected in the 4-fold dilution of the extract.

that show the presence of these flavonoids, as well as quercetin and kaempferol, in *Ginkgo biloba* samples[42-44].

Additional peaks with *m/z* 425, 431, 447, and 593 were detected. Fragmentation of the parent ion *m/z* 425 yielded no additional signature aglycone fragments, making its identification difficult. Fragmentation of the parent ions of *m/z* 431, 447, and 593 yielded the fragment ion *m/z* 285, suggesting these peaks could be kaempferol or luteolin glycosides, that have been reported in *Ginkgo biloba* extracts previously[45]. While authentic standards would be required to determine these unknown compounds unequivocally, it can be presumed that they are kaempferol glycosides, as no borate adducts were detected that would signify the presence of the catechol moiety of luteolin glycosides.

2.4 Conclusions

A sheath liquid CE-MS method using a borate based buffer was developed for the detection and identification of the natural flavonoids apiin, apigenin, apigetrin, chrysin, eriodoctyl, galangin, kaempferol, luteolin, naringenin, naringin, pinocembrin, quercetin, quercitrin, and rutin in under 13 min. Flavonoid glycosides typically migrated faster than aglycones, followed by flavonones, flavonols, and flavones. The catechol containing compounds all migrated slowest due to borate complexation. MS studies showed that these borate complexes were detectable as *m/z* M+26, 44, 58, and 72, and these ions could be used diagnostically to differentiate catechol containing flavonoids from non-catechol containing flavonoids of the same *m/z*. MS/MS studies were conducted on the flavonoid standards, and the data was used to determine the presence of

these compounds in *Ginkgo biloba* extract. The highest abundance flavonoids were quercetin and kaempferol, followed by apigetrin, rutin, and apigenin. The method described here shows the utility of CE to achieve high resolution separations. It also demonstrates the breadth of information that can be obtained from MS and MS/MS for the fingerprinting studies of flavonoids in a complex plant material, such as *Ginkgo biloba*.

2.5 References

1. L. H. Yao, Y. M. Jiang, J. Shi, F. A. TomÁS-BarberÁN, N. Datta, R. Singanusong and S. S. Chen, *Plant. Foods Hum. Nutr*, **2004**, *59*, 113-122.
2. M. L. Lee, R.; Shen, L.' Yang, L.; Yen, K.; Hou, W., *J. Agric. Food Chem.*, **2001**, *49*, 5551-5555.
3. M. Serafini, I. Peluso and A. Raguzzini, *Proc. Nutr. Soc.*, **2010**, *69*, 273-278.
4. M. O. Nandave, S. K.; Arya, D. S.;, *Nat. Prod. Radiance*, **2005**, *4*, 166-176.
5. B. Tanwar and R. Modgil, *Spatula DD*, **2012**, *2*, 59-68.
6. A. R. S. Tapas, D. M.; Kakde, R. B.;, *Trop. J. of Pharm. Res.*, **2008**, *7*, 1089-1099.
7. P. Pietta, *J. Nat. Prod.*, **2000**, *63*, 1035-1042.
8. A. H. Hopia, Marina, *J. Am. Oil Chem. Soc.*, **1999**, *76*, 139-144.
9. C. J. Fehske, K. Leuner and W. E. Muller, *Pharmacol. Res.*, **2009**, *60*, 68-73.
10. H. Amieva, C. Meillon, C. Helmer, P. Barberger-Gateau and J. F. Dartigues, *PloS one*, **2013**, *8*, e52755.
11. J. C. T. Winter, D.;, *Pharmacol. Biochem. Behav.*, **1999**, *62*, 543-547.

12. Y.-C. Ko, R.-J. Lee, H.-T. Feng and M.-R. Lee, *J. Chinese Chem. Soc.*, **2013**, *60*, 1333-1338.

13. F. Deng and S. W. Zito, *J. Chroma. A*, **2003**, *986*, 121-127.

14. K. Sutthanut, B. Sripanidkulchai, C. Yenjai and M. Jay, *J. Chroma. A*, **2007**, *1143*, 227-233.

15. K. C. B. De Souza, E. E. S. Schapoval and V. L. Bassani, *J.Pharma. Biomed. Anal.*, **2002**, *28*, 771-777.

16. R. G. Peres, G. A. Micke, M. F. Tavares and D. B. Rodriguez-Amaya, *J. Sep. Sci.*, **2009**, *32*, 3822-3828.

17. S. Sanli and C. E. Lunte, *Anal. Methods*, **2014**, *6*, 3858-3864.

18. C. Huck, G. Stecher, W. Ahrer, W. M. Stogg, W. Buchberger and G. K. Bonn, *J. Sep. Sci.*, **2002**, *25*, 904-908.

19. J. Zhu, K. Yu, X. Chen and Z. Hu, *J. Chroma. A*, **2007**, *1166*, 191-200.

20. W. Wang, P. Lin, L. Ma, K. Xu and X. Lin, *J. Sep. Sci.*, **2016**, DOI: 10.1002/jssc.201501287.

21. H. P. Hendrickson, A. D. Kaufman and C. E. Lunte, *J. Pharma. Biomed. Anal.*, **1994**, *12*, 325-334.

22. T. Wu, Y. Guan and J. Ye, *Food Chem.*, **2007**, *100*, 1573-1579.

23. S. M. S. Sawalha, D. Arráez-Román, A. Segura-Carretero and A. Fernández-Gutiérrez, *Food Chem.* **2009**, *116*, 567-574.

24. A. Carrasco-Pancorbo, C. Neususs, M. Pelzing, A. Segura-Carretero and A. Fernandez-Gutierrez, *Electrophoresis*, **2007**, *28*, 806-821.

25. E. de Rijke, P. Out, W. M. Niessen, F. Ariese, C. Gooijer and U. A. Brinkman, *J. Chroma. A*, **2006**, *1112*, 31-63.

26. G. Vanhoenacker, A. De Villers, K. Lazou, D. De Keukeleire and P. Sandra, *Chromatographia*, **2001**, *54*, 309-315.

27. P. Bednář, B. Papoušková, L. Müller, P. Barták, J. Stávek, P. Pavloušek and K. Lemr, *J. Sep. Sci.*, **2005**, *28*, 1291-1299.

28. K. Brensinger, C. Rollman, C. Copper, A. Genzman, J. Rine, I. Lurie and M. Moini, *Forensic Sci. Int.*, **2016**, *258*, 74-79.

29. M. Vaher and M. Koel, *J. Chroma. A*, **2003**, *990*, 225-230.

30. C. A. Ballus, A. D. Meinhart, R. G. de Oliveira and H. T. Godoy, *Food Res. Inter.* **2012**, *45*, 136-144.

31. P. Tong, L. Zhang, Y. He, S. Tang, J. Cheng and G. Chen, *Talanta*, **2010**, *82*, 1101-1106.

32. X. B. Xu, D. B. Liu, X. M. Guo, S. J. Yu and P. Yu, *J. Chroma. A*, **2014**, *1366*, 65-72.

33. N. M. Schiavone, S. A. Sarver, L. Sun, R. Wojcik and N. J. Dovichi, *J. Chroma. B, Anal Tech Biomed Life Sci.*, **2015**, *991*, 53-58.

34. J. F. Banks Jr., *J. Chroma. A*, **1995**, *712*, 245-252.

35. S.-P. Wang and K.-J. Huang, *J. Chroma. A*, **2004**, *1032*, 273-279.

36. F. Cuyckens, Y. L. Ma, G. Pocsfalvi and M. Claeysi, *Analusis*, **2000**, *28*, 888-895.

37. G. C. Justino, C. M. Borges and M. H. Florencio, *Rapid Comm. Mass Spectrom*, **2009**, *23*, 237-248.

38. F. Cuyckens, R. Rozenberg, E. de Hoffmann and M. Claeys, *J. Mass Spectrom.*, **2001**, *36*, 1203-1210.

39. N. Fabre, I. Rustan, E. de Hoffmann and J. Quetin-Leclercq, *J. Amer. Soc. Mass Spectrom.*, **2001**, *12*, 707-715.

40. C. Yan, S. Liu, Y. Zhou, F. Song, M. Cui and Z. Liu, *J. Amer. Soc. Mass Spectrom*, **2007**, *18*, 2127-2136.

41. T. A. van Beek and P. Montoro, *J. Chroma. A*, **2009**, *1216*, 2002-2032.

42. J. Wang and S. Han, *Chromatographia*, **2013**, *76*, 715-718.

43. R. Z. Guo, X. G. Liu, W. Gao, X. Dong, S. Fanali, P. Li and H. Yang, *J. Chroma. A*, **2015**, *1422*, 147-154.

44. Y. Cao, Q. Chu, Y. Fang and J. Ye, *Anal. Bioanal. Chem.*, **2002**, *374*, 294-299.

45. J. L. Luo, F.; Liu, Y.; Shih, Y.; Lo, C.; , *Journal Food Drug Anal.*, **2013**, *21*, 27-39.

Chapter 3

The Development of a Sheathless Interface for Capillary Electrophoresis Electrospray Ionization Mass Spectrometry using a Cellulose Acetate Cast Capillary

3.1 Introduction

Over the past 15 years, sheathless interfaces have predominated over sheath liquid interfaces due to superior limits of detection. However, sheathless interfaces do suffer from a multitude of drawbacks that make their implementation difficult or impractical. A brief review of sheathless interfaces and their associated pros and cons is presented in this chapter. Then, the development of a novel interface capable of overcoming many negative attributes of other designs is described.

3.2 Tip Shaping

The shape of the emitter tip used in sheathless CE-ESI-MS is an important factor in determining the conditions that permit stable electrospray. As reported by Chowdhury and Chait, reduction of the tip O.D. is required to easily produce stable spray from electrolyte containing aqueous solution[1]. Smaller tip O.D.s decrease the onset potential required for electrospray formation by increasing the local electric field strength[2]. Utilizing lower ESI potentials decreases the likelihood of corona discharge. Additionally, sharpening the tip can eliminate the necessity of auxiliary gas, greatly simplifying the construction of the interface.

The most common method to achieve reduced emitter size is to pull the fused silica capillary to a thin filament. Capillary pulling can be conducted using a Bunsen burner, butane torch, or high power laser. A weight can be suspended

from the capillary during heating to provide constant tension for reproducible tip shapes. The capillary I.D. is closed post-pull so the thin filament must be trimmed with a cutting stone[3]. The trimming step is a source of tip diameter irreproducibility. Also, if the tip I.D. is too small relative to the rest of the capillary, a small back pressure is generated that can counter the EOF. However, when implemented, pulled tips are capable of the best sensitivity relative to other tip shaping methods. Pulled tips require lower onset potential for spray formation, reducing the occurrence of discharge and electrochemical reactions, thereby increasing capillary lifetimes. However, pulled tips are quite susceptible to clogging from particulates in the rinse solutions, BGE, and sample. Pressure can be applied at the tip to push the particulate out the capillary inlet. Due to the fragile nature of the pulled tip, this often results in breakage and the capillary must be replaced.

Mechanical sharpening and etching with HF acid are two alternative tip shaping methods that avoid frequent clogging. Both of these methods reduce the O.D. of the CE capillary without affecting its I.D. As such, the droplets formed from etched and mechanically sharpened tips are larger, rendering them less sensitive than pulled tips. Mechanically sharpened tips have been fabricated by grinding with a rotating wet sanding machine[4] or emery cloth[5]. These tips are sturdy and robust but difficult to reproduce. To etch a tip, the capillary terminus is submerged in a solution of HF while gas or water is pushed through the capillary[6]. The HF eats away at the capillary outer diameter resulting in a conical terminus. HF etched capillary tips are quite reproducible and can be mass produced. However,

experience and training with HF is required due to its poisonous and corrosive nature.

3.3 Sheathless CE-ESI-MS

The most important consideration for all CE-ESI-MS interfaces is the method used to maintain the CE and ESI electrical connections simultaneously. Sheath flow interfaces meet this requirement with the sheath solution. However, the matter is substantially more complicated for sheathless interfaces.

Sheathless interfaces are categorized as one-piece and two-piece designs. Two-piece designs utilize a separation capillary and an emitter capillary distinct from one another. The ESI connection is usually introduced at the gap between the two capillaries. One-piece designs utilize one capillary for both separation and electrospray. The benefit of two-piece designs is that the emitter capillary can be replaced independently from the CE capillary and vice versa. However, the gap between the CE capillary and emitter tip is a source of dead volume and dilution. One-piece interfaces often involve more fabrication, but do not suffer from the aforementioned drawbacks.

3.3.1 Two-piece Interfaces

The original two-piece interface was the liquid junction interface discussed in the Chapter 1[7]. Since then, the separation and emitter capillaries have been butted together with the assistance of microdialysis tubing[8] or a micro-tee[9]. Commercial stainless steel emitter tips can also be used with these interfaces to increase system lifetimes, robustness, and sensitivity[10]. A benefit of these designs is that they permit post separation acidification of analytes via the

junction between the two capillaries[11]. Another two-piece interface utilizes narrow O.D. glass emitters inserted directly into the capillary terminus. The outlet of the CE capillary is submerged in a buffer reservoir. A fraction of the CE effluent enters the emitter while the remaining solution flows into the BGE reservoir to establish electrical contact with the shared electrode[12].

Two-piece interfaces suffer from misalignment of the separation and emitter capillaries. Even with the assistance of connectors, it is difficult to match the outer diameter of the capillary with the inner diameter of the connector. This can result in a non-linear flow path and band broadening[13]. Until this issue is resolved, commercialized two-piece interfaces are unlikely.

3.3.2 One-piece Interfaces

Interfaces that use the CE capillary for separation and as the ESI emitter are more common than two-piece interfaces. The original one-piece sheathless interface (Figure 3.1A), which utilized a metal coated CE tip[14], has since been recreated using gold[15], silver[16], nickel[17], copper[18], and graphite[19]. While the lifetimes of these capillaries are short, they are relatively easy to fabricate and are still implemented today.

Another method used to introduce a terminus voltage is electrode insertion into the capillary outlet[20] (Figure 3.1B) or into the capillary wall near the terminus[21] (Figure 3.1C). Large I.D. capillaries are required for the electrode to fit without completely blocking flow. Still, turbulent flow occurs that is a source of band broadening and unstable electrospray. Instead of inserting an electrode into the capillary wall, a conductive epoxy can be used to fill the hole[13] (Figure 3.1D).

In this design, the conductive epoxy is submerged in a BGE reservoir where the outlet voltage is applied. It has been reported, however, that these interfaces are vulnerable to bubble forming electrolysis reactions that terminate the CE circuit.

Split-flow sheathless interfaces have also been developed, in which a small hole is introduced near the capillary terminus. A fraction of the CE effluent exits through the hole and contacts the ESI electrode[22]. Similarly, the hole can be encased within a small metal sleeve containing BGE (Figure 3.1E). The hole has been introduced into the capillary wall using a dental drill and by cracking the capillary with a cutting stone (Figure 3.1F). This design does not greatly disrupt flow, so separation resolution is maintained. However, the holes and cracks are difficult to reproduce. To circumvent the use of hand tools, a portion of the capillary can instead be submerged in HF acid until the walls become porous[23] (Figure 3.1G). The porous section is then submerged in BGE where the terminus voltage can be applied. If etching is carried out at the tip of the capillary, the creation of the electrical connection and tip shaping can be conducted in a single step[24] (Figure 3.1H). All the split-flow interfaces have shown satisfactory CE-ESI, but are structurally fragile. Protective housing is required to prevent breakage.

In this chapter, we describe the design and fabrication of a robust one-piece sheathless CE-ESI-MS interface, which is an elaboration of the Osbourn-Lunte cellulose acetate decoupler used for CE-electrochemical detection[25]. The interface-decoupler features the use of a CO_2 laser for the fabrication of conductive channels, with subsequent coating with a polymer providing for structural robustness among other functions. As with previous interfaces, use is made

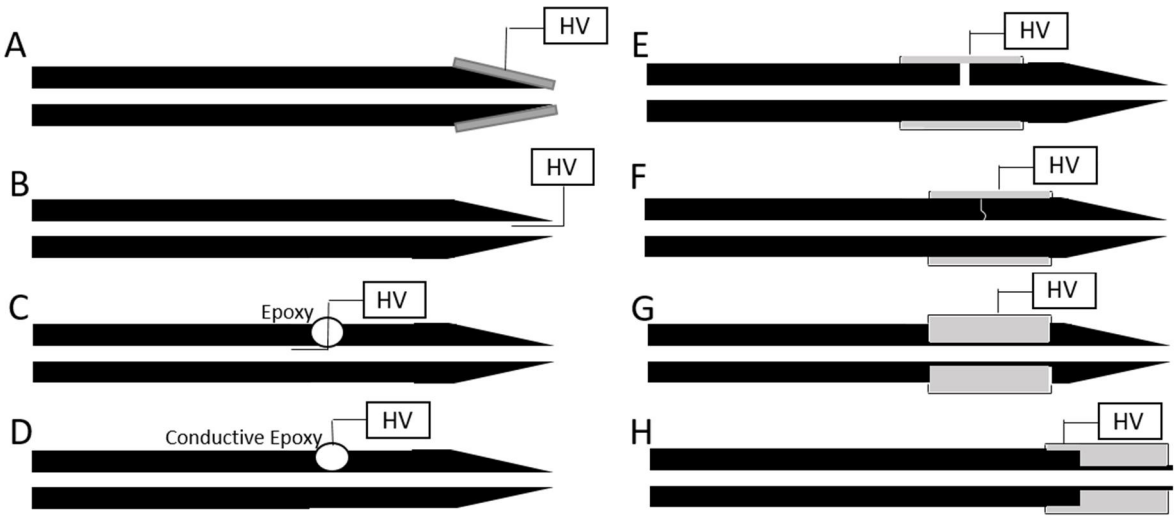

Figure 3.1: One-piece sheathless interface designs. A) Metal coated tip, B) electrode insertion into the capillary outlet, C) electrode insertion into the capillary wall, D) conductive epoxy used to fill hole in capillary wall, E) hole drilled into capillary wall contained in metal sleeve with BGE, F) small crack in the wall contained in metal sleeve with BGE, G) porous HF etched walls contained in metal sleeve with BGE, H) HF etched porous tip design.

of a BGE reservoir in completion of the needed circuits and further allows pH perturbation of post CE separation zones for enhancement of ionization efficiency, thus detection sensitivity. Fabrication details, operational aspects and preliminary results are presented herein.

3.4 Experimental

3.4.1 Reagents

Angiotensin II, Val-Tyr-Val, Leu-enkephalin, Met-enkephalin, cellulose acetate, ammonium acetate, and glacial acetic acid were purchased from Sigma-Aldrich (St. Louis, MO, USA). Acetone (HPLC grade), water (MS grade) and ammonium hydroxide stock were purchased from Fisher Scientific (Waltham, MA, USA). Peptide stock solutions were prepared in MS grade water and diluted into 30 mM ammonium acetate background electrolyte (BGE). Cellulose acetate solution was prepared as 6% weight/volume (w/v) in acetone. Buffers were prepared from solid ammonium acetate and adjusted to the appropriate pH using aqueous 1 M acetic acid or ammonium hydroxide.

3.4.2 Instrumentation and Apparatus

3.4.2.1 CE-UV

The separation of peptide standards was optimized using a P/ACE MDQ Capillary Electrophoresis System equipped with a diode array detector (Beckman Coulter, Palo Alto, CA, USA). A 65 cm length x 50 μm i.d. x 360 μm o.d. capillary (Polymicro Technologies, Tucson, AZ, USA) with a 55 cm effective length was used for all CE-UV studies. Prior to injection, CE capillaries were sequentially conditioned at 10 psi for 5 minutes each with nanopure water, 0.1 M ammonium

hydroxide, and BGE. For all the sample injections, hydrodynamic injection of 5 psi for 2 seconds was performed.

3.4.2.2 CE-ESI-MS Interface Fabrication

The capillary tip was sharpened using a Dremel (6500 rpm, Mt. Prospect, IL, USA) quipped with 600 grit wet sanding paper. A 46 µm tungsten wire from California Fine Wire (Grover Beach, CA, USA) was threaded 10 cm into the outlet of a 55 cm length capillary. The capillary inlet was secured to a second Dremel to provide constant rotation of the capillary. The capillary outlet was placed against the sanding disc at a 20^{o} angle for 5 min and then inspected under microscope to ensure tip uniformity.

Without removing the tungsten wire from the capillary outlet, a CO_2 laser (Boss Laser, Sanford, FL, USA) set to 30% power, 20 mm/s speed, with six replicate ablations was used to introduce 24 channels perpendicular to the capillary length. The channels were made 5 cm from the capillary outlet spanning a 1 cm section. The tungsten wire was displaced 1 cm to provide a smooth surface for coating. Using a 20G syringe, cellulose acetate dissolved in acetone (6% w/v) was used to coat the ablated portion of the capillary. The coated capillary was baked at 90^{o}C for one hour and tweezers were used to remove the tungsten wire from the capillary outlet. The coated capillary was sequentially rinsed with nanopure water and 0.1 M ammonium hydroxide at 10 psi for 1 h for conditioning.

The modified capillary was inserted into a machined PEEK housing attached to an XYZ positioner and secured using PEEK fittings. The PEEK housing contained a buffer reservoir with a platinum electrode for the application of the

terminus voltage. Two CZE1000R Spellman high voltage power supplies (Hauppauge, NY, USA) were used to apply CE and ESI potentials. The CE and ESI power supplies were operated in positive voltage mode. The schematic in Figure 3.2 shows the electrical configuration and design of the interface. All CE-MS experiments were conducted using a LTQ-XL MS from Thermo Scientific (Waltham, MA, USA). Detection was performed in positive ion mode using single reaction monitoring of Val-Tyr-Val (m/z 380.5 -> 263), Leu-enkephalin (m/z 556.5 -> 425), Met-enkephalin (m/z 574.5 -> 425), and angiotensin II (m/z 1047 -> 932) at an 'enhanced' scan rate.

3.5 Results and Discussion

3.5.1 Interface Design

Past efforts in the development of CE-ESI-MS interfaces have been based on sheath-flow and sheathless approaches. Presently we have focused on the development of an interface not compromising sensitivity, while seeking to develop a reproducible fabrication procedure that provides for operational robustness. In order to achieve maximum sensitivity, one is essentially limited to the sheathless interface design. Structural elements required of the interface include a beveled tip at the terminus, a conductive region somewhat proximal to the terminus and a polymeric coating of the conductive region. Functionally, the beveled terminus serves to facilitate an efficient ESI spray, the conductive region allows one to establish electrical connections for CE and ESI simultaneously, and encircling the conductive region with a polymeric coating serves to prevent dilution, provide structural integrity and allows the transport of small ions thus the ability to modify

pH in the post-CE region. These concepts and features are illustrated in Figure 3.2.

3.5.2 Interface Fabrication

With the design details identified, the next aspect was the development of a series of practical and reproducible operations for interface fabrication. While the details are provided in the experimental section, it is instructive to present an overview of the various steps, in particular the order and reasons that they were implemented. Initially one selects a length of capillary (typically 55 cm length, 360 μm o.d, 50 μm i.d.) and inserts a tungsten wire into the capillary outlet, which serves to stabilize the various critical regions of the capillary during fabrication operations. Using a Dremel Tool fitted with a sanding disk, rotating motion served to create the desired beveled terminal region. With the tungsten wire still in place, the next step involved utilization of a programmable CO_2 laser to simultaneously create a series of ablations in each of a group of capillaries a short distance from the capillary terminus. In a final step, the ablated region was coated with a solution of cellulose acetate dissolved in acetone. Subsequent heating resulted in the formation of a membrane that provides structural support; however, cellulose membranes formed from casting of acetone solutions are known to exhibit limited permeability to water vapor[30] and would not be expected to provide for the necessary transport properties for the various ions and protons necessary for the establishment of the electrical circuit, nor the ability to achieve pH perturbation of the CE running buffer. Consequently, after removal of the tungsten wire, the entire capillary was rinsed with a strongly basic solution for one hour in order to increase

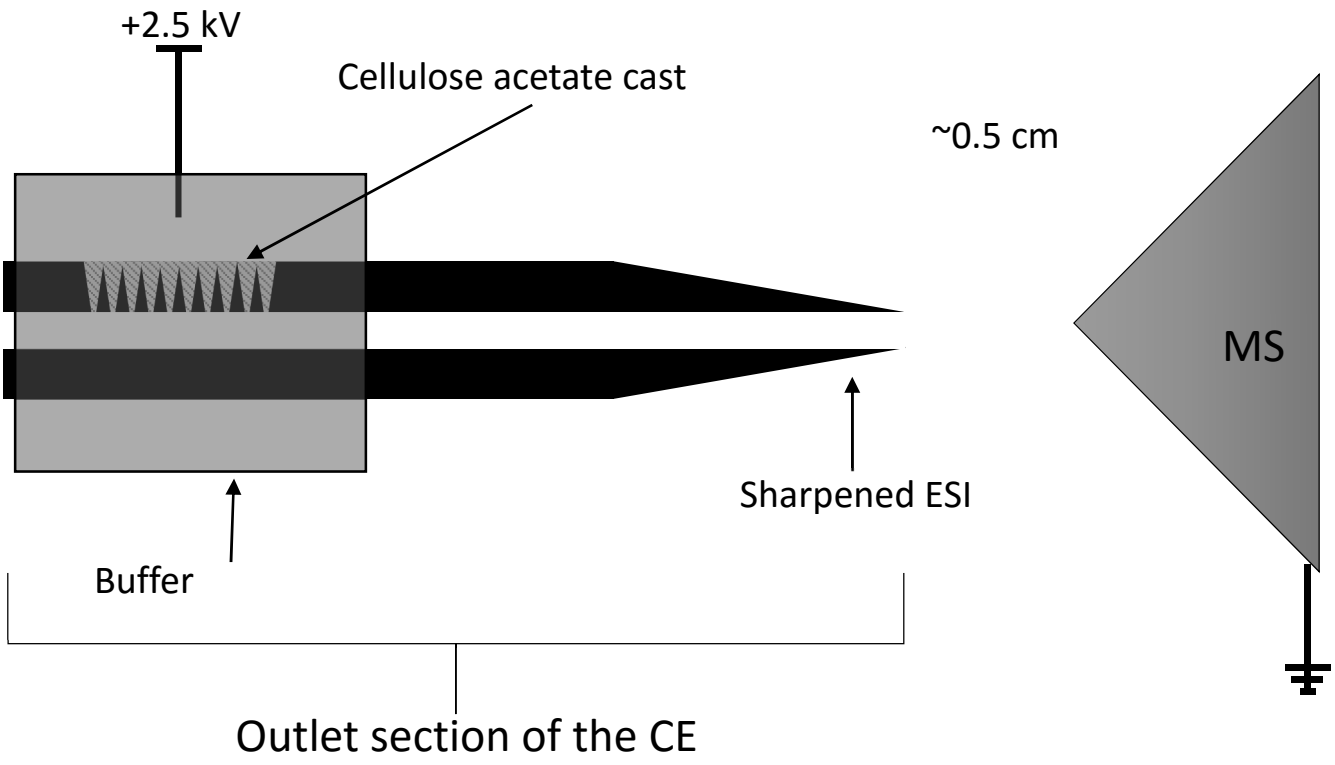

Figure 3.2: A schematic of the cellulose acetate cast CE-ESI-MS interface.

the cast membrane permeability.

3.5.3 Perspectives and Operational Aspects

Fused-silica capillary electrospray tips have been fabricated previously using flame pulling[26], etching with hydrofluoric acid[24], and mechanical sharpening[5]. For the cellulose acetate cast capillaries, mechanical sharpening was chosen because the resulting capillary tips were not as susceptible to clogging as pulled tips and did not require the use of hydrofluoric acid. A tungsten wire was initially inserted at the capillary outlet during the sharpening process to prevent debris produced during the ablation process from getting lodged inside the capillary. The tungsten wire serves two additional purposes with respect to the fabrication of the cellulose acetate cast. First, during the ablation process, the wire ensures the laser pierces only one side of the capillary wall. The opposing side of the capillary diameter is protected from the laser and remains intact. Second, the tungsten wire prevents cellulose acetate from leaking into the ablated holes, which could result in clogging or coating of the silanol walls. The cellulose acetate does not bind to the tungsten, which allows it to be removed without damage to the inner diameter upon drying.

The cellulose acetate cast capillary for sheathless CE-ESI-MS has several advantages over existing designs. The absence of a metal tip allows the interface to be situated less than 0.5 cm from the MS inlet without corona discharge and bubble forming redox reactions. In our experiments, the modified capillaries produced stable spray and were only replaced in rare cases of clogging. The cellulose acetate cast capillary is also mechanically stable, which can be attributed

to the remaining polyimide opposite the laser ablations and refortification with cellulose acetate polymer. Securing the capillary into the interface housing further fortifies the interface. Nafion casts can also be used instead of cellulose acetate[31] if additional structural support is desired, but may result in loss of cationic analytes. Lastly, the fabrication of the laser-ablated capillaries is automated, allowing for high-throughput and reproducible capillary fabrication. One disadvantage of this design is that prominent solvents for non-aqueous CE, like acetonitrile or acetone, cannot be used without causing leakage through the cellulose acetate polymer. However, pure methanol, ethanol, and 2-propanol were tested and did not result in leakage through the membrane.

Capillary rinsing prior to CE-ESI-MS is an essential step to prevent contamination of the MS and inconsistencies in electroosmotic flow. Infusion of water for an hour, from the inlet to outlet direction, at 10 psi ensures that no particulates remain lodged within the capillary. Ammonium hydroxide (0.1 M) rinses are conducted prior to capillary use and between CE-ESI-MS runs to deprotonate the silanol walls and generate reproducible electroosmotic flow (EOF). Alternatively, one can create a permanent charge[27,28] by coating the capillary wall with a polymer containing; however, such an approach typically requires chemical derivatization that may involve multiple steps, and if surface leaching occurs potentially represents an additional source of contamination to the MS. Utilizing the conditioning/reconditioning step with ammonium hydroxide results in an appropriate and consistent EOF.

Several parameters were tested to ensure that each capillary was capable of achieving reproducible migration times and stable spray. To ensure that the capillary was not clogged during the fabrication process, a plug of 10 μM Val-Tyr-Val was infused through the capillary and compared to the theoretical elution time for a 50 μm I.D. x 55 cm length capillary at 10 psi (calculation per standard mobility equations). The elution time of the plug was consistent with that of an unmodified capillary, i.e. a capillary had not been subjected to laser ablation and casting with cellulose acetate. Prior to utilizing each capillary in the CE-ESI-MS format, CE current stability was monitored with the capillary containing background electrolyte with current variation of only 0.4-0.6% being observed. In further evaluations, migration time reproducibility and signal precision of four replicate injections of 10 μM Val-Tyr-Val were used to evaluate the interface. The migration time relative standard deviation for these injections was 1.1% and the signal precision was 4.1% for a 10 psi 1 sec injection. Detection response linearity was evaluated over a concentration range from 100 nM – 10 μM, with an r^2 = 0.998. Based on S/N 3, the estimated LOD of Val-Tyr-Val was 8 nM or 0.2 femtomole using the aforementioned injection conditions. This value is in agreement with other CE-ESI-MS interfaces for peptide standards[32]. Lastly, the spray stability at acidic and basic pH and with the assistance of pressure did not compromise the electrospray process. These observations demonstrate that the interface is suitable for routine CE-ESI-MS analysis.

3.5.4 Comparison of the CE-ESI-MS Interface to a Commercial CE-UV System

To demonstrate that the CE separation does not degrade in the cellulose acetate cast capillary, CE-UV and CE-ESI-MS electropherograms for a peptide mixture containing angiotensin II, Val-Tyr-Val, Leu-enkephalin, and Met-enkephalin were obtained. The background electrolyte used for both analyses was 30 mM ammonium acetate adjusted to pH 2.8. Peptide standards of 50 μM and 1 μM were injected into the CE-UV and CE-ESI-MS systems, respectively. As shown in Figure 3.3, Baseline separation of the peptides was achieved with either method and migration times were comparable. A relative increase of 0.25 min peak widths was observed for CE-ESI-MS results. This was attributed to Joule heating, which is prevented with the thermostatically controlled Beckman CE-UV system. As opposed to several other CE-ESI-MS methods to establish spray at low pH, our method did not require pressure assistance or permanent capillary wall coating to create electrospray at low EOF strengths. These results demonstrate that with this interface, analytical separations are not compromised when compared to those from an unmodified capillary.

3.5.5 Post-Junction pH Modification

To achieve enhanced ionization efficiency, post-separation pH modification of the electrophoresis BGE buffer was evaluated using an acidic solution in the interface reservoir. This feature is desirable if the pH of the electrophoresis buffer does not provide optimal response or if the compound is to be separated as one charge and detected as another. For peptide Val-Tyr-Val with electrophoresis being conducted in 10 mM ammonium acetate of pH 6.7, comparisons were

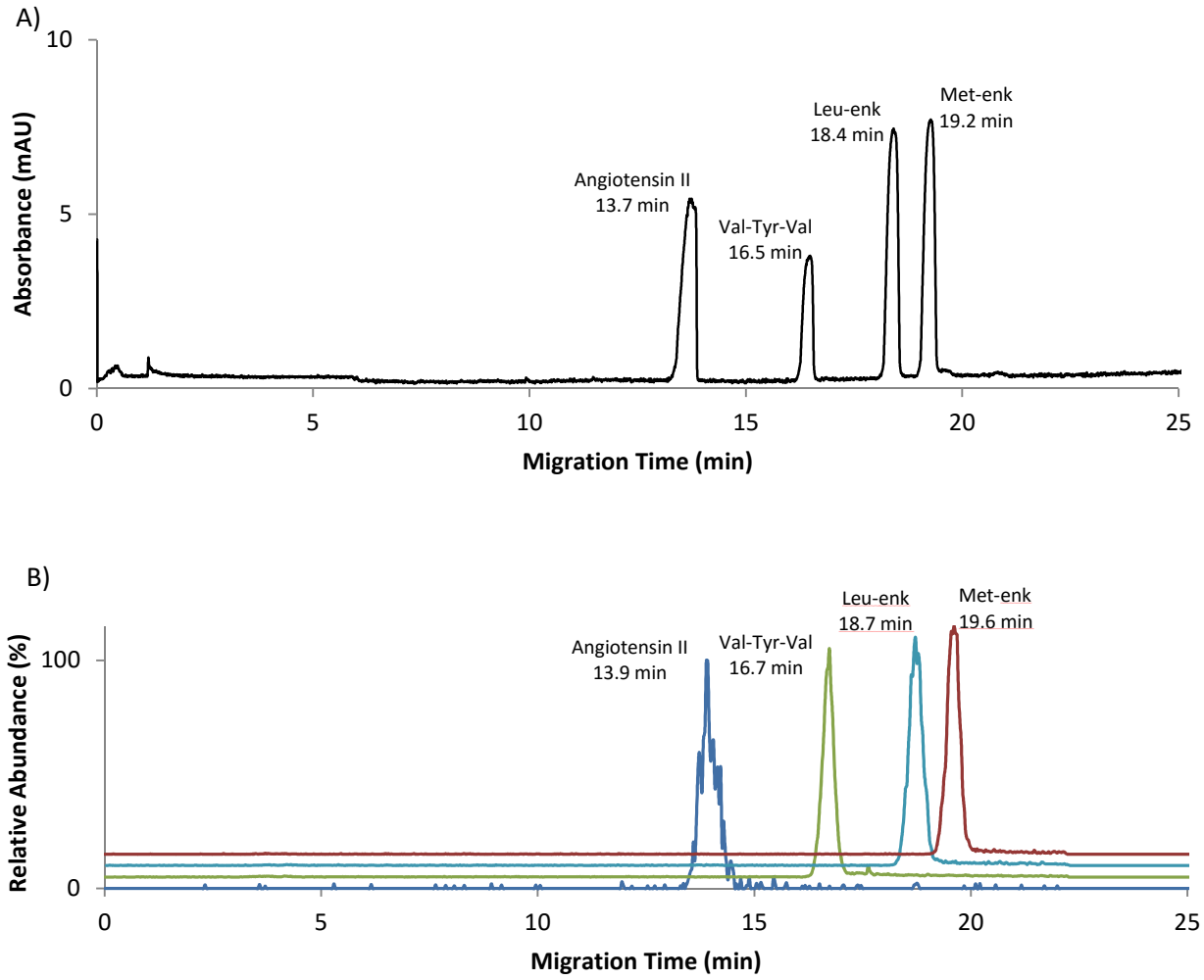

Figure 3.3: A) The CE-UV separation of four peptide standards with commercial instrumentation; B) The CE-ESI-MS separation of the same peptide standards with an in-house fabricated CE-System using the laser ablated – cellulose acetate interface.

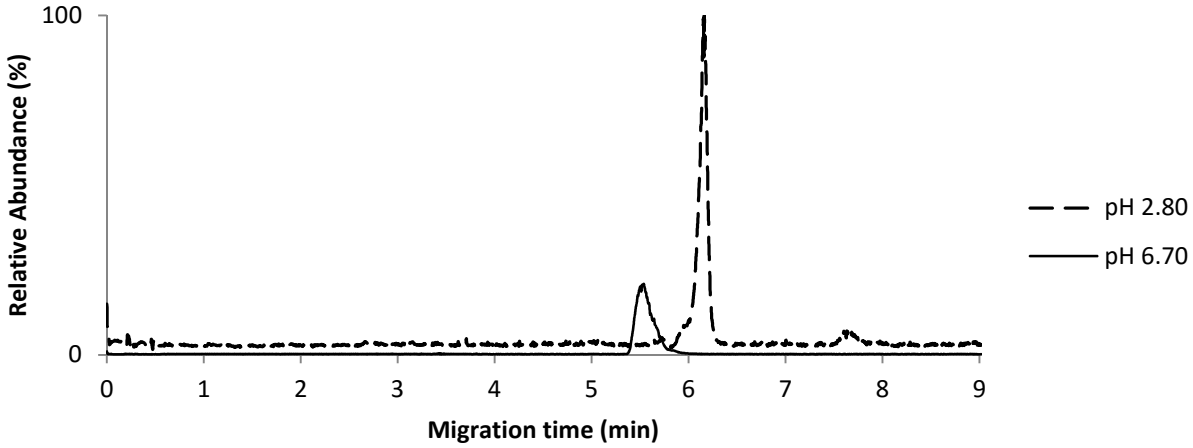

Figure 3.4: CE-ESI-MS spectra of Val-Tyr-Val conducted using 10 mM ammonium acetate at pH 6.7 BGE. The solid line is the electropherogram obtained when the buffer reservoir contains 10 mM ammonium acetate at pH 6.7 as BGE, while the dotted line shows an overlay of electropherograms obtained when the buffer reservoir contained 100 mM ammonium acetate at pH 2.8.

made with differing solutions in the interface reservoir. The first experimental condition utilized a pH 6.7 solution of 10 mM ammonium acetate, while in the next experiment a pH 2.8, 100 mM ammonium acetate buffer system was employed. With the more acidic buffer, an approximately 3.30-fold signal enhancement in the signal intensity was observed (n = 3). The migration time using the acidic buffer was 0.5 min longer due to the decreased electroosmotic flow near the outlet (Figure 3.4). The time required for the equilibration of pH between the reservoir and the capillary is dependent on the concentration and buffer capacity of the electrophoresis buffer. In our experience, equilibration was nearly instanteous because the chosen pH 6.7 BGE has limited buffer capacity. Previous workers have reported that up to 8 hours may be required to achieve full titration of a BGE in its buffering range[29].

3.6 Conclusions

In the work described in this chapter, a novel CE-ESI-MS sheathless interface utilizing a cellulose acetate cast membrane has been described, which possesses several advantages over existing designs. The fabrication methodology allows several capillaries to be manufactured simultaneously in a procedure that avoids the tedious procedures and/or the highly caustic acids of previous designs. The use of a programmable laser omits the need for hand tools, resulting in reproducible ablations. The design is mechanically stable upon coating with cellulose acetate and does not require difficult alignment steps that two-piece sheathless interfaces present. The interface produces a stable electrospray with lifetimes similar to that of unmodified fused silica capillaries. Additionally, this

design does not inherently present a significant dead volume and due to the semi-permeable membrane, permits post-CE pH modification without introducing sample dilution.

3.7 References

[1] Chowdhury, S. K.; Chait, B. T. Anal. Chem., **1991**, 63 (15), 1660-1664.

[2] Banks, F. J. Electrophoresis, 1997, 18, 2255-2266.

[3] Hannis, J. C.; Muddiman, D. C. Rapid Comm. Mass Spectrom., **1998**, 12, 443-448.

[4] Petersson, M. A.; Hulthe, G.; Fogelqvist, E. J. Chroma. A., **1999**, 854, 141-154.

[5] Barnidge, D. R.; Nilsson, S.; Markides, K. E.; Rapp, H.; Hjort, K. Rapid Comm. Mass Spectrom. **1999**, 13, 994-1002.

[6] Kelly, J. F.; Ramaley, L.; Thibault, P. Anal. Chem. **1997**, 69, 51-60.

[7] Lee, E. D.; Muck, W.; Henion, J. D.; Covey, T. R. *Biol. Mass Spectrom.*, **1989**, *18* (9), 844-850.

[8] Severs, J. C.; Smith, R. D. Anal. Chem. **1997**, 69, 2154-2158.

[9] Tong, W.; Link, A.; Eng, J. K.; Yates, III, J. R. Anal. Chem. **1999**, 71, 2270-2278.

[10] Ishihama, Y.; Katayama, H.; Asakawa, N.; Oda, Y. Rapid Comm. Mass Spectrom., **2002**, 16, 913-918.

[11] Severs, J. C.; Harms, A. C.; Smith, R. D. Rapid Comm. Mass Spectrom., **1996**, 10, 1175-1178.

[12] Jussila, M.; Sinervo, K.; Porras, S. P.; Riekkola, M-L, Electrophoresis, **2000**, 21, 3311-3317.

[13] Maxwell, J. E.; Chen, D. D. Y. Anal. Chim. Acta, **2008**, 627, 25-33.

[14] Olivares, J. A.; Nguyen, N. T.; Yonker, C. R; Smith, R. D. *Anal. Chem.*, **1987**, *59*

(8), 1230-1232.

[15] Ramsey, R. S.; McLucky, S. A., *J. Microcolumn Sep*., **1995**, *7*, 461-469.

[16] Chen, Y-R., *Rapid Comm. Mass Spectrom*., **2003**, *17*, 437-441.

[17] Bendahl, L.; Hansen, S. H.; Olson, J., *Rapid Comm. Mass Spectrom.* **2002**, *16*, 2333-2340.

[18] Zamfir, A. D.; Dinca, C.; Sisu, E.; Peter-Katalinic, J., *J. Sep. Sci*., **2006**, *29*, 414-422.

[19] Zhu, X.; Thiam, S.; Valle, B. C.; Warner, I. M. *Anal. Chem*. **2002**, *74*, 5405-5409.

[20] Fang, L.; Zhang, R.; Williams, E. R.; Zare, R. N.; *Anal. Chem.*, **1994**, *66* (21), 3696-3701.

[21] Cao, P.; Moini, M., *Am. Soc. Mass Spectrom*., **1997**, *8*, 561-564.

[22] Moini, M., *Anal. Chem*., **2001**, *73* (14), 3497-3501.

[23] Whitt, J. T.; Moini, M., *Anal. Chem*., **2003**, *75* (9), 2188-2191.

[24] Moini, M., *Anal. Chem*., **2007**, *79* (11), 4241-4246.

[25] Osbourn, D. M.; Lunte, C. E., *Anal. Chem.* **2001**, *73*, 5961-5964.

[26] Wu, Y.-T.; Chen, Y.-C., *Anal. Chem.* **2005**, *77*, 2071-2077.

[27] Soga, T.; Ohashi, Y.; Ueno, Y.; Naraoka, H.; Tomita, M.; Nishioka, T., *J Proteome Res* **2003**, *2*, 488-494.

[28] Melanson, J. E.; Baryla, N. E.; Lucy, C. A. Trends Anal Chem **2001**, 6-7, 365-374.

[29] Zhou, J.; Lunte, S. M. *Anal Chem* **1995**, *67*, 13-18.

[30] Yuan, J.; Dunn, D.; Clipse, N. M.; Newton Jr., R., *J. Pharm. Technol.* **2009**, *33*, 88-100.

[31] O'Shea, T. J.; Greenhagen, R. D.; Lunte, S. M.; Lunte, C. E.; Smyth, M. R.; Radzik, D. M.; Watanabe, N., *J. Chroma. A* **1992**, *593*, 305-312.

[32] Pont, L.; Benavente, F.; Barbosa, J.; Sanz-Nebot, V., *J. Sep. Sci.* **2013**, *36*, 3896-3902.

Chapter 4

CE-ESI-MS Method Development for Lipid Peroxidation Biomarkers of Oxidative Stress

4.1 Introduction

4.1.1 Oxidative Stress

Molecular oxygen (O_2) present in a biological system can undergo reduction reactions that yield reactive oxygen species (ROS) such as superoxide ($O_2^{\cdot -}$), peroxide (O_2^{2-}), and hydroxyl radical ($OH^{\cdot}$). Additionally, nitric oxide ($NO^{\cdot}$) in the vasculature can react with superoxide in order to produce peroxynitrite ($ONOO^-$). From peroxynitrite, secondary reactions can occur resulting in further production of reactive nitrogen species (RNS) and ROS. In high concentrations relative to antioxidants, these reactive species can upset the balance of the cellular redox state, causing what is known as oxidative stress[1,2].

Oxidative stress presents a source of structural damage to important macromolecules like DNA, proteins, and lipids. When DNA undergoes reaction with ROS, the nucleotides can become modified at either the base or sugar unit, resulting in structural damage and possible mutagenic carcinogenesis[3]. Oxidation of proteins by ROS causes changes in the protein's structure and function[4]. For example, cysteine residues can become oxidized by ROS to form unintended disulfide linkages. The result of these adverse modifications can be denaturation or loss of function. Lastly, when lipids react with ROS in a process known as 'lipid peroxidation', a chain reaction occurs between the newly oxidized fatty acids and neighboring unmodified fatty acids. This chain reaction causes

the propagation of damage throughout the membrane, altering its hydrophobicity and in effect, its permeability[5]. Reaction products of oxidized macromolecules and their metabolites are often used to measure the extent of oxidative stress occurring within a biological system[6-10].

4.1.2 Lipid Peroxidation

Oxidative deterioration of unsaturated fatty acids, glycolipids, cholesterol, and phospholipids is common during a stress event. The damage can occur non-enzymatically via direct attack by ROS or enzymatically by proteins upregulated during oxidative stress.

The non-enzymatic pathway for lipid peroxidation involves a three step process: initiation, propagation, and termination[11]. Polyunsaturated fatty acids (PUFAs) are particularly at risk of initiation because their methylene group (-CH_2-) hydrogen atoms are highly susceptible to abstraction by hydroxyl radical. This abstraction results in the formation an alkyl radical. In aerobic conditions, this radical is converted to a peroxyl radical (ROO$\cdot$). The peroxyl radical is also capable of hydrogen abstraction from proximal PUFAs, producing additional alkyl radicals and lipid peroxides (ROOH). Subsequently, lipid peroxides can undergo a transition metal catalyzed reaction to form alkoxyl radicals (RO$\cdot$), which are also capable of hydrogen abstraction. One common end product of lipid peroxidation is a hydroxylated lipid (ROH), which is significantly more hydrophobic than the original. This change in membrane hydrophobicity is detrimental to the viability of a cell, as it is unable to efficiently regulate the compounds that pass through it[5].

Enzymatic lipid degradation is catalyzed by lipooxygenases (LOX), cyclooxygenases (COX), and cytochrome P450[12]. In a healthy system, these enzymes react with lipids to produce signaling molecules that maintain biological homeostasis and regulate pathological function[13]. Certain isoforms of these enzymes can be upregulated by stimuli and cellular stress, resulting in the overproduction of lipid metabolites. For example, COX-2 can be upregulated by excitatory amino acids during oxidative stress, increasing the production of the lipid mediators of inflammation[14].

4.1.3 Biomarkers of Enzymatic Lipid Peroxidation

One of the most abundant lipids degraded by these enzymatic pathways is arachidonic acid. Arachidonic acid (AA) is an essential omega-6 PUFA that is stored in membranes by esterification as phospholipids. During ischemic injury and inflammation, calcium ion influx increases the activity of phospholipase A_2 (PLA_2). PLA_2 releases AA from the membrane to be rapidly metabolized by LOX to produce leukotrienes (LTBs) and hydroxyl-eicosatetraenoic acids (HETEs), COX to produce prostaglandins (PGs) and thromboxanes (TXBs), and cytochrome P450 to produce 20-HETE, leukotoxins, and prostacyclin[15]. A general scheme for the arachidonic cascade is shown in Figure 4.1. These AA metabolites are known as ‘eicosanoids.’ Eicosanoids participate in a wide variety of biological activities, including vasodilation, bronchoconstriction and dilation, signaling for cell aggregation, and chemoattraction[16].

When tissue is damaged, by direct injury, heat, toxins, etc., the body’s inflammatory response triggers increases in ROS, COX-2 (isoform of COX), and

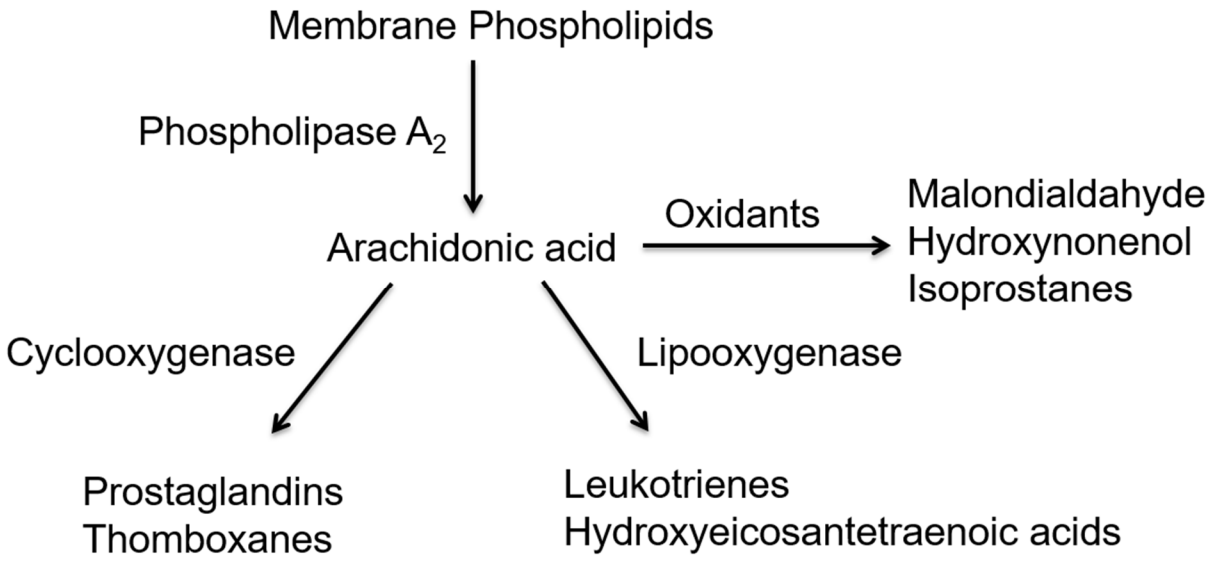

Figure 4.1: Arachidonic acid cascade to the formation of markers of oxidative stress

several LOX isoforms in order to oxidize AA. Eicosanoids can be used as biomarkers to determine the influence of each metabolic cycle. This information can be used to measure the extent of oxidative damage that has occurred or to manipulate the inflammatory response[17,18] (e.g. ibuprofen).

Immunoassays[19], fluorescent labelling[20, 21], and LC-MS/MS[22] are common methods used to determine eicosanoid content. Commercially available immunoassays are not capable of determining multiple eicosanoids simultaneously and often require preconcentration of large volumes of sample (5-10 mL). Eicosanoids do not exhibit strong light absorbing properties, so they require derivatization to achieve sufficient detection limits with spectroscopic techniques. Post derivatization, however, the analytes' increasing molecular size and similarity result in more difficult separation. LC/MS/MS with ESI and APCI[23] has proven to be the strongest platforms for eicosanoid detection. A drawback of this methodology is that the ionization of lipid molecules tends to be quite low. As such, additives or derivatization are often required[24]. Additionally, if the sample volume is less than 10 μL, as in microdialysis sampling, only one or two trials can be conducted per sample.

Here, a CE-ESI-MS/MS method was developed for the detection of Prostaglandin E_2 (PGE_2), prostaglandin $F_{2\alpha}$ ($PGF_{2\alpha}$), prostaglandin D_2 (PGD_2), Leukotriene B_4 (LTB_4), and thromboxane B_2 (TXB_2) in rat brain microdialysis samples. The structure of these analytes is shown in Figure 4.2. CE-MS is ideal for this application due to its low sample consumption, which allows for improved

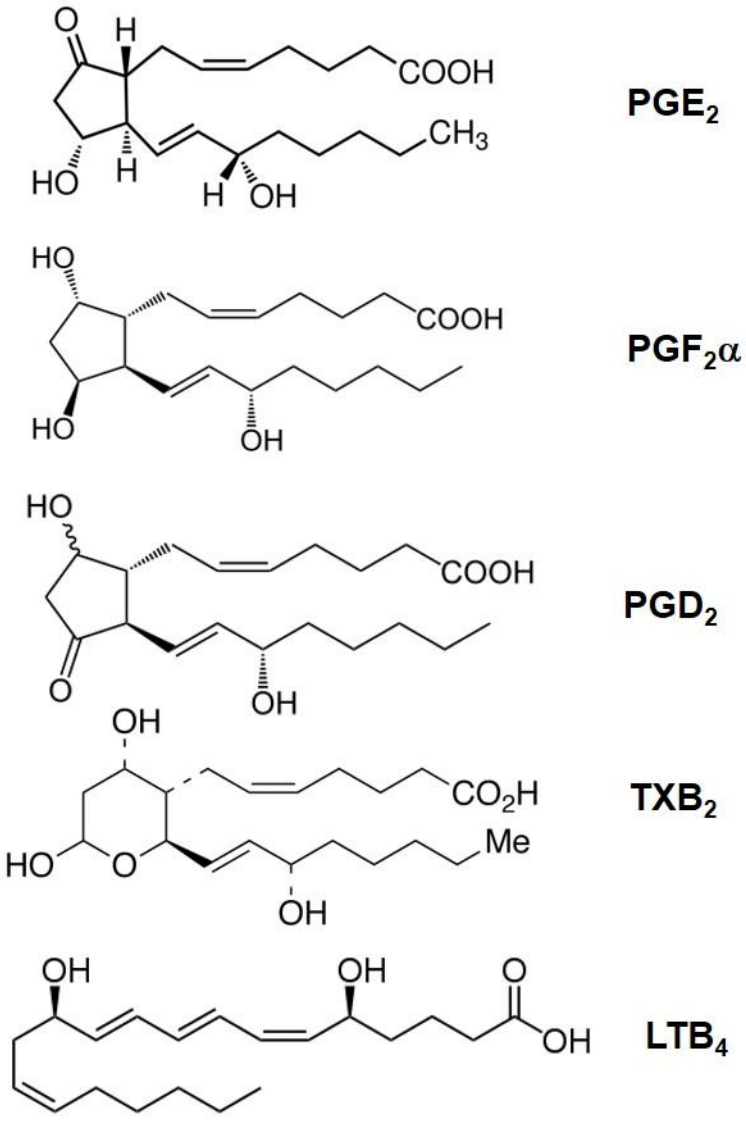

Figure 4.2: Structure of the lipid peroxidation biomarkers investigated in this study.

temporal resolution during sampling. The method utilizes an AMP+ derivatization agent to increase ESI-MS sensitivity and aqueous solubility. Additionally, the derivatized eicosanoids fragment differently from one another, unlike free eicosanoids, limiting the need for a rigorous separation.

4.2 Microdialysis Sampling

Microdialysis is a minimally invasive *in-vivo* sampling technique which relies on diffusion of extracellular molecules across a semipermeable membrane. The membrane is composed of a low molecular weight cut-off polymer that prevents collection of large molecules. Small molecules diffuse across the membrane via a concentration gradient. Through the inlet of the probe, saline or artificial cerebral spinal fluid (ACSF) is introduced at a flow rate of 1-10 μL/min, while the analytes which passively diffuse into the probe are collected at the outlet. A general schematic of a microdialysis probe is shown in Figure 4.3. The microdialysis probe can be implanted in most tissue, including skin[25], brain[26], and liver tissue[27].

` One advantage of microdialysis sampling is that it provides site specific real-time collection of extracellular components. Collection from microenvironments is easily achieved compared to other *in vivo* techniques that require removal of whole brain. Another advantage of microdialysis sampling is that the probe is capable of delivery and recovery. Basal sample collection allows a test subject to act as its own control. Subsequently, the extracellular space can be sampled during and after administration of drug compounds. Lastly, microdialysis can be used to sample analyte concentrations

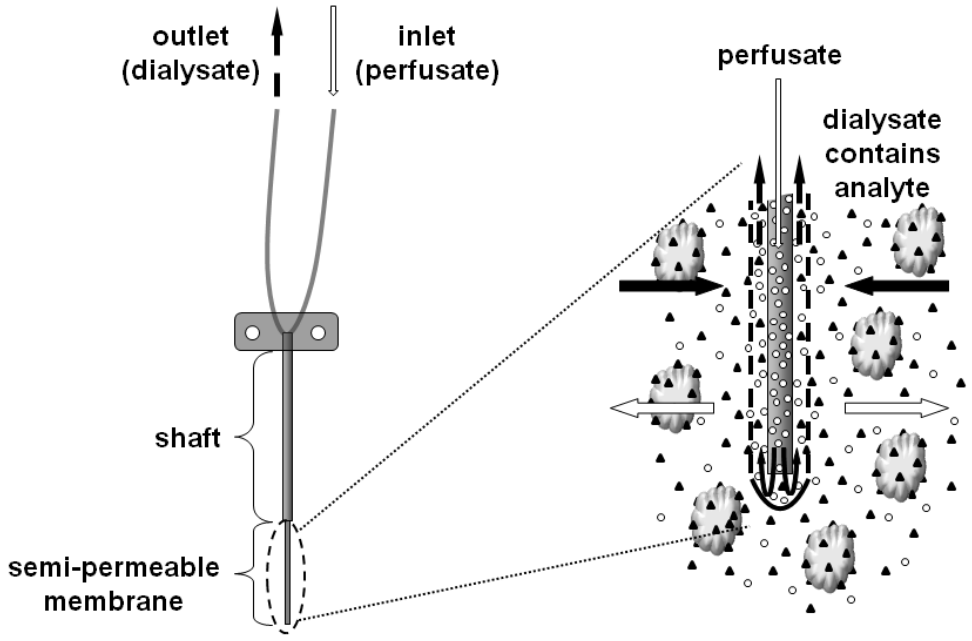

Figure 4.3: A microdialysis probe

for hours, days, and weeks. So far, it is the only technique capable of long term *in vivo* sampling studies.

4.3 Experimental

4.3.1 Reagents

PGE_2, PGD_2, $PGF_{2\alpha}$, TXB_2, and LTB_4 and the AMP+ derivatization kit was purchased from Cayman Chemical (Ann Arbor, MI, USA). Ammonium acetate and Ringer's salts were purchased form Sigma-Aldrich (St. Louis, MO, USA). MS Grade water, methanol, and reagent grade ammonium hydroxide and ethanol were purchased from Fisher Scientific (Fair Lawn, NJ, USA).

Stock solutions of PGE_2, PGD_2, $PGF_{2\alpha}$, and TXB_2 were prepared by dissolving 1 mg solid in 1 mL of ethanol. LTB_4 was purchased as a 50 μg/500 μL solution in ethanol. Eicosanoid mixtures were made to 1 μM in Ringer's solution or methanol and prepared fresh daily to prevent degradation. All eicosanoid solutions were stored at -20 °C. Ringer's solution was made from solid and contained 147 mM NaCl, 3 mM KCl, 1 mM $MgCl_2$, and 1.2 mM $CaCl_2$.

4.3.2 Instrumentation

Initial method development for the separation of native eicosanoids was conducted using a P/ACE MDQ Capillary Electrophoresis System equipped with a diode array detector (Beckman Coulter, Palo Alto, CA, USA). A 65 cm x 50 μm i.d. x 360 μm o.d. capillary (Polymicro Technologies, Tucson, AZ, USA) was used with a 55 cm effective length for all CE-UV studies.

All CE-MS studies were conducted using the interface described in the Chapter 3. The interface was situated 1 cm from an LTQ-XL MS from Thermo Scientific (Waltham, MA, USA). The ESI voltage on the instrument control was set to zero and no drying or cone gas was used. The ion transfer tube temperature was set to 350ºC with the MS inlet voltages being optimized by tuning each compound using the instrument's auto-tuner. The CE power supply was operated in the range of 20-25 kV while the ESI power supply was operated at positive or negative 3 kV. The optimum CID energy for the derivatized eicosanoids was determined by infusing each compound through the CE capillary individually.

4.3.3 Sample Preparation

Solid phase extraction (SPE) was conducted using Oasis HLB cartridges with 10 mg stationary phase (Waters Corp., Milford, MA, USA) and with Ziptips (Millipore, Billerica, MA, USA). For the Oasis HLB cartridges, the SPE bed was activated with 1 mL of water and equilibrated with two 0.75 mL additions of 95/5 water/methanol. A small volume (10 μL) of eicosanoid test standards or brain dialysate samples were diluted to 210 μL and loaded onto the SPE cartridge. The sample tube was then washed with 200 μL of the equilibration solution and added to the cartridge to ensure the entire sample had been transferred. The cartridge was then washed with two 1 mL volumes 95/5 water/methanol. Elution of the sample was conducted using 1 mL of pure MS grade methanol into a 1.5 mL glass vial. For the Ziptips, the bed was activated with 10 μL of acetonitrile and equilibrated with four 10 μL rinses of 95/5 water/methanol. Four microliters

(4 μL) of sample was introduced to the cartridge and plunged through 10 times. The sample was then eluted into 10 μL of acetonitrile.

Prior to derivatization, the SPE eluent was evaporated to dryness using a gentle stream of argon gas and reconstituted in 20 μL of 50/50 dimethylformamide/acetonitrile. The derivatization agents were then added as follows: 10 μL of 1-hydroxybenzotriazole, 20 μL of cold 1-Ethyl-3-(3-dimethylaminopropyl)carbodiimide (EDC), and 30 μL of AMP+ derivatization agent. The AMP+ agent usually required heating to dissolve particulates in the vial prior to addition to the sample. The contents of the sample were vortex mixed for 30 seconds and then heated at 60ºC using a heating block for 30 minutes.

Post derivatization, the sample was allowed to cool to room temperature. The solution was then evaporated once more and reconstituted in water (10 μL for Oasis and 4 μL for ZipTip) prior to CE-ESI-MS analysis.

To develop calibration curves for the analytes, 25, 100, and 500 nM standards were dissolved in Ringer's solution and desalted using Ziptips. Subsequently, the samples were derivatized using the AMP+ kit. This process was completed in triplicate. The resultant samples were then analyzed by CE-MS/MS in duplicate, resulting in six data points per concentration, per analyte.

4.3.4 Microdialysis

Microdialysis samples were obtained from the hippocampus of female Sprague-Dawley rats. A perfusion flow rate of Ringers solution at 1 μL/min was

used. Postop microdialysate samples were collected for one hour and pooled prior to sample preparation and CE-MS/MS analysis.

4.4 Method Development

4.4.1 CE-UV and CE-MS of Native Eicosanoids

4.4.1.1 CE-UV Studies

Published CE methods capable of separating eicosanoids rely on greater than 50% acetonitrile content in the BGE. Of these, none utilize MS detection and are incapable of low nM LODs. The cellulose acetate interface is not compatible with acetonitrile, so alternative separation conditions were investigated. In the case that novel conditions were unachievable, alternative interface designs could have been utilized.

Initially, the separation of the eicosanoids was optimized on a CE-UV system. Ammonium acetate BGE was utilized due to its ESI compatibility and buffering range. To achieve separation of the eicosanoids with CE, the pH must be greater than 4.5 to ensure the compounds are charged.

The starting BGE conditions were 15 mM ammonium acetate at pH 5.5, with a CE voltage of 20 kV. At these conditions, $PGF_{2\alpha}$ and PGD_2 were detected, but co-migrated. Twenty percent methanol was added to the BGE, which diminished the EOF and separated the two PGs. However, when PGE_2 was added to the mixture, it co-migrated with $PGF_{2\alpha}$ and PGD_2. The methanol concentration was doubled once more, to 40%, which improved the separation slightly. At >40% methanol BGE concentrations, the run times were greater than

30 minutes, rendering these conditions undesirable. The effects of methanol concentration on the separation are shown in the electropherograms presented in Figure 4.4.

The buffer ionic strength was then increased to 30 mM ammonium acetate, where PGE_2 and PGD_2 began to resolve (Figure 4.5A). These two PGs share the same molecular mass and fragmentation spectra (Figure 4.6); therefore, they must be electrophoretically separated to be differentiated by CE-MS/MS. LTB_4, possessing different structural characteristics than PGs, was detected approximately 1 min later at these conditions (Figure 4.5B). Adjustring the BGE to pH 5 resulted in baseline separation of the four compounds (Figure 4.5C). Under these conditions, TXB_2 co-migrated with $PGF_{2\alpha}$. However, the MS would be able to resolve these analytes based on mass differences.

Additional modifications to the BGE were made in attempt to improve resolution and permit segmented scanning MS analysis (data not shown). For example, BGE ionic strengths of 60, 80, 120, and 200 mM were investigated. Under these conditions, Joule heating caused increasing current and peak broadening. To reduce these effects, the capillary inner diameter was decreased to 25 μm I.D. While this reduced Joule heating, the resolution of the analytes was unaffected. In fact, the EOF was of the same magnitude for all BGE concentrations greater than 60 mM. These results suggest that at 40% methanol BGE concentrations, the EOF is repressed to a minimal magnitude.

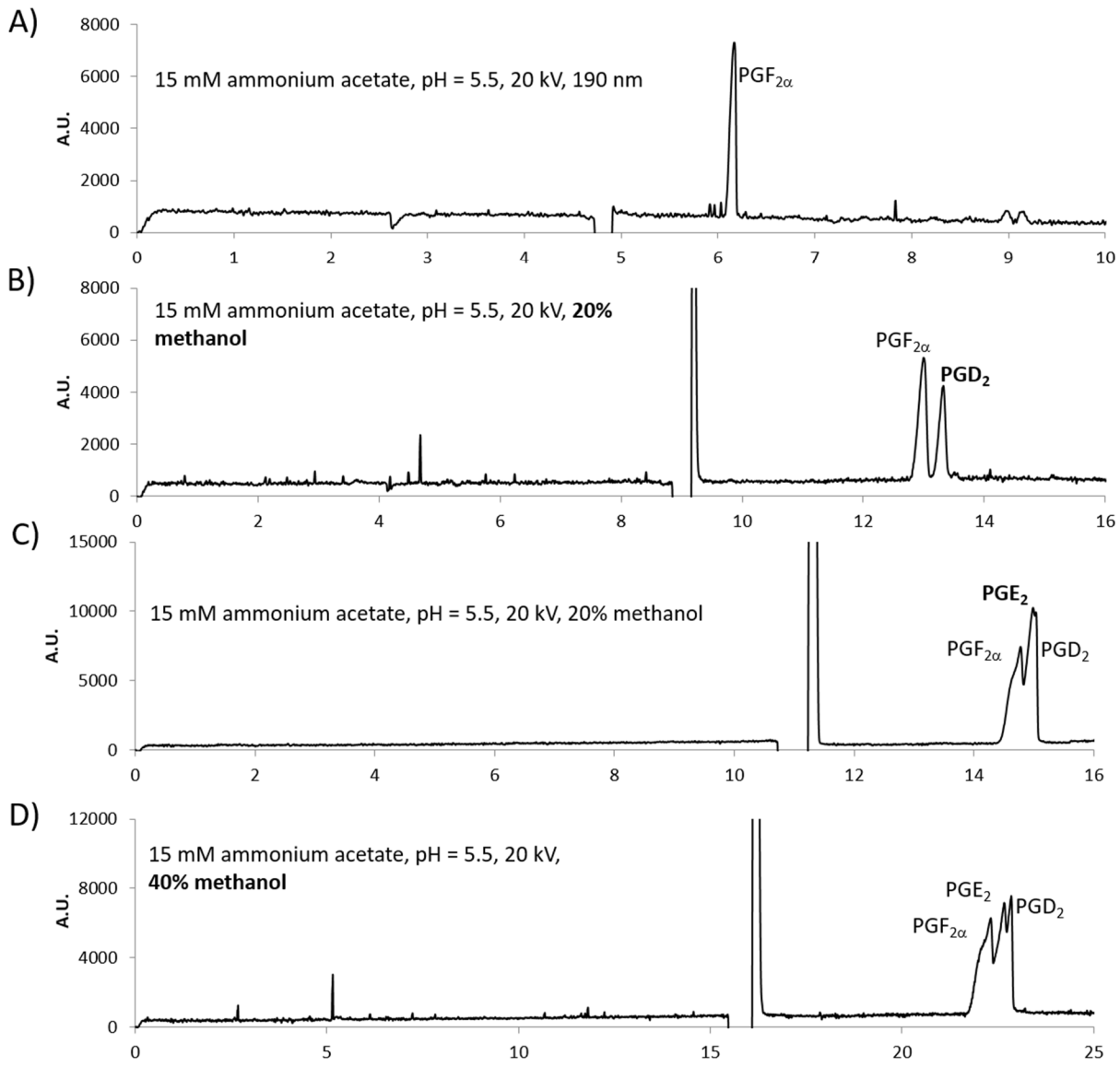

Figure 4.4: Method development: BGE methanol concentration with 100 μM prostaglandin standards; A) 0% methanol, PGF2α, B) 20% methanol, PGF2α and PGD2, C) 20% methanol, PGF2α, PGD2, PGE2, and D) 40% methanol, PGF2α, PGD2, and PGE2.

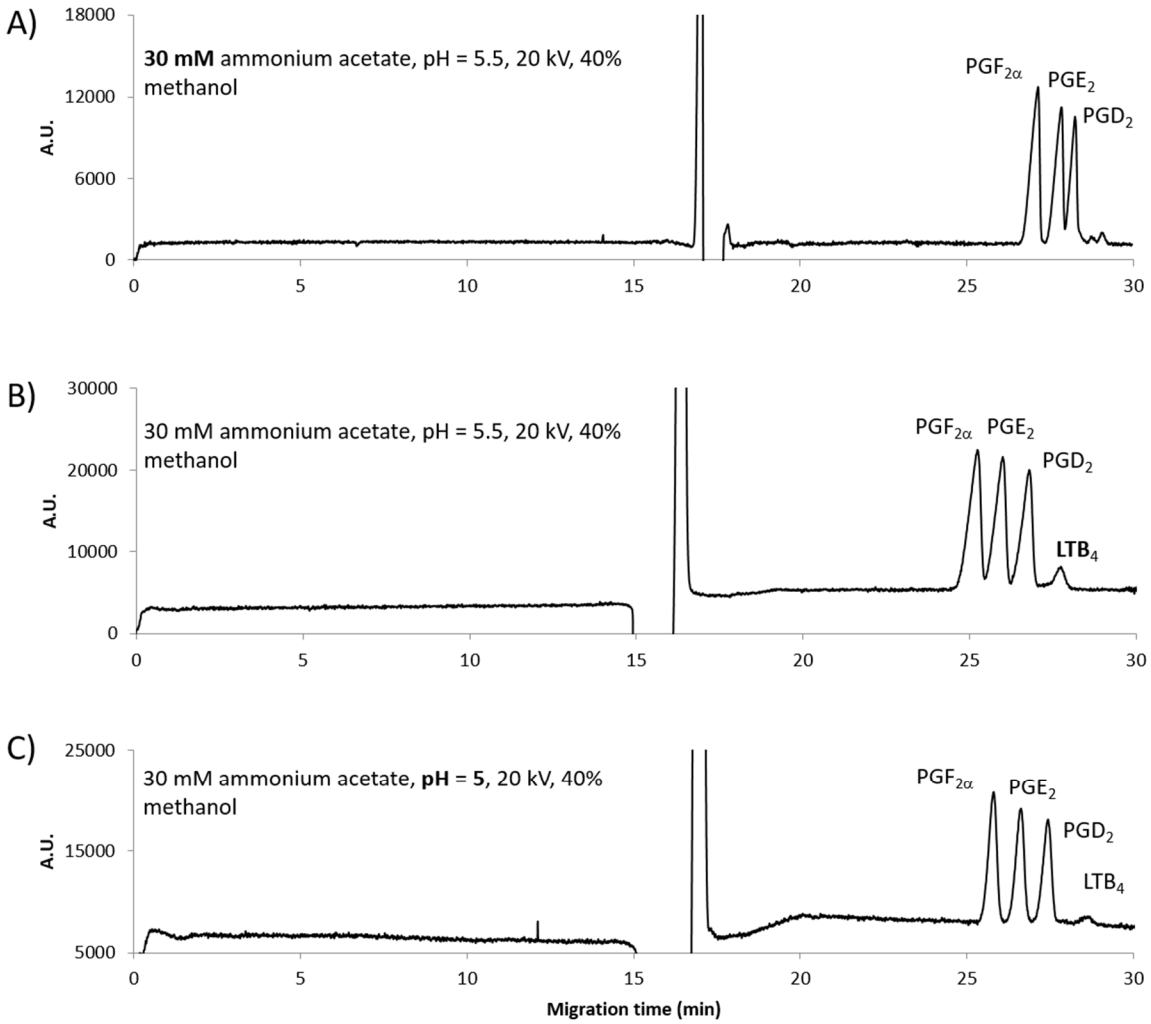

Figure 4.5: Method development: ionic strength and pH with 100 mM eicosanoid standards. A) 30 mM ammonium acetate, pH = 5.5, $PGF_{2\alpha}$, PGE_2, PGD_2, B) 30 mM ammonium acetate, pH = 5.5, PGF2a, PGE_2, PGD_2, and LTB_4, C) 30 mM ammonium acetate, pH = 5, $PGF_{2\alpha}$, PGE_2, PGD_2, and LTB_4.

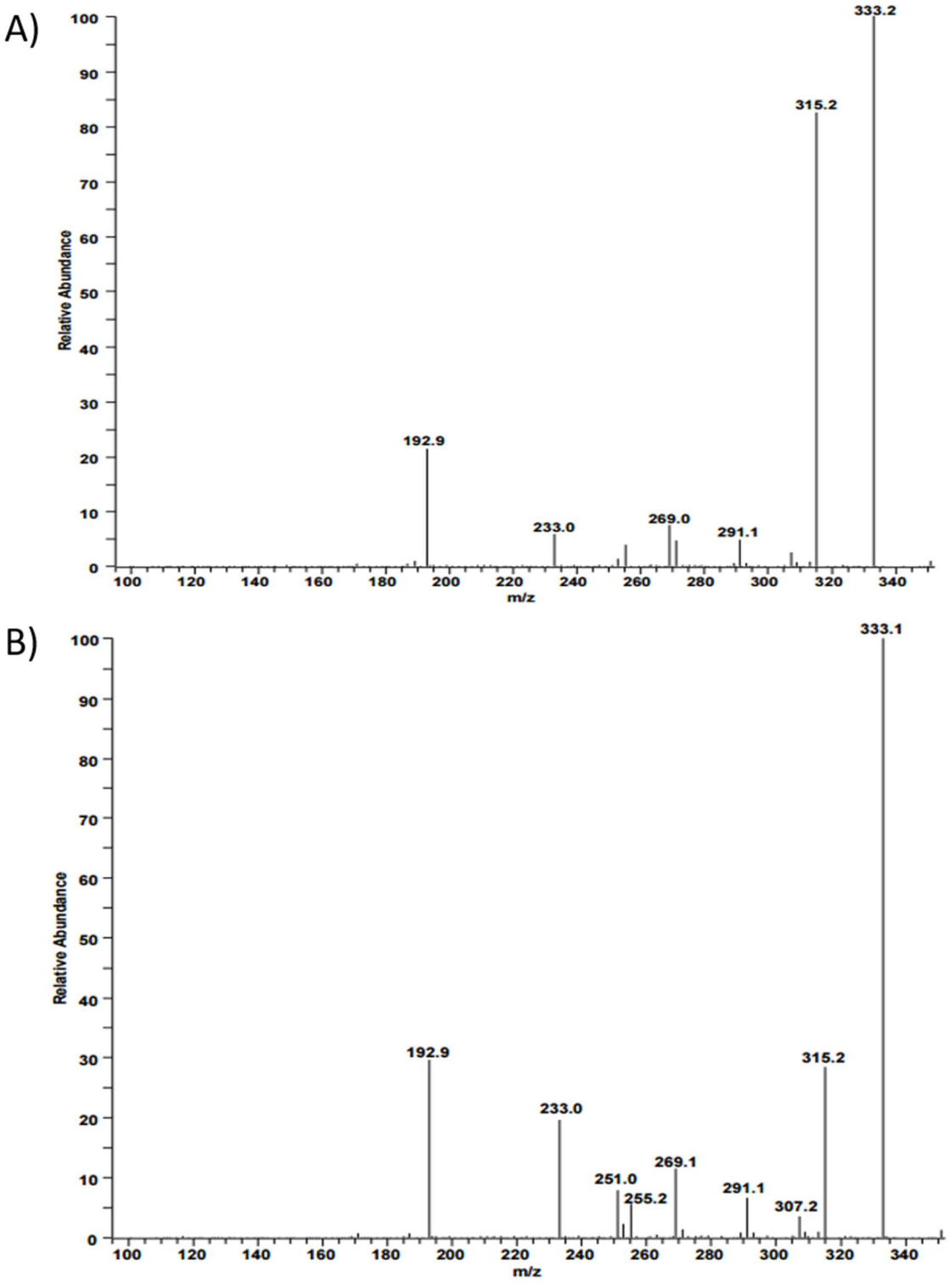

Figure 4.6: A) Fragmentation of PGE_2 and B) PGD_2

Lastly, cyclodextrins (CDs) were added to the BGE to potentially increase separation selectivity and aqueous solubility for the eicosanoids. Hydroxypropyl β-CD additive decreased the total run time but resulted analyte co-migration. As an uncharged β-CD, this was expected because PGs migrate faster when complexed with the CD. Subsequently, sulfobutyl-β-CD, a negatively charged CD, was investigated. With this additive, the resolution of the eicosanoids was improved, but peak shapes were non-Gaussian. Ultimately, neither β-CDs were sufficient in achieving better separation conditions than the CD-free buffer, therefore this approach was not pursued further.

4.4.1.2 CE-MS Studies

As described in Chapter 1, anion analysis by CE-ESI-MS is notoriously difficult. In normal mode CE, when the EOF reaches the shared electrode, a gap in conductivity can cause the current to fail. In this case, anions do not reach the mass spectrometer. Pressure assistance and high EOF velocities can be used to overcome the conductivity gap [28, 29]. Another option is to reverse the polarity of the CE system. This can be done using static or dynamic silanol wall coating. Dynamic wall coating is not often applied in CE-ESI-MS because the coating molecules are not volatile. Static coating is often used in CE-ESI-MS, but does require derivatization of the capillary walls [28, 29], which can be time consuming. Additionally, leaching of the coating molecules can cause unstable electrospray and contamination of the spectrometer.

Table 4.1: Infusion of $PGF_{2\alpha}$ in 1 mM and 2 mM ammonium acetate with differing amounts of methanol organic modifier (n = 1).

Methanol Content	Ion Counts (1 mM)	Ion Counts (2 mM)
0%	6.20E+01	1.40E+02
20%	2.80E+02	8.90E+04
40%	2.50E+05	2.90E+05
60%	4.70E+05	2.90E+05
80%	8.30E+05	3.90E+05

Table 4.2: Infusion of $PGF_{2\alpha}$ in 1 mM ammonium acetate and 80% of different organic modifiers (n = 1).

Organic Modifier (80%)	Ion Counts
Methanol	8.30E+05
Isopropanol	1.20E+06
Acetonitrile	5.00E+05

Optimized conditions from the CE-UV studies were transferred to the CE-ESI-MS system to achieve better sensitivity and specificity for the eicosanoids. In our electrophoresis experiments using the optimized separation parameters, the eicosanoids were not detected. With the use of pressure assistance and high EOF velocities, the analytes co-migrated and demonstrated poor sensitivity.

The cause of poor sensitivity was determined to be low solubility of the eicosanoids in the optimized BGE. An examination of 1 μM $PGF_{2\alpha}$ signal as a function of methanol concentration is shown in Table 4.1. At 80% methanol concentration in the BGE, 8.3E5 ion counts were obtained, as opposed to 2.8E2 for 20% methanol. Isopropanol and acetonitrile were tested as well, as shown in Table 4.2. For isopropanol and methanol, high organic content slows the EOF and greatly increases run time. The use of the organic modifier acetonitrile does not slow the EOF, but does dissolve the cellulose acetate polymer of the interface. An ideal solvent that did not dissolve the cellulose acetate or slow the EOF was not found.

To overcome the problem of low solubility and poor sensitivity, two options were considered. The first was to derivatize the eicosanoids in order to obtain a product with properties optimal as regards with a CE-ESI-MS detection sensitivity. The second was to redevelop an eicosanoid method using acetonitrile BGE modifier and an interface that did not rely on cellulose acetate. The former option was chosen because redeveloping a method with another interface would be difficult and time consuming. Additionally, there are several commercialized derivatization kits designed to improve MS detection of

eicosanoids. These kits have shown nM limits of detection for eicosanoids from biological samples.

4.4.2 CE-MS of Derivatized Eicosanoid Standards

The AMP+ mass spectrometry kit from Caymen was used to derivatize the eicosanoids standards. The analyte undergoes “charge reversal” derivatization, where its negatively charged carboxylic group is converted to an amide linked to an aromatic system with a fixed positive charge. The reaction is as follows:

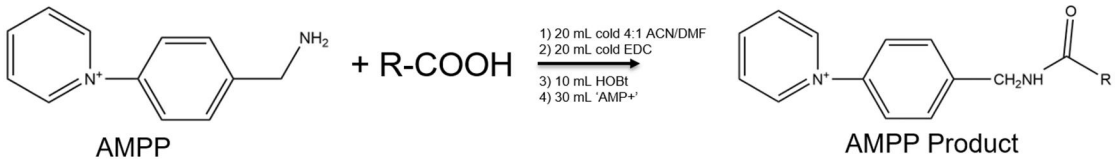

where EDC is the coupling agent, HOBt is hydroxbenzotriazole, AMPP is the tag, and R-COOH is the free eicosanoid. The derivatized eicosanoid is more water soluble and 10- to 20-fold more sensitive in positive mode than the free eicosanoid in negative mode[30].

Initially, the derivatization was carried out per the instructions from Caymen as described in the experimental section. However, significant broadening due to peak destacking was observed with these conditions (Figure 4.7A). The derivatization cocktail was sequentially diluted in acetonitrile until narrow peaks were detected without compromising peak area, as shown in Figure 4.7B-C.

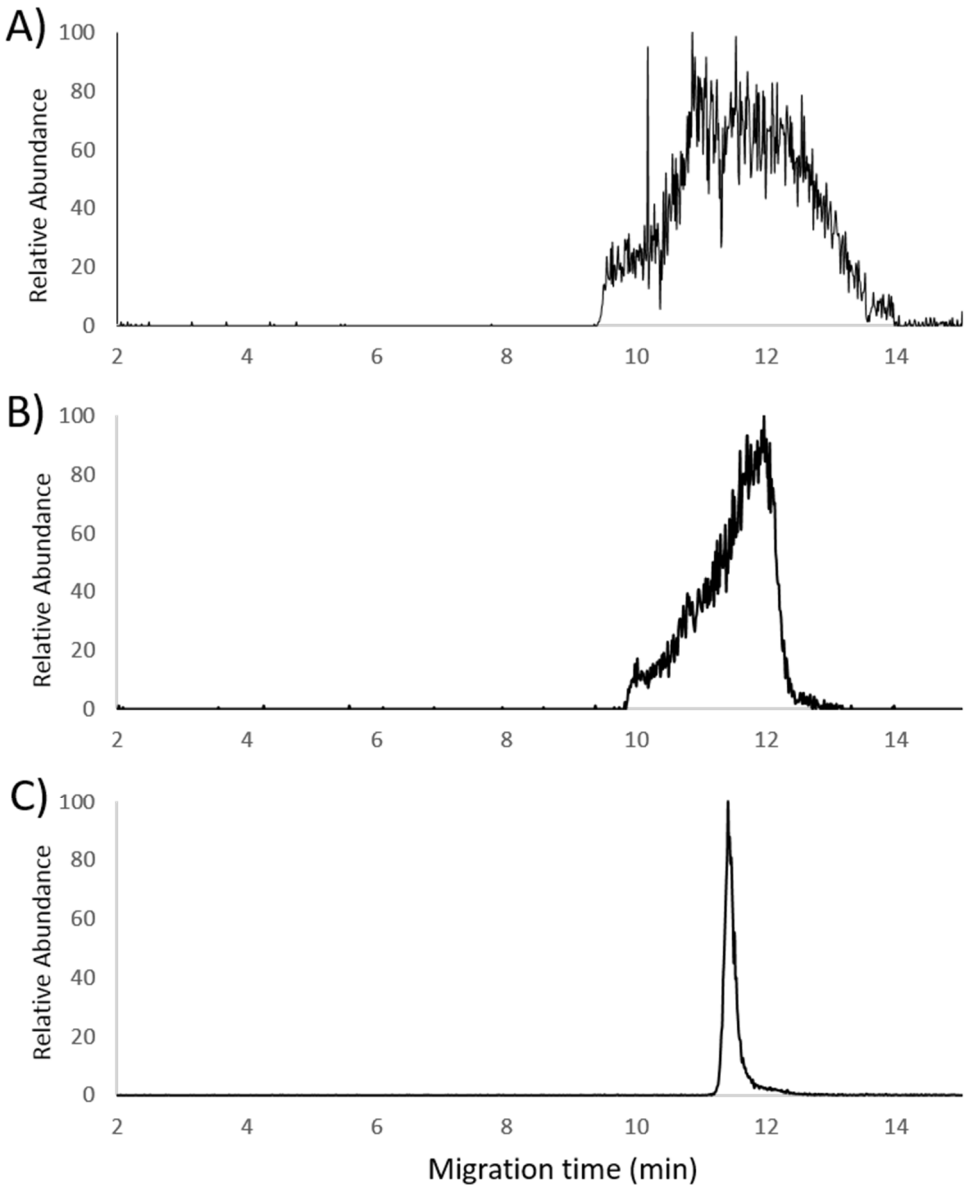

Figure 4.7: CE-ESI-MS of $PGF_{2\alpha}$ derivatized using A) ½ (TIC 1.4E2) B) 1/16th (1.6E2) and C) 1/1000th (1.3E3) the derivatization recipe.

Table 4.3: Most abundant daughter ions from the derivatized eicosanoids

Analyte	Parent Ion (m/z)	Isolation Width (m/z)	Normalized CID energy (%)	Product Ions (m/z)
$PGF_{2\alpha}$	521.5	1.5	50	477
PGE_2	519.5	1	50	239, 491
PGD_2	519.5	1	50	295
TxB_2	538.5	2	35	337
LTB_4	503.5	1.5	35	323, 391

Table 4.4: LODs for derivatized eicosanoid standards. Estimated temporal resolution calculated assuming 10% recovery of 10 nM in vivo eicosanoids at 1 μL/min collection rate

Analyte	LOD (nM) (n =3)	pg	Est. Temporal Res. (sec)
$PGF_{2\alpha}$	3.37 +/- 1.34	0.06	7.2
PGD_2	5.73 +/- 1.54	0.1	12
PGE_2	3.28 +/- 0.84	0.06	7.2
TxB_2	9.1 +/- 0.39	0.16	19.2
LTB_4	13.5 +/- 7.94	0.22	26.4

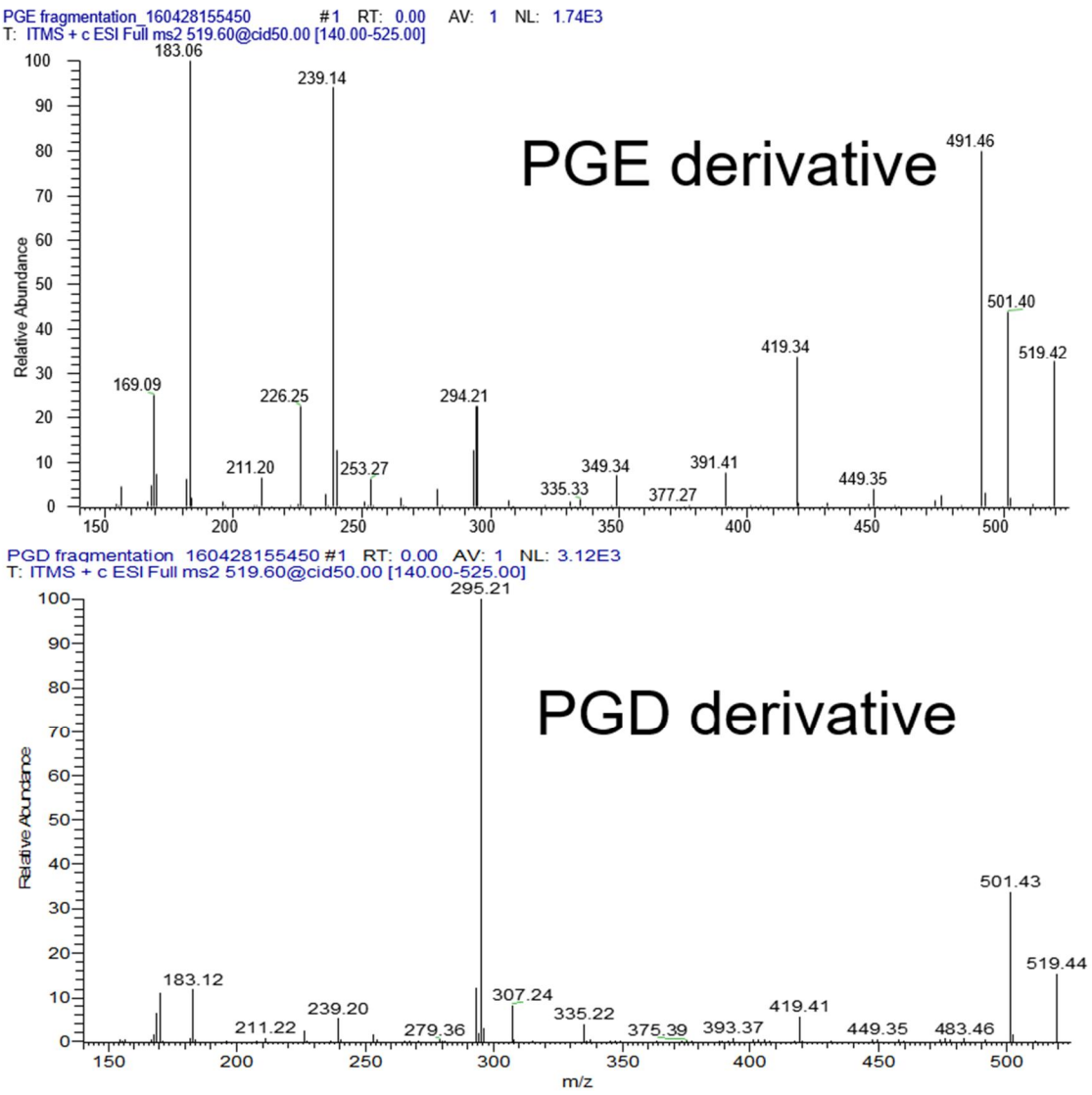

Figure 4.8: CID fragmentation of PGE and PGD derivatized with AMP+

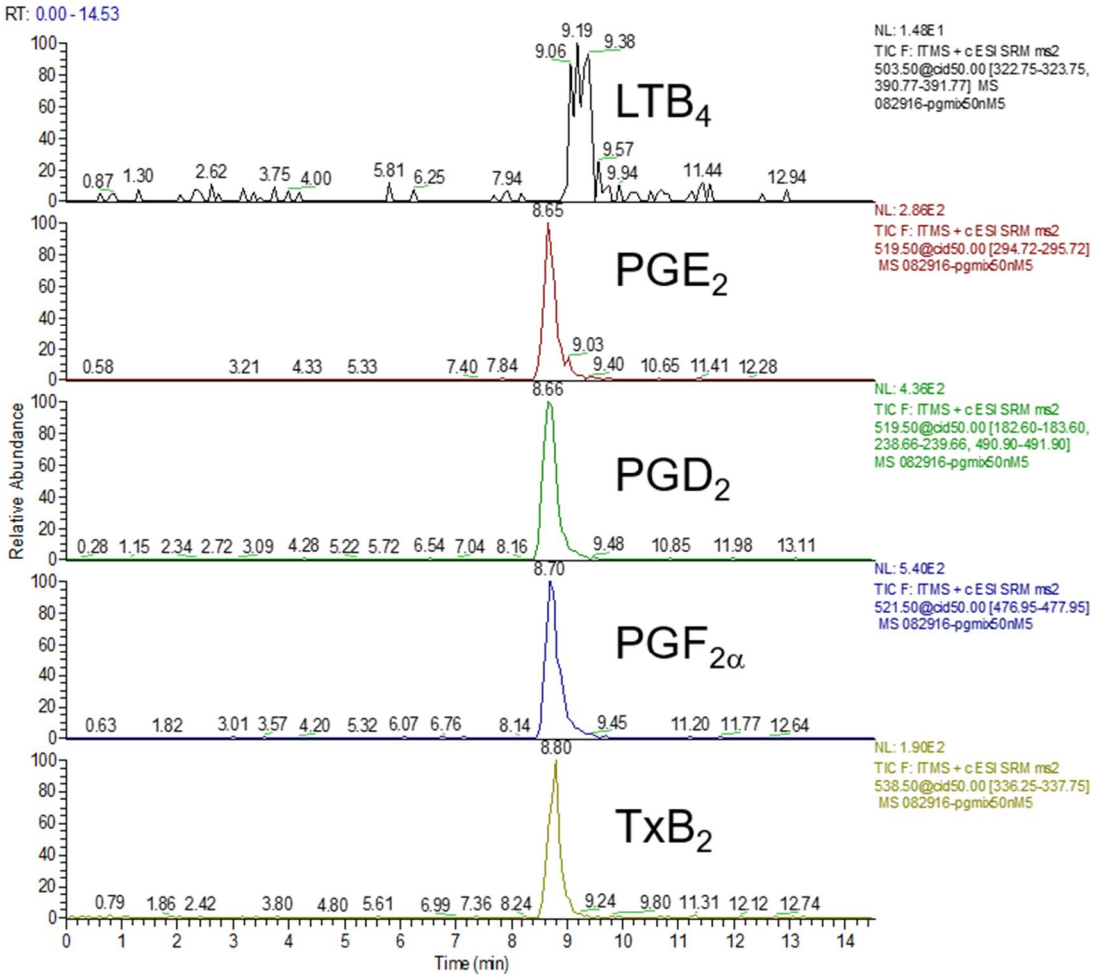

Figure 4.9: CE-ESI-MS/MS of 50 nM derivatized eicosanoid standards. Conditions: 50 mm I.D. x 360 mm O.D. x 60 cm L_{tot}, 30 mM ammonium acetate, pH = 6.7, 10% meOH, 283 V/cm, +3.2 kV ESI kV, CID energy = 50.

The fragmentation conditions and most abundant daughter ions from the derivatized eicosanoid standards are shown in Table 4.3. Interestingly, the fragmentation of PGE_2 and PGD_2 derivatives differed from one another as shown in Figure 4.8. Because of this, a rigorous CE separation was not entirely necessary. Instead, the purpose of CE was to introduce nanoliters of sample to the MS and to improve concentration sensitivity relative to infusion.

The CE-ESI-MS analysis of 50 nM derivatized eicosanoids is shown in Figure 4.9. Generic BGE conditions were used that resulted in comigration of all the eicosanoids with the exception of LTB_4. However, all five analytes were uniquely detected by MS/MS. Table 4.4 shows that the LODs for the eicosanoids were 3-15 nM. Biological levels of eicosanoids in tissue are in this range and can certainly increase above this range in cases of oxidative stress.

One important reason for utilizing CE-ESI-MS for the investigation of oxidative biomarkers found in microdialysate is to achieve higher temporal resolution than other analytical systems. To demonstrate this method's utility toward achieving this goal, an estimation of the lowest temporal resolution was conducted (Table 4.4). The estimation took into account the low recovery (10%) and low biological concentration (10 nM) of eicosanoids during a microdialysis experiment[31]. Even in this case, the time required to detect the eicosanoids at a flow rate of 1 μL/min was as low as 7.2 seconds (120 nL). Other LC-MS methods utilized in the C. Lunte lab have required up to 10 minutes to collected the necessary sample for detection. Additionally, the low sample consumption of this CE method permits further utilization of the sample to explore other oxidative

biomarkers, increasing the amount of information from a single sample and decreasing the number of experiments required to conduct a full metabolic profile.

Even though the previously described method is sufficient for salt-free samples, microdialysate contains sodium, chloride, magnesium, and calcium that will negatively affect spray volatility and sensitivity as shown in Figure 4.10. To remove matrix components, two sample clean-up methods were explored. First, Oasis HLB cartridges were tested. Bollinger and coworkers reported approximately 60% yields for eicosanoids using these cartridges on mouse serum and lung epithelial cells[30] (procedure in experimental section). Their eicosanoid method relied on an LC separation that diverted salt from the detector, so salt that was not removed during SPE did not greatly influence their spectra. Our CE method, however, suffered from peak destacking and losses in sensitivity due to the presence of salt post-SPE. Larger rinse volumes and higher aqueous washes were tested to remove excess salt, but resulted in significant loss of analyte.

Ziptips, which are low volume pipet tips that contain a few milligrams of C18 bonded silica phase, were employed to improve retention of eicosanoids relative to the Oasis HLB cartridges and allow for large aqueous rinses. Additionally, because the elution volume from the Ziptip is 10 μL (as opposed to 1000 μL), the evaporation step prior to derivatization was not required, decreasing sample prep time and sample loss. Using the procedure described in

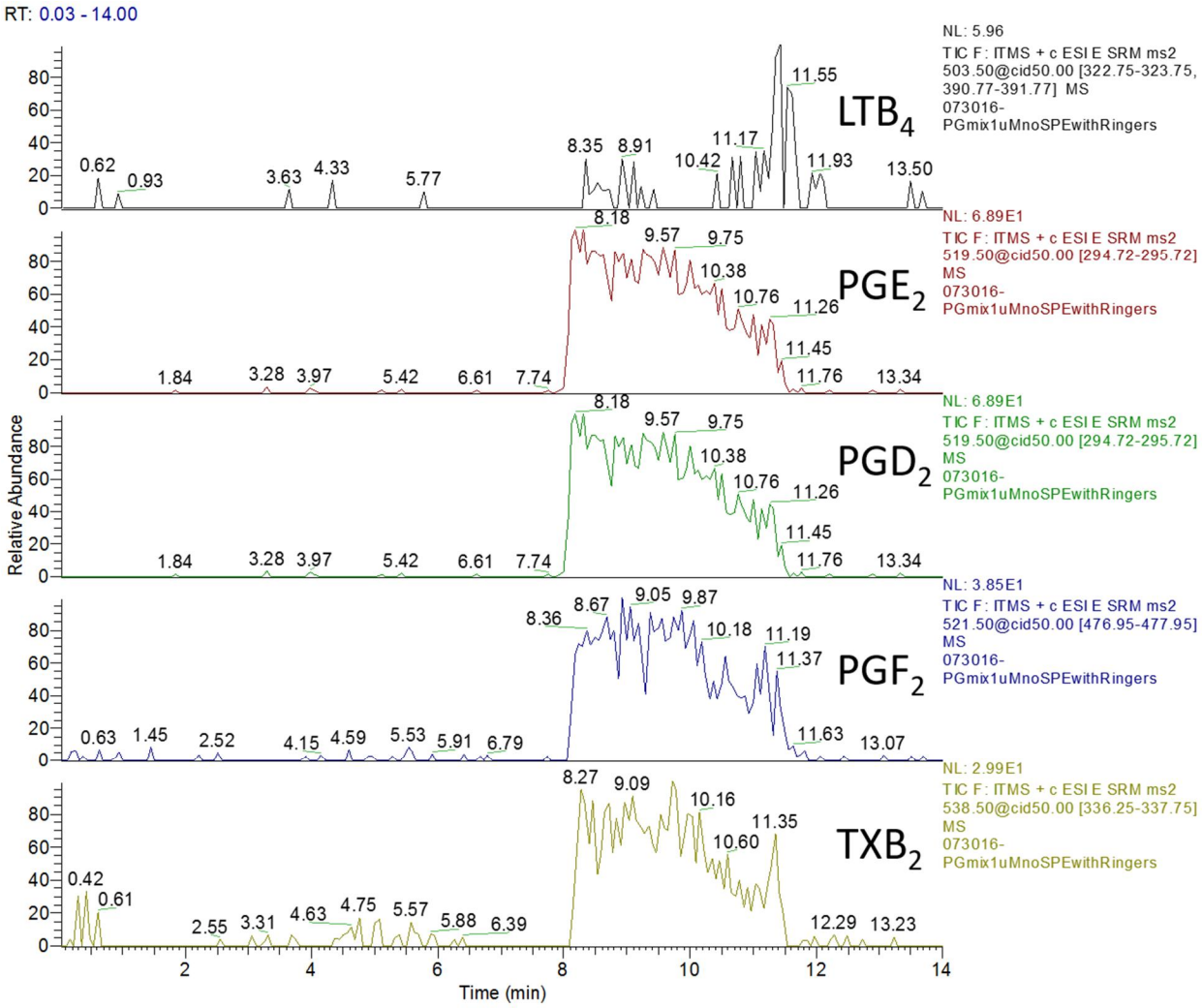

Figure 4.10: CE-MS/MS spectra of 1 μM derivatized eicosanoid standards. Standards were dissolved in Ringer's prior to derivatization.

the experimental section, 95-125% of $PGF_{2\alpha}$, PGE_2, PGD_2, and TXB_2 were recovered from the SPE material, while LTB had approximately 50% recovery (n = 3). Eicosanoid spectra that have been dissolved in Ringer's solution and extracted by Ziptips are shown in Figure 4.11. Peak destacking was not apparent for the extracted eicosanoids, suggesting that a majority of salt had been removed from the sample. Sample acidification prior to desalting was also investigated, but resulted in poor derivatization and low signal for the eicosanoids (data not shown).

The CE-MS/MS calibration curves for the eicosanoids dissolved in Ringer's solution, desalted by Ziptips, and derivatized by AMP+ are shown in Figure 4.12. Detected response linearity was evaluated over a concentration range from 25 - 500 nM, with $r^2 = 0.99$ for all analytes (n = 6). The estimated LOD for the prostaglandin and thromboxane standards was 25 nM while LTB_4 was difficult to detect at concentrations lower than 75 nM. LTB_4 is not well retained by the Ziptip due to its polarity, resulting in a high LOD relative to the other analytes. Separate sample preparation procedures would need to be developed to detect LTB_4 at low nM concentrations. The remaining LODs are high compared to those of samples dissolved in water instead of Ringer's. The cause of the increased LOD is two-fold. First, the SPE step presents a potential source of sample loss. Second, it is likely that some salt from the Ringer's solution is still present in the final elution.

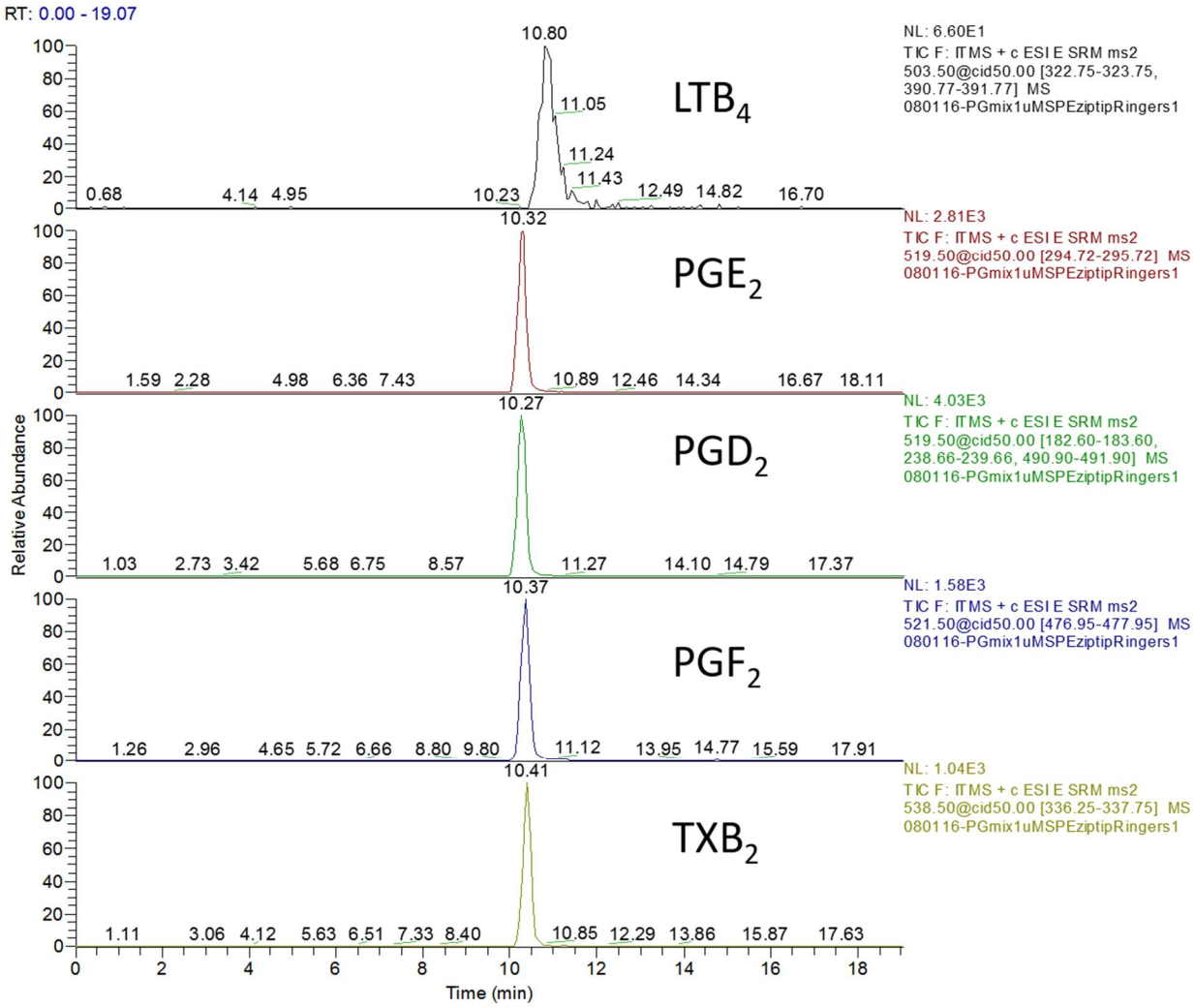

Figure 4.11: CE-MS/MS spectra of 1 μM derivatized eicosanoid standards dissolved in Ringer's solution and desalted with Ziptips.

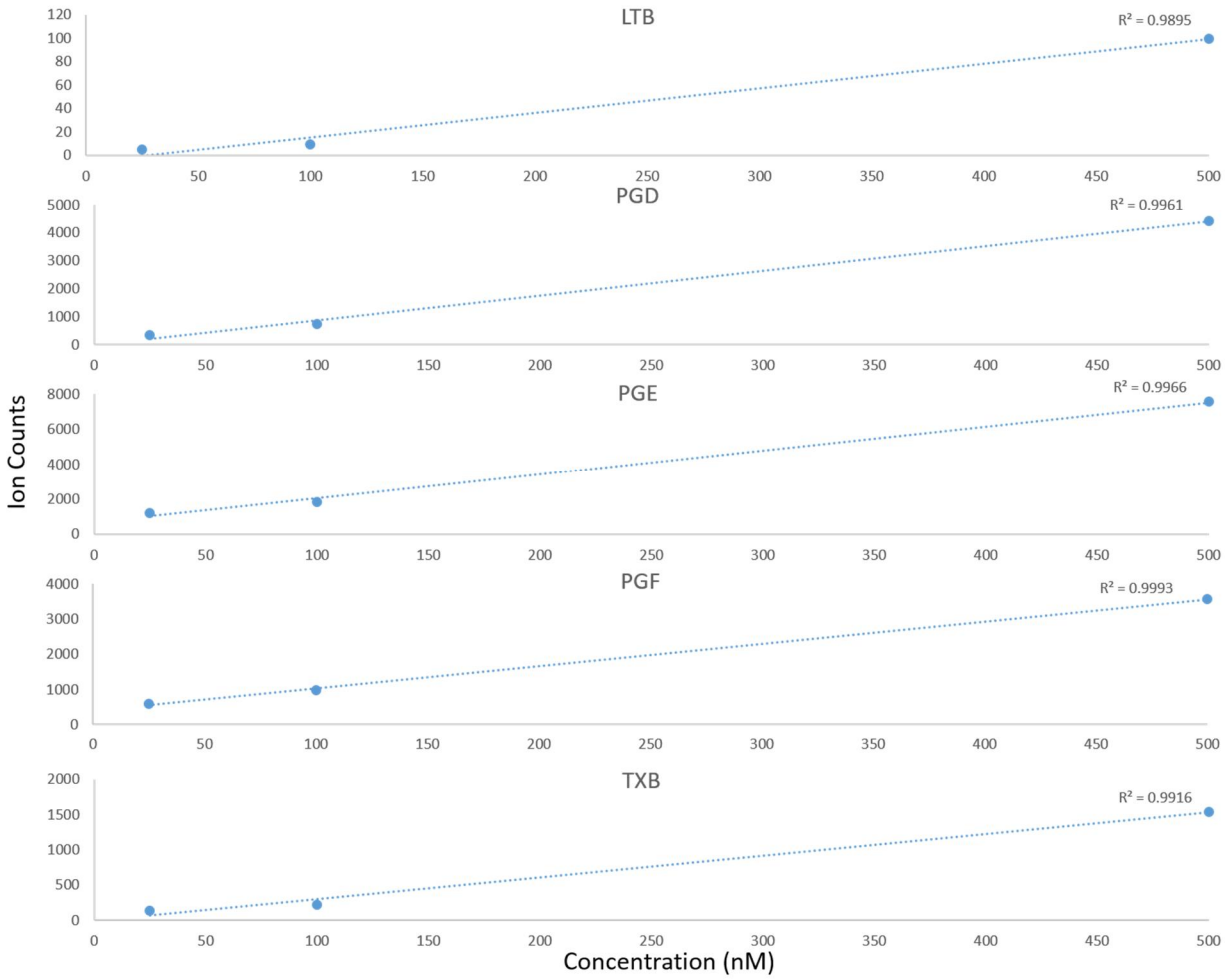

Figure 4.12: Calibration curves for desalted eicosanoids dissolved in Ringer's solution using CE-MS/MS

4.4.3 Application of CE-ESI-MS Method for Eicosanoids in Microdialysis Samples

The sample preparation, derivatization, and CE-MS/MS method were carried out on postop microdialysis samples collected from the hippocampal region of female Sprague-Dawley rats. The samples were collected at 1 μL/min for one hour (60 μL) and stored at -80ºC to prevent degradation prior to analysis. The samples were expected to contain slightly higher than basal levels of eicosanoids due to the inflammation that occurs immediately after probe implantation. Unfortunately, the MS response for the various eicosanoids was below the detection limits of the method (Figure 4.13). One-hundred nanomolar standards were spiked to the sample and the signals for $PGF_{2\alpha}$, PGE_2, and TXB_2 increased expectedly. LTB_4 was not detected in the spiked sample, suggesting that signal suppression for this analyte is greater from microdialysis samples than from pure Ringer's solution.

There are several improvements that could be made to the described method to achieve signal above the detection limits for the eicosanoids in microdialysis samples. First, the microdialysis recovery of the eicosanoids could be improved. For pure Ringer's solution perfused through the probe, 5-20% recovery of the eicosanoids has been reported. Wang et al. improved the recovery of eicosanoids from *in vitro* microdialysis samples by modifying the makeup of the probe's membrane and the addition of cyclodextrin to the perfusate[31]. For the eicosanoids investigated in this study, the identity of the membrane used had little effect on their recovery. However, the addition of

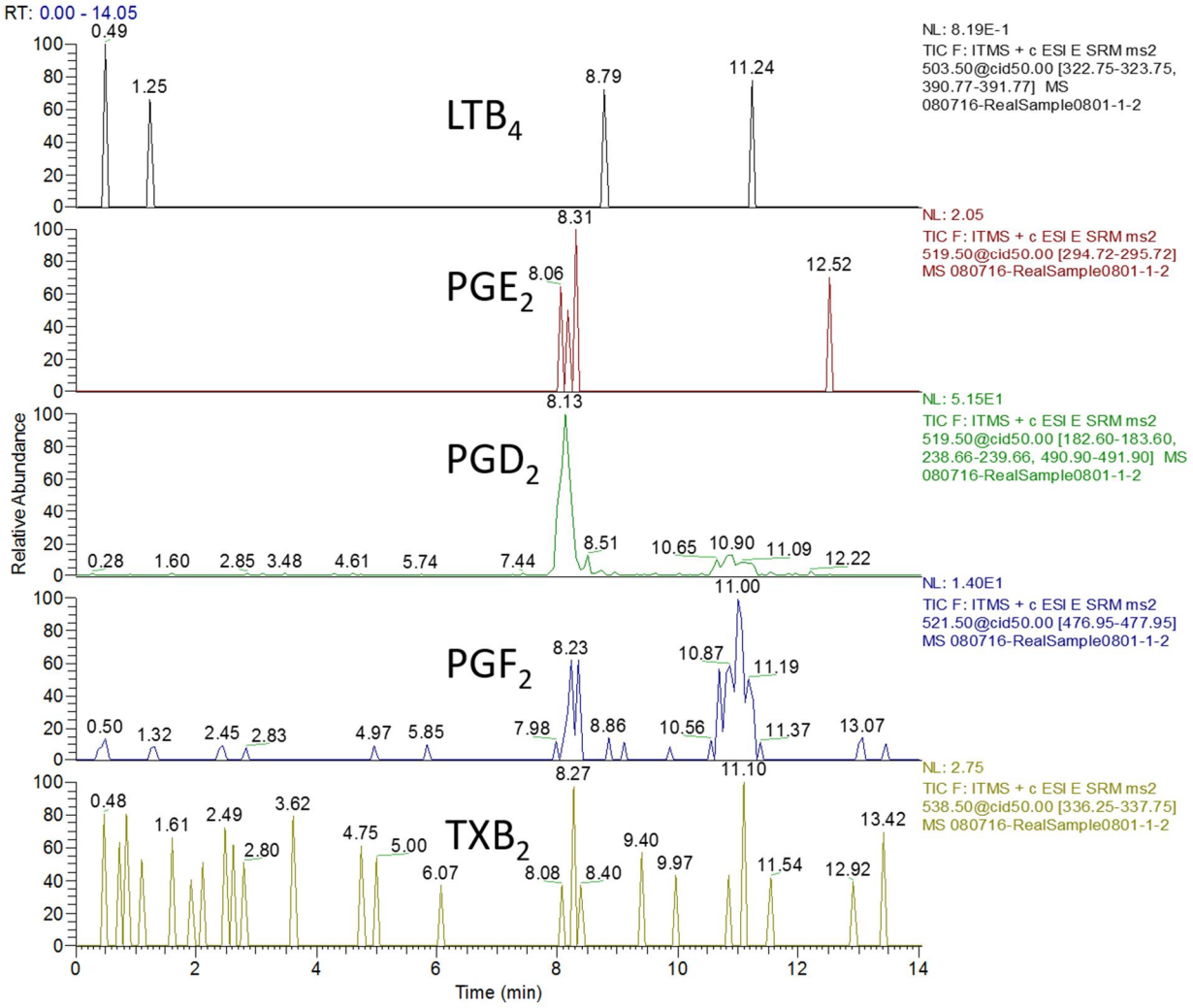

Figure 4.13: CE-MS/MS results for postop (1 hr) microdialysis sample

hydroxypropyl-β-cyclodextrin had a tremendous impact on the recovery, in some cases increasing recovery to 65%. With these modifications, they were able to achieve 2 nM detection limits for an LC-MS/MS method that was previously insufficient under normal conditions. A second improvement that could be made is the utilization of preconcentration. With the current method, 4 μL of sample is desalted, derivatizated, evaporated and reconstituted in 4 μL of water. If low volume injection vials are used instead of the 200 μL centrifuge tubes used in this study, the sample could be reconstituted in a much smaller volume. Lastly, if necessary, a more thorough separation of the analytes can be developed and coupled to segmented MS/MS analysis. Segmented MS can improve sensitivity relative to the current parameters that scan five masses simultaneously.

4.5 Conclusions

A CE-UV method for eicosanoids was developed, but was not for ideal ESI-MS. To improve solubility and ionization of the eicosanoids, charge reversal derivatized with AMP+ was conducted. Low nM detection limits were achieved for derivatized standards dissolved in water. However, when the eicosanoids were dissolved in Ringers solution, peak destacking hindered the method's sensitivity. A desalting step that utilized c18 Ziptips was added to the method, thereby preventing peak destacking. With this prep step added, the method was capable of 25-100 nM detection limits for the analytes. This was not sufficient for basal microdialysis samples. Modifications to the method, such as improving recovery and preconcentration were described.

4.6 References

[1] Sies, H., *Exp. Physiol.*, **1997**, *82*, 291-295.

[2] Finkel, T.; Holbrook, N. J., *Nature*, **2000**, *408*, 239-247.

[3] Lyras, L.; Cairns, N. J.; Jenner, A.; Jenner, P.; Halliwell, B., *J. Neurochem.,* **1997**, *68* (5), 2061-2069.

[4] Floyd, R. A.; Carney, J. M., *Ann. Neurol.,* **1992**, *32*, 22-27.

[5] Gutteridge, J. M. C., Clin. Chem., **1995**, *41*(12), 1819-1828.

[6] Valavanidis, A.; Vlachogianni, T.; Flotakis, C., J. Environ. Sci. and Health, **2009**, *27*, 120-139.

[7] Mateos, R.; Lecumberri, E.; Ramos, S.; Goya, L.; Bravo, L., J. Chroma. B., **2005**, *827* (1), 76-82.

[8] Montuschi, P.; Collins, J. V.; Ciabattoni, G.; Lazzeri, N.; Corradi, M.; Kharitonov, S. A.; Barnes, P. J., Am. J. Resp. Crit. Care Med., **2000**, *162* (3), 1175-1177.

[9] Weiss, D. J.; Lunte, C. E., Electrophoresis, **2008**, *21*(10), 2080-2085.

[10] Hoque, M. E.; Arnett, S. D.; Lunte, C. E., J. Chroma. B., **2005**, *827*(1), 51-57.

[11] Vaca, C. E.; Wilhelm, J.; Ringdahl-Harms, M., Mutat. Res., **1988**, *195*, 137-149.

[12] Zhang, R.; Brennan, M-L.; Shen, Z.; MacPherson, J. C.; Schmitt, D.; Molenda, C. E.; Hazen, S. L., J. Bio. Chem., *277* (48), **2002**.

[13] Gemmell, E.; Marshall, R. I.; Seymour, G. J., Periodontology 2000, **1997**, *14*(1), 112-143.

[14] Crofford, L. J., J Rheumatology, **1997**, *49*, 15-19.

[15] Balboa, M. A.; Balsinde, J., Biochim. Biophys. Acta, **2006**, *1761*, 385-391.

[16] Kinsella, J. E.; Lokesh, B., Crit. Care. Med., **1990**, *18*(2), 94-114.

[17] Basu, S., Mol. Cells, **2010**, *30*(5), 383-391.

[18] Seet, R. C. S.; Lee, C-Y. J.; Loke Mun, W.; Huang, S. H.; Huang, H.; Looi, W. F.; Chew, E. S.; Quek, A. M. L., Lim, E. C. H., Halliwell, B., Free Rad. Bio. Med., **2011**, *50*, 1787-1793.

[19] Farman, N.; Pradelles, P.; Bonvalet, J. P., Am. J. Physio., **1986**, 251(2), 238-244.

[20] Duenges, W., Anal. Chem., **1977**, *49*(3), 442-445.

[21] Imagawa, R. T. H. S. T.; Sawada, T. K. T. O. T., Anal. Chem., **1997**, *69*(24), 5006-5010.

[22] Tsikas, D.; Zoerner, A. A., J. Chroma. B. Anal. Tech. Biomed. Life Sci., **2014**, *964*, 79-88.

[23] Mesaros, C.; Lee, S. H.; Blair, I. A., J. Chroma B. Anal. Tech. Biomed. Life Sci., **2009**, *877*(26), 2736-2745.

[24] Puppolo, M.; Varma, D.; Jansen, S. A., J. Chroma. B, **2014**, *964*, 50-64.

[25] Ault, J. M.; Riley, C. M.; Meltzer, N. M.; Lunte, C. E., Pharma. Res., **1994**, *11*(11), 1631-1639.

[26] Zhou, S. Y.; Zuo, H.; Stobaugh, J. F.; Lunte, C. E.; Lunte, S. L., Anal. Chem., **1995**, *67*(3), 594-599.

[27] Davies, M. I.; Lunte, C. E., Drug Metab. Dispos., **1995**, *23*(10), 1072-1079.

[28] Soga, T.; Yuki, U.; Naraoka, H.; Matsuda, K.; Tomita, M.; Nishioka, T., Anal. Chem., **2002**, *74*(24), 6224-6229.

[29] Harada, K.; Fukusake, E.; Kobayashi, A., J. Biosci. Bioeng., **2006**, *101*(5), 403-409.

[30] Bollinger, J. G.; Thompson, W.; Lai, Y.; Oslund, R. C.; Hallstrand, T. S.; Sadilek, M.; Turecek, F.; Gelb, M. H., Anal. Chem., **2010**, *82*, 6790-6796.

[31] Wang, Y., Dissertation, University of Kansas, **2015**.

Chapter 5

Conclusions and Future Directions

5.1 Conclusions

Two CE-ESI-MS interfaces were constructed. The first interface, a sheath liquid design first developed by Mark Schieferecke, Ryan Krisko, and Craig Lunte, was used to develop a novel CE-MS method for common natural aglycone and glycone type flavonoids. The method overcame issues associated with negative mode CE-ESI-MS analysis, such as current drops and corona discharge, without the use of static wall coating or pressure-assistance. It also demonstrated the utility of borate BGE for CE-ESI-MS. Borate is known to complex polyphenolic compounds, resulting in improved CE resolution. We demonstrated that catechol containing flavonoids remain complexed in the gas phase. The complexes form an increasing pattern of masses in the mass spectra that can be used to identify a catechol functionality on polyphenolic compounds. Examples of these complexes and their fragmentation were presented along with a demonstration of the method on *Ginkgo biloba* supplements.

The second CE-ESI-MS interface was an adaptation of Damon Osbourn and Craig Lunte's cellulose acetate decoupler for CE-EC. The capillary is ablated using a programmable laser near the capillary terminus. Cellulose acetate, a semipermeable membrane, is used to coat the holes and allow for the passage of current. In the case of CE-EC, the modified section is grounded. Conversely, for CE-ESI-MS, a high voltage is applied to generate electrospray

from the terminus. The novel design for CE-ESI-MS did not require the use of hydrofluoric acid, hand tools, or complicated alignment procedures like other designs. Our design was mechanically robust and produced stable electrospray. The separations achieved using the novel system were comparable to a commercial CE-UV system, while also demonstrating low limits of detection. Lastly, the interface was capable of pH modification post separation, which can be used to achieve separate CE and ESI conditions within a single analytical run.

Finally, the novel interface was used to develop an analytical method for five eicosanoids that are found in microdialysis samples at low levels. The eicosanoids investigated in this study were arachidonic acid metabolites generated by the excitable enzymes COX and LOX. CE-ESI-MS was chosen to investigate these compounds due to the volume limitations presented by microdialysis sampling. A CE-UV separation was developed that baseline resolved four of the five compounds. However, these conditions were inadequate for ESI-MS of the lipophilic compounds. To overcome this problem, the analytes were derivatized to improve solubility and sensitivity. A new method was developed for the derivatized eicosanoids, resulting in as low as 3 nM detection limits in the absence of salt. The LODs increased significantly when the analytes were dissolved in Ringer's solution. Ziptips were employed to prevent peak destacking, thereby improving LODs. The Ziptips were somewhat effective but were a source of sample loss and did not completely remove the salt content, resulting in LODs in the 25-100 nM range. This was not sufficient for detection in microdialysis samples. Improvements like adding cyclodextrin to

the microdialysis perfusate and preconcentration post-SPE were suggested to overcome the insufficiency in detection.

5.2 Future Directions

The features offered by CE-MS, such as high resolution, high peak capacity, reasonable cost, versatility, and low sample volume requirements are offset by problems like poor migration time reproducibility and interface robustness. Both problems are major factors preventing CE-MS widespread adoption in various laboratory environments. Recently, the application of CE has increased due to expansion of the protein therapeutics field; however, due to the lack of a suitable interface that allows for high sensitivity MS detection, CE-MS has not grown much with this expansion. In order to see CE-MS grow, its robustness must rival that of LC-MS. To get to this point, incremental advancements in the mechanical and electrical stability, interface housing, high throughput production, and ease of implementation must be made.

Along the way, the advantages and applications of the interface must be showcased. We aim to demonstrate its utility toward applications with sample limitations like microdialysis or blood spots. SCIEX, a company that manufactures a sheathless CE-MS interface, demonstrated their interface's utility toward peptide and protein identification and its complimentary nature with LC-MS (Figure 5.1). Other groups are demonstrating the utility of coupling CE to high mass accuracy mass spectrometers[1,2].

Another direction for electrophoretic techniques coupled to mass spectrometers is the utilization of microchips. Microchip electrophoresis (MCE) is

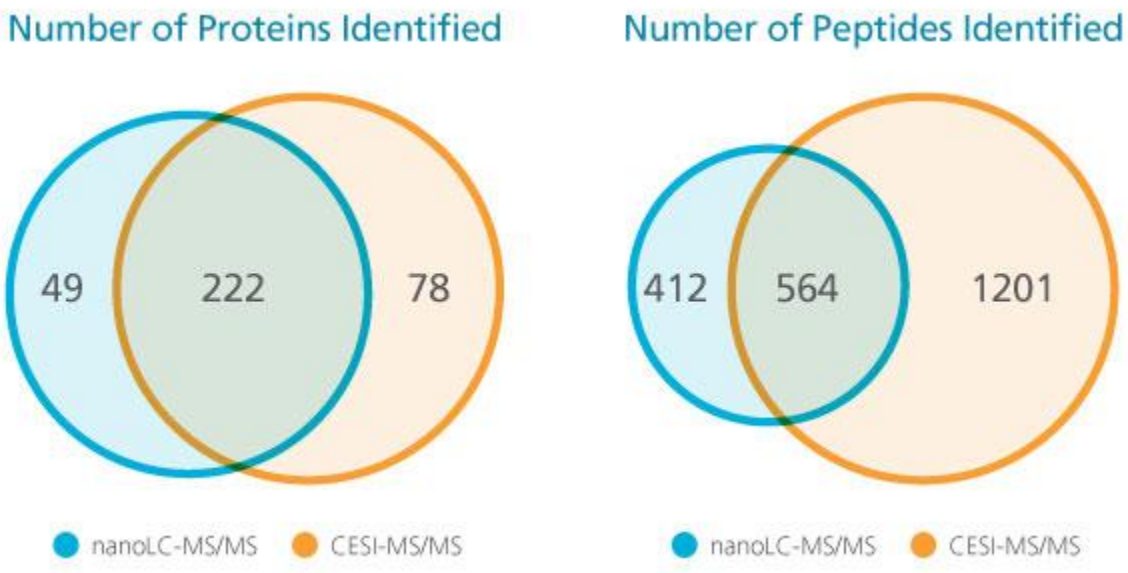

Figure 5.1: Protein and peptide coverage from yeast mitochondrial extract using CESI-MS (image from: https://sciex.com/applications/pharma-and-biopharma/biologics-characterization/biologics-analysis-by-cesi-ms/cesi-proteomics).

most commonly coupled to laser induced fluorescence, but mass spectrometry removes the requirement of a fluorophore. As in the capillary format, sheath liquid, liquid junction, and sheathless MCE-ESI-MS systems have been fabricated[3]. The sheath liquid MCE-MS interface utilizes a fused silica capillary attached to a conventional coaxial sheath flow interface. As such, dilution of the sample by the sheath liquid limits the utility of this design. For sheathless MCE-MS, a piece of sharpened fused silica capillary or standard ESI needle is glued to the microchannel exit. However, these designs suffer from dead volumes at the junction where the ESI connection is applied, short lifetimes, and clogging. Utilization of the decoupler design from Chapter 3 could theoretically be adapted for MCE-ESI-MS to eliminate dead volume and dilution issues. This advancement will be explored further by the S. Lunte laboratory.

5.3 References

[1] Zhao, Y.; Riley, N. M.; Sun, L.; Hebert, A. S.; Yan, X.; Westphall, M. S.; Rush, M. J. P.; Zhu, G.; Champion, M. M.; Medie, F. M.; Champion, P. A. D.; Coon, J. J.; Dovichi, N. J., Anal. Chem., 2015, 87(10), 5422-5429.

[2] Faserl, K.; Kremser, L.; Muller, M.; Teis, D.; Lindner, H. H., Anal. Chem., 2015, 87(9), 4633-4640.

[3] Li, F-A.; Huang, J-L.; Her, G-R., Electrophoresis, 2008, 29, 4938-4943.